MINISTRY OF AVIATION

AERONAUTICAL RESEARCH COUNCIL
REPORTS AND MEMORANDA

Drag Reduction of Thin Wings at Supersonic Speeds, by the Use of Camber and Twist

By

G. M. ROPER, M.A., Ph.D.

LONDON: HER MAJESTY'S STATIONERY OFFICE

1959

PRICE £1 7s. 6d. NET

Drag Reduction of Thin Wings at Supersonic Speeds, by the Use of Camber and Twist

By

G. M. ROPER, M.A., Ph.D.

COMMUNICATED BY THE DIRECTOR-GENERAL SCIENTIFIC RESEARCH (AIR),
MINISTRY OF SUPPLY

Reports and Memoranda No. 3132*

July, 1957

Summary.—Camber and twist is applied to the problem of reducing the drag due to incidence, of thin triangular or swept-back wings, at supersonic speeds, with subsonic leading edges and supersonic or sonic trailing edges. Two cases are considered: (i) with leading-edge suction forces ignored, (ii) with leading-edge suction forces included. It is found that twist, especially towards the wing tips, is more effective in reducing drag, for given lift, for the larger values of $\tan \gamma / \tan \mu$, where γ is the semi-apex-angle and μ is the Mach angle, and that camber is more effective for the smaller values, though, in general, the best results are obtained by a suitable combination of camber and twist. For triangular wings, with suction ignored, the maximum percentage drag reduction varies from about 10 per cent (for sonic leading edges) to 50 per cent (for very slender plan-forms) and, if suction forces are included, from zero (for very slender plan-forms) to about 10 per cent (when the leading edges are sonic). The effect of the swept-back trailing edge is, in general, to increase the maximum percentage drag reduction for given lift if suction forces are ignored; but to decrease the maximum reduction for smaller values of $\tan \gamma / \tan \mu$, and to increase the maximum reduction for values of $\tan \gamma / \tan \mu$ near to one, if suction forces are included.

---

1. *Introduction.*—In Ref. 1, the effect of camber and twist on the pressure distribution and drag on some triangular wings of zero thickness, at supersonic speeds but with subsonic leading edges, is investigated. The shapes of some cambered and twisted wings are found such that the thrust loading on the leading edges is removed or modified, while certain requirements with respect to camber and twist, or aerodynamic properties, are satisfied. The effect of additional incidence is also calculated. In Ref. 2, Part II, the effect of a change of Mach number on the aerodynamic characteristics of a wing with given camber and twist is calculated.

In these investigations, no particular attention was paid to the problem of obtaining a wing of minimum drag, but it was found that for some wings (mainly those with twist towards the wing tips), with modified pressure singularities of strength P on the leading edges, there was a certain range of positions of $P = 0$ for which the drag was less than that on the flat wing. For wings with no leading-edge singularities, the drag was found to be greater than that for the corresponding flat wing.

For a wing with given plan-form and given lift, in incompressible or subsonic flow, elliptic spanwise distribution of chord load gives minimum lift-dependent drag. In supersonic flow, wave drag appears, and it is necessary to consider the distribution of load over the whole wing.

---

* R.A.E. Report Aero. 2585, received 6th March, 1958.

In this report, the use of camber and twist is applied to the problem of reducing the drag due to incidence, camber and twist, for given lift of :

(a) triangular wings with subsonic leading edges, and unswept trailing edges

(b) swept-back wings with subsonic leading edges, and straight supersonic or sonic trailing edges.

Unless a special effort is made, an infinite suction (corresponding to a singularity) will occur (theoretically) on the infinitely thin leading edge, giving rise to a finite thrust locally. This infinite suction will not occur in practice, neither is the practical wing infinitely thin. In incompressible flow, it is well known that the equivalent thrust at the leading edge does appear (at least, when there is no leading-edge separation). It is not yet known, in the cases now considered, how much suction will occur; therefore two cases are considered*:

(i) with leading-edge suction forces included in the optimising process,

(ii) with leading-edge suction forces ignored in the optimising process.

Physically we are assuming, in the latter case, that the effect on the rest of the pressure distribution, of the presence or absence of the suction force, is insignificant. It is known that this is not always true, but it may well give useful results in some cases.

In Ref. 1, the surfaces corresponding to certain basic velocity potentials, and in Ref. 2, the velocity potentials corresponding to certain cambered and twisted surfaces, are given. In this report, the velocity potentials for three further (higher order) camber and twist solutions are found using the results of Ref. 2, Part II, Appendix III.

The load distributions on the nine† separate surfaces $z = - \delta x^{n-2s} y^{2s} (n (> 2s) = 1, 2, 3, 4, 5;$ $s = 0, 1, 2)$ are found, where δ is a small arbitrary constant, x is measured downstream from the apex, y is measured to starboard, and z is measured vertically upwards, and general formulae for the total lift, drag and pitching moments for the separate camber and twist solutions, for both triangular wings and swept-back wings with subsonic leading edges, and straight supersonic or sonic trailing edges are deduced.

In the numerical examples worked, one, two, three or four of the basic camber and twist solutions are combined with that of the flat plate $(n = 1, s = 0)$, so as to obtain the maximum reduction of drag for given type of plan-form and given lift. The choice of surfaces is not entirely arbitrary. It is possible, from a study of the grouping, etc., of the simplest combinations, to choose the camber and twist distributions most likely to give optimum results.

The results obtained are optimum for the number of surfaces, from those available, which are combined. The method can be extended to include a greater number of surfaces, but there are already signs of convergence. Some general formulae (which could be used for more extensive calculations on an electronic computor), will be given in a further report.

It is also shown how the position of the centre of pressure (at given lift) can be fixed in any desired position, with a (generally) slight increase in the value of the corresponding minimum drag.

2. *Mathematical Analysis of the Problem.*—2.1. *Formulae for the Calculation of the Minimum Drag for Given Wing Combinations.*—In the linearised theory of supersonic inviscid flow, the drag due to incidence, camber and twist, for a wing with subsonic leading edges, is given by

$$T = D - S, \qquad \qquad \qquad \qquad \qquad \qquad \qquad (1)$$

where D is the drag component of the pressure integral, and S is the component in the free stream direction of the suction force, which is determined by the strength of the singularities in the pressure on the leading edges of the wing.

---

* Deliberate design of wings with no leading-edge singularities, but still of low drag, is also possible, and further work on this is in hand.

† Further higher order camber and twist solutions have been worked out and used since this report was written, and will be given in further reports.

If α_r is the local surface slope in the negative streamwise direction, and p_r the load per unit area, at any point of the surface given by $z_r = F(x, y)$, the local surface slope and load per unit area for a surface given by

$$z = \sum_{r=1}^{n} (A_r z_r), \qquad \text{where the } A_r \text{ are constants,} \qquad .. \qquad (2)$$

are (using linear theory):

$$\alpha = \sum_{r=1}^{n} (A_r \alpha_r), \quad .. \qquad .. \qquad .. \qquad .. \qquad .. \qquad .. \qquad (3)$$

and

$$p = \sum_{r=1}^{n} (A_r p_r). \quad .. \qquad .. \qquad .. \qquad .. \qquad .. \qquad .. \qquad (4)$$

Hence the lift L, and the pressure integral D, are given by:

$$L = \int_S (A_1 p_1 + A_2 p_2 + \ldots + A_n p_n) \, dS \equiv \sum_{r=1}^{n} (A_r L_r), \quad .. \qquad .. \qquad .. \qquad .. \qquad (5)$$

$$D = \int_S (A_1 p_1 + A_2 p_2 + \ldots + A_n p_n)(A_1 \alpha_1 + A_2 \alpha_2 + \ldots + A_n \alpha_n) \, dS$$
$$= \sum (A_r^2 D_r) + \sum (A_r A_s D_{r,s}) \qquad (r = 1, 2, \ldots n; s = 2, 3, \ldots n; r < s), \qquad (6)$$

integration being over the plan-form of the wing, and where

$$L_r = \int_S p_r \, dS,$$

$$D_r = \int_S p_r \alpha_r \, dS,$$

are the total lift and pressure integral respectively for surface z_r, and

$$D_{r,s} (\equiv D_{s,r}) = \int_S (p_r \alpha_s + p_s \alpha_r) \, dS$$

is the 'interference' pressure integral for surfaces z_r, z_s (from the pressure distribution of one surface acting on the surface slope of the other).

. If P_r is the strength of the singularity in the x component, u, of the perturbation velocity on the leading edge of the surface z_r, the strength, P, of the singularity for the surface z is given by

$$P = \sum_{r=1}^{n} (A_r P_r), \quad .. \qquad .. \qquad .. \qquad .. \qquad .. \qquad .. \qquad (7)$$

and the component, in the free-stream direction, of the suction force due to the leading-edge singularity is (equation (140), Ref. 1):

$$S = 2\pi\rho\varkappa \int_0^{x_1} P^2 \, dx = 2\pi\rho\varkappa \int_0^{x_1} (A_1 P_1 + A_2 P_2 + \ldots + A_n P_n)^2 \, dx$$

$$= \sum (A_r^2 S_r) + \sum (A_r A_s S_{r,s}) \qquad (r = 1, 2, \ldots n; s = 2, 3, \ldots n; r < s), \quad .. \qquad (8)$$

where $S_r = 2\pi\rho\varkappa \int_0^{x_1} P_r^2 \, dx$ is the suction force for surface z_r, $S_{r,s} (\equiv S_{s,r}) = 2\pi\rho\varkappa \int_0^{x_1} (2P_r P_s) \, dx$ is the 'interference' suction force for surfaces z_r and z_s, $x = x_1$ at the wing tips, and $\varkappa^2 = 1 - (\tan \gamma / \tan \mu)^2$.

The total drag is

$$T = D - S = \sum (A_r^2 T_r) + \sum (A_r A_s T_{r,s}), \qquad .. \qquad .. \qquad .. \qquad .. \qquad .. \qquad (9)$$

where $T_r = D_r - S_r$, and $T_{r,s} = D_{r,s} - S_{r,s}$.

3

For surfaces z_r, z_s of the same given plan-form, it can be shown that D_r, S_r and $D_{r,s}$, $S_{r,s}$ are proportional to L_r^2 and $(L_r L_s)$ respectively. Hence, writing $D_r/L_r^2 = d_r$, $D_{r,s}/(L_r L_s) = d_{r,s}$, $S_r/L_r^2 = s_r$, $S_{r,s}/(L_r L_s) = s_{r,s}$, and $A_r L_r = a_r$, formulae (5), (6), (8) and (9) can be written (d_r, $d_{r,s}$, s_r, $s_{r,s}$ depend on $\varkappa$ and the types of surfaces z_r, z_s):

$$L = \sum_{r=1}^{n} a_r , \qquad \qquad \qquad \qquad \qquad \qquad \qquad (10)$$

$$D = \sum (a_r^2 d_r) + \sum (a_r a_s d_{r,s}) , \qquad \qquad \qquad \qquad (11)$$

$$S = \sum (a_r^2 s_r) + \sum (a_r a_s s_{r,s}) , \qquad \qquad \qquad \qquad (12)$$

$$T = \sum (a_r^2 t_r) + \sum (a_r a_s t_{r,s}) , \qquad \qquad \qquad \qquad (13)$$

where $t_r = d_r - s_r$, $t_{r,s} = d_{r,s} - s_{r,s}$. Hence

$$t \equiv T/L^2 = \left[\sum (a_r^2 t_r) + \sum (a_r a_s t_{r,s}) \right] \bigg/ \left[\sum a_r \right]^2 \qquad \qquad (14)$$

$$\equiv d - s ,$$

where $d = D/L^2$, $s = S/L^2$, the summation in each case being for $r = 1, 2, \ldots n$; $s = 2, 3, \ldots n$; $r < s$.

For minimum d,

$$\frac{1}{D} \frac{\partial D}{\partial a_r} - \frac{2}{L} \frac{\partial L}{\partial a_r} = 0 , \text{ for } r = 1, 2, \ldots n , \qquad \qquad \qquad (15a)$$

and for minimum t,

$$\frac{1}{T} \frac{\partial T}{\partial a_r} - \frac{2}{L} \frac{\partial L}{\partial a_r} = 0 , \text{ for } r = 1, 2, \ldots n . \qquad \qquad \qquad (15b)$$

The n equations (15a) or (15b) determine the coefficients a_1, a_2, $\ldots a_n$.

Formulae giving the values of a_r and minimum d ($\equiv d_{\text{opt}}$) are given in equations (16) to (26). For minimum t ($\equiv t_{\text{opt}}$), d_r and $d_{r,s}$ are replaced by t_r and $t_{r,s}$ respectively, and d_{opt} by t_{opt} in these formulae. Combining two surfaces given by $r = 1$, 2, it can be shown that

$$\frac{a_1}{2d_2 - d_{1,2}} = \frac{a_2}{2d_1 - d_{1,2}} = \frac{2L(d)_{\text{opt}}}{4d_1 d_2 - (d_{1,2})^2} = \frac{L}{2(d_1 + d_2 - d_{1,2})} . \qquad \qquad (16)$$

Hence the optimum d is given by

$$d_{\text{opt}} = \frac{4d_1 d_2 - d_{1,2}^2}{4(d_1 + d_2 - d_{1,2})} , \qquad \qquad \qquad \qquad \qquad \qquad (17)$$

$$\frac{\Delta d}{d_1} \equiv \frac{d_1 - d_{\text{opt}}}{d_1} = \frac{(2d_1 - d_{1,2})^2}{4d_1(d_1 + d_2 - d_{1,2})} . \qquad \qquad \qquad \qquad (18)$$

For the combination of three surfaces given by $r = 1$, 2, 3:

$$\frac{a_1}{\Delta_1} = \frac{a_2}{\Delta_2} = \frac{a_3}{\Delta_3} = \frac{2L(d)_{\text{opt}}}{\Delta_{\text{III}}} = \frac{L}{\Delta_1 + \Delta_2 + \Delta_3} , \qquad \qquad \qquad (19)$$

where

$$\Delta_{\text{III}} = \begin{vmatrix} 2d_1 & d_{1,2} & d_{1,3} \\ d_{2,1} & 2d_2 & d_{2,3} \\ d_{3,1} & d_{3,2} & 2d_3 \end{vmatrix} \qquad \qquad \qquad \qquad \qquad (20)$$

and

$$\left. \begin{aligned} \Delta_1 &= d_{2,3} d_{1,2} + d_{2,3} d_{1,3} + 4d_2 d_3 - 2d_3 d_{1,2} - 2d_2 d_{1,3} - d_{2,3}^2 \\ \Delta_2 &= d_{3,1} d_{2,3} + d_{3,1} d_{2,1} + 4d_3 d_1 - 2d_1 d_{2,3} - 2d_3 d_{2,1} - d_{3,1}^2 \\ \Delta_3 &= d_{1,2} d_{3,1} + d_{1,2} d_{3,2} + 4d_1 d_2 - 2d_2 d_{3,1} - 2d_1 d_{3,2} - d_{1,2}^2 \end{aligned} \right\} \qquad \qquad (21)$$

4

Hence

$$(d)_{\text{opt}} = \tfrac{1}{2}\Delta_{\text{III}}/(\Delta_1 + \Delta_2 + \Delta_3)$$

$$= (4d_1d_2d_3 - d_1d_{2,3}^2 - d_2d_{3,1}^2 - d_3d_{1,2}^2 + d_{1,2}d_{2,3}d_{3,1})/$$

$$\{4(d_1d_2 + d_2d_3 + d_3d_1) - (d_{1,2}^2 + d_{2,3}^2 + d_{3,1}^2) - 4(d_1d_{2,3} + d_2d_{3,1} + d_3d_{1,2})$$

$$+ 2(d_{1,2}d_{2,3} + d_{2,3}d_{3,1} + d_{3,1}d_{1,2})\} \, . \quad .. \qquad .. \qquad .. \qquad .. \qquad .. \qquad .. \qquad (22)$$

For the combination of four surfaces given by $r = 1, 2, 3, 4$:

$$\frac{a_1}{\Delta_1} = \frac{a_2}{\Delta_2} = \frac{a_3}{\Delta_3} = \frac{a_4}{\Delta_4} = \frac{2L(d)_{\text{opt}}}{\Delta_{\text{IV}}} = \frac{L}{\Delta_1 + \Delta_2 + \Delta_3 + \Delta_4}, \, .. \qquad .. \qquad .. \qquad .. \qquad (23)$$

where

$$\Delta_{\text{IV}} = \begin{vmatrix} 2d_1 & d_{1,2} & d_{1,3} & d_{1,4} \\ d_{2,1} & 2d_2 & d_{2,3} & d_{2,4} \\ d_{3,1} & d_{3,2} & 2d_3 & d_{3,4} \\ d_{4,1} & d_{4,2} & d_{4,3} & 2d_4 \end{vmatrix} \qquad .. \qquad .. \qquad .. \qquad .. \qquad .. \qquad .. \qquad (24)$$

and

$$\Delta_1 = 8d_2d_3d_4 + 2d_{2,3}d_{3,4}d_{4,2}$$

$$+ 2\{d_2d_{3,4}(d_{1,3} + d_{1,4}) + d_3d_{2,4}(d_{1,2} + d_{1,4}) + d_4d_{2,3}(d_{1,2} + d_{1,3})\}$$

$$- d_{1,2}d_{3,4}(d_{2,3} + d_{2,4} - d_{3,4}) - d_{1,3}d_{2,4}(d_{3,4} + d_{3,2} - d_{4,2})$$

$$- d_{1,4}d_{2,3}(d_{4,2} + d_{4,3} - d_{2,3}) - 2(d_2d_{3,4}^2 + d_3d_{4,2}^2 + d_4d_{2,3}^2)$$

$$- 4(d_2d_3d_{1,4} + d_3d_4d_{1,2} + d_2d_4d_{1,3}) \, , \quad .. \qquad .. \qquad .. \qquad .. \qquad .. \qquad .. \qquad (25)$$

with corresponding formulae for Δ_2, Δ_3, Δ_4. Hence

$$(d)_{\text{opt}} = \tfrac{1}{2}\Delta_{\text{IV}}/(\Delta_1 + \Delta_2 + \Delta_3 + \Delta_4)$$

$$= \left\{ 8d_1d_2d_3d_4 + 2\sum_4 (d_1d_{2,3}d_{3,4}d_{2,4}) + \tfrac{1}{2}\sum_3 (d_{1,2}^2 d_{3,4}^2) \right.$$

$$\left. - 2\sum_6 (d_1d_2d_{3,4}^2) - \sum_3 (d_{1,2}d_{2,3}d_{3,4}d_{4,1}) \right\} / \left[8\sum_4 (d_2d_3d_4) \right.$$

$$+ 2\sum_4 (d_{2,3}d_{3,4}d_{4,2}) + 4\sum_4 \{d_1(d_{2,3}d_{3,4} + d_{3,4}d_{4,2} + d_{4,2}d_{2,3})\}$$

$$- 2\sum_3 \{(d_{1,2} + d_{3,4})(d_{1,3}d_{2,4} + d_{1,4}d_{2,3} - d_{1,2}d_{3,4})\}$$

$$\left. - 2\sum_4 \{d_1(d_{2,3}^2 + d_{3,4}^2 + d_{4,2}^2)\} - 8\sum_6 (d_1d_2d_{3,4}) \right]$$

(The number under the summation sign denotes the number of terms in the sum.)

For the combination of n surfaces given by $r = 1, 2, \ldots n$:

$$\frac{a_r}{\Delta_r} = \frac{2L(d)_{\text{opt}}}{\Delta_N} = \frac{1}{\displaystyle\sum_{r=1}^{n} \Delta_r}, \qquad .. \qquad .. \qquad .. \qquad .. \qquad .. \qquad .. \qquad .. \qquad .. \qquad (26)$$

where Δ_N is of the same form as Δ_{III}, Δ_{IV}, but with N rows and columns, and Δ_r $(r = 1, 2, \ldots n)$ is equal to Δ_N with each term in the rth column replaced by 1.

The formulae given above are quite general, and do not depend on the type of camber and twist used, suffixes $_{1, 2, 3, 4, \ldots n}$ referring to arbitrary surfaces. The formulae giving minimum d can also be used for thin wings with supersonic leading edges, or for symmetrical wings at zero incidence.

5

For orthogonal loadings, that is, loadings for which $d_{r,s} = 0$ for all values of r and s, the above formulae for d_{opt} reduce to those obtained by Graham[9]. For example, the formula for the combination of orthogonal loadings given by $r = 1, 2, 3, 4$ would reduce to:

$$\frac{1}{d_{\text{opt}}} = \frac{1}{d_1} + \frac{1}{d_2} + \frac{1}{d_3} + \frac{1}{d_4}, \qquad \cdots \quad \cdots \quad \cdots \quad \cdots \quad \cdots \quad (26a)$$

but to form these (unknown) orthogonal loadings, it would be necessary to combine known camber and twist solutions, given by $r = 1, a, b, c$ (say), and d_2, d_3, d_4 would be functions of the ten quantities $d_r, d_{r,s}$ $(r = 1, a, b, c; s = a, b, c; r < s)$, so that the result $(26a)$ could be expressed in the same form as (24) with a, b, c in place of $2, 3, 4$.

2.2. *Formulae for the Calculation of the Minimum Drag for Given Wing Combinations when the Centre of Pressure is Fixed (at Design C_L).*—The distance of the centre of pressure of the wing from the apex is given by

$$\frac{\bar{x}}{c} = \frac{\int p x \, dS}{c \int p \, dS} = \frac{\bar{M}}{cL} \equiv \nu, \qquad \cdots \quad \cdots \quad \cdots \quad \cdots \quad \cdots \quad (27)$$

where $\bar{M}$ is the pitching moment about the apex, and c is the length of the root chord.

For the surface given by equation (2),

$$\bar{M} = \sum_{r=1}^{n} (A_r M_r) = \sum_{r=1}^{n} \left(a_r \frac{M_r}{L_r}\right) = c \sum_{r=1}^{n} (a_r \nu_r), \qquad \cdots \quad \cdots \quad (28)$$

where $M_r = \int p_r x \, dS$ is the pitching moment about the apex of the surface given by z_r, and $M_r / c L_r = \nu_r$.

If ν is a given constant, the conditions for minimum d are the n equations $(15a)$ and the additional condition

$$\frac{1}{c} (d\bar{M}) = \nu(dL). \qquad \cdots \quad \cdots \quad \cdots \quad \cdots \quad \cdots \quad \cdots \quad \cdots \quad (29)$$

Hence it can be shown that

$$\frac{a_r}{\Delta_r} = \frac{2L(d)_{\text{opt}}}{\Delta_{N-1}} = \frac{(\nu_n - \nu)L}{\sum\limits_{r=1}^{n-1} (\nu_n - \nu_r)\Delta_r} = \frac{-(\nu_n - \nu)a_n}{\sum\limits_{r=1}^{n-1} (\nu_r - \nu)\Delta_r} \qquad r = 1, 2, \ldots (n-1), \quad \cdots \quad (30)$$

where, in this case,

$$\Delta_{N-1} = \begin{vmatrix} a_{1,1} & a_{1,2} \ldots \ldots a_{1,r} \ldots \ldots a_{1,n-1} \\ a_{2,1} & a_{2,2} \ldots \ldots \ldots \ldots \ldots a_{2,n-1} \\ \ldots \ldots \ldots \ldots \ldots \ldots \ldots \ldots \ldots \\ a_{n-1,1} & a_{n-1,2} \ldots \ldots \ldots a_{n-1,n-1} \end{vmatrix}, \qquad \cdots \quad \cdots \quad \cdots \quad \cdots \quad \cdots \quad \cdots \quad \cdots \quad (31)$$

Δ_r is here equal to Δ_{N-1} with each term of the rth column replaced by 1, and

$$a_{r,r} = 2\left[d_r(\nu_n - \nu)^2 - d_{n,r}(\nu_n - \nu)(\nu_r - \nu) + d_n(\nu_r - \nu)^2\right] \Big/ \left[(\nu_n - \nu)(\nu_n - \nu_r)\right] \qquad (32)$$

$$(\nu_n - \nu_r)a_{r,s} = \left[d_{r,s}(\nu_n - \nu)^2 - d_{n,s}(\nu_r - \nu)(\nu_n - \nu) - d_{n,r}(\nu_s - \nu)(\nu_n - \nu)\right.$$

$$\left. + 2d_n(\nu_r - \nu)(\nu_s - \nu)\right] \Big/ (\nu_n - \nu)$$

$$= (\nu_n - \nu_s)a_{s,r}, \qquad \cdots \quad \cdots \quad \cdots \quad \cdots \quad \cdots \quad \cdots \quad \cdots \quad \cdots \quad \cdots \quad (33)$$

remembering that $d_{s,r} = d_{r,s}$.

For numerical calculations, a limiting process is avoided, if suffix n is chosen to denote a surface for which $v_n \neq v$.

If suction forces are included, d_r, $d_{r,s}$, d_{opt} are replaced by t_r, $t_{r,s}$, t_{opt} respectively in formulae (30) to (33).

2.3. *Variation of C_D with C_L (or with Incidence) for a Given Wing.*—The shape of the final wing is given by an equation of the form

$$z = \sum_{r=1}^{n} (A_r z_r) = C_{L0} f(x, k^2 y^2) \, ,$$

where $k = \cot \gamma$, C_{L0} is the design lift coefficient, and $f(x, k^2 y^2)$ is a rational algebraic function of x and $k^2 y^2$, whose coefficients are functions of $\varkappa = \{1 - (\tan \gamma / \tan \mu)^2\}^{1/2}$. The wing is designed to give optimum results with respect to the drag for given plan-form, given design lift and given Mach number, though the optimum value of d, or t, and the percentage decrease when compared with the corresponding flat wing, depend only on the value of $\varkappa$ (for the triangular wing). The addition of a small arbitrary function of y to the equation of the wing does not alter the pressure distribution or local surface slope, according to the linear theory used in this report.

The drag on a given wing can be expressed in terms of the design lift coefficient, C_{L0}, and the total lift coefficient, C_L; or in terms of the drag at any lift $\bar{C}_{L0}$ and the additional incidence, α. A formula for C_D in terms of C_{L0} and ΔC_L, the additional lift, is given in Ref. 1, for the types of wings considered in that paper. The general formula, using the notation of the previous paragraphs, for the drag coefficient can be written in the form:

$$C_D = \frac{kE(\varkappa)}{2\pi} \left[t_0 C_{L0}^2 + t_{1,0} C_{L0} \cdot \Delta C_L + t_1 (\Delta C_L)^2 \right] \quad \cdots \quad \cdots \quad \cdots \quad (34)$$

$$= \frac{kE(\varkappa)}{2\pi} \left[t_1 C_L^2 + (t_{1,0} - 2t_1) C_L C_{L0} + (t_1 + t_0 - t_{1,0}) C_{L0}^2 \right] \quad \cdots \quad \cdots \quad (35)$$

where

$$t_{1,0} = \frac{1}{L} \left[2a_1 t_1 + a_2 t_{1,2} + a_3 t_{1,3} + \ldots + a_n t_{1,n} \right], \quad \cdots \quad \cdots \quad \cdots \quad \cdots \quad (36)$$

and t_0 is written for t_{opt}.

$$\frac{kE(\varkappa)}{2\pi} t_0 C_{L0}^2 = C_{D0} , \qquad \text{the drag coefficient at design lift } C_{L0};$$

$$\frac{kE(\varkappa)}{2\pi} t_{1,0} C_{L0} \Delta C_L = C_{D1,0} , \qquad \begin{array}{l}\text{the 'interference' drag coefficient of the given wing} \\ \text{at lift } C_{L0}, \text{ and the flat wing of the same plan-form} \\ \text{at lift } \Delta C_L;\end{array} \quad (37)$$

$$\frac{kE(\varkappa)}{2\pi} t_1 (\Delta C_L)^2 = \Delta C_{D1} , \qquad \text{the drag coefficient for the flat wing at lift } \Delta C_L$$

(For a given wing, and design lift coefficient C_{L0}, the coefficients of ΔC_L and $(\Delta C_L)^2$ in (34), or of C_L and C_L^2 in (35) depend only on the plan-form and Mach number.)

When the suction forces are ignored, t_0, $t_{1,0}$, t_1 are replaced by d_0, $d_{1,0}$, d_1 respectively in formulae (34) to (37).

Formula (34) can also be written in the form

$$C_D = \bar{C}_{D0} + \bar{C}_1 \alpha + \bar{C}_2 \alpha^2 , \quad \cdots \quad \cdots \quad \cdots \quad \cdots \quad \cdots \quad \cdots \quad \cdots \quad (38)$$

where $\bar{C}_{D0}$ is the drag coefficient at any arbitrary lift $\bar{C}_{L0}$, α is the additional incidence, and

$$\bar{C}_1 = \bar{C}_{L0} + \frac{4}{kE(\varkappa)} \int \frac{x \alpha_0}{(x^2 - k^2 y^2)^{1/2}} dS - \frac{8\pi \varkappa}{V k E(\varkappa)} \int_0^{x_1} \left(\frac{x}{2}\right)^{1/2} P_0 \, dx \quad \cdots \quad (39)$$

$$\bar{C}_2 = \frac{2\pi}{kE(\varkappa)} \left(1 - \frac{\varkappa}{2E(\varkappa)}\right) , \quad \cdots \quad \cdots \quad \cdots \quad \cdots \quad \cdots \quad \cdots \quad \cdots \quad (40)$$

α_0, P_0 being the local surface slope and strength of leading edge singularity respectively of the wing at lift $\bar{C}_{L0}$.

If $\bar{C}_{L0}$ is taken as zero, formula (38) gives the drag coefficient at any small incidence, α (measured from the position of zero lift), $\bar{C}_{D0}$ being the drag coefficient of the cambered and twisted wing at zero lift (in this case the equation of the surface is of the form

$$z = C_{L0} f(x, k^2 y^2) + \alpha_0 x \, ,$$

where $2\pi/\{kE(\varkappa)\} \cdot \alpha_0 = C_{L0}$, and C_{L0} is the design lift coefficient).

Formula (38) also gives the total drag of a wing with thickness, if the wave drag due to thickness is included in the term $\bar{C}_{D0}$.

For a triangular wing of zero thickness, for small $A\sqrt{(M^2 - 1)}$, where A is the aspect ratio, $\tan \gamma / \tan \mu \to 0$ and $\varkappa \to 1$, and it can be shown that

$$\bar{C}_1 = \bar{C}_{L0} + 0\left\{\left(\frac{\tan \gamma}{\tan \mu}\right)^3\right\},$$

$$\bar{C}_2 \to \frac{\pi}{kE(\varkappa)} = \frac{1}{2}\frac{\partial C_L}{\partial \alpha},$$

since

$$C_L = \bar{C}_{L0} + \frac{2\pi}{kE(\varkappa)}\,\alpha \, . \qquad \qquad \qquad \qquad \qquad \qquad \qquad (41)$$

Therefore, in this case,

$$C_D = \bar{C}_{D0} + \left[\bar{C}_{L0} + 0\left\{\left(\frac{\tan \gamma}{\tan \mu}\right)^3\right\}\right]\alpha + \frac{1}{2}\frac{\partial C_L}{\partial \alpha}\alpha^2$$

$$= \bar{C}_{D0} + \frac{1}{2}\frac{\partial C_L}{\partial \alpha}\alpha^2 \, , \text{ approximately, if } \bar{C}_{L0} = 0 \, . \qquad \qquad \qquad (42)$$

Ward[36] gives the formula $C_D = \bar{C}_{D0} + \frac{1}{2}(\partial C_L/\partial \alpha)\alpha^2 + 0(t^4 \log^2 t)$ for slender bodies of thickness t, at incidence α. It has been verified that the terms $0\{(\tan \gamma / \tan \mu)^3 \alpha\}$ $(= 0\,(t^3 \alpha)$ in this case), would come from the integral neglected by Ward.

When $\varkappa \to 1$, $t_{1,r} = 1$ for all surfaces z_r, and $t_1 = \frac{1}{2}$ (*see* Appendix VII), and therefore

$$t_{1,0} = \frac{\sum\limits_{r=1}^{n} (2a_r t_1)}{L} = 2t_1 \, .$$

Hence formula (35) becomes

$$C_D = \frac{kE(\varkappa)}{2\pi}\left[t_1 C_L^2 + (t_1 + t_0 - t_{1,0})C_{L0}^2\right] \, . \qquad \qquad \qquad \qquad \qquad (43)$$

For cambered wings (*i.e.*, wings for which the local surface slope is a function of x only), $t_1 + t_0 - t_{1,0} = 0$ when $\varkappa \to 1$ (*see* Appendix VII), and $C_D = C_{D1}$, i.e., no reduction is possible in the total lift-dependent drag.

This result for $\varkappa \to 1$ agrees with the result recently obtained by Mangler[43], using slender-wing theory.

3. *The Load Distributions on the Basic Cambered and Twisted Surfaces.*—In Ref. 1, the linearised supersonic-flow equation is solved by the method of hyperboloido-conal co-ordinates[3], the velocity potential being obtained in terms of two kinds of Lamé functions, which are such that solutions can be applied to the required swept-back plan-form and the boundary conditions on the Mach cone of the apex are satisfied. The shapes of the corresponding cambered and twisted surfaces are found, it being assumed that the surfaces all lie close to the plane $z = 0$.

For our present purpose, it is convenient to separate the basic surfaces given by equations of the form $z = -\delta x^{n-2s} y^{2s}$ $(n > 2s)$, and to find their corresponding pressure distributions.

8

In Ref. 2, formulae for the velocity potentials of the surfaces up to $n = 4$ are given, and also the shapes of surfaces with velocity potentials proportional to $x^4 X$, $k^2 y^2 x^2 X$, $k^4 y^4 X$, where $\cot^{-1} k = \gamma$, the apex semi-angle, and $X = (x^2 - k^2 y^2)^{1/2}$. Hence it can be shown that the velocity potentials for the surfaces given by $n = 5$ are as follows:

TABLE 1

Surface	Velocity potential, ϕ, on the surface
$z = -\dfrac{\delta}{c^4} x^5$	$\dfrac{V \delta F_3}{c^4 k E(\varkappa)} \left[f_{14} x^4 + f_{15} k^2 y^2 x^2 + f_{16} k^4 y^4 \right] X$
$z = -\dfrac{\delta}{c^4} k^2 y^2 x^3$	$\dfrac{- V \delta F_3}{c^4 k E(\varkappa)} \left[f_{17} x^4 + f_{18} k^2 y^2 x^2 + f_{19} k^4 y^4 \right] X$
$z = -\dfrac{\delta}{c^4} k^4 y^4 x$	$\dfrac{V \delta F_3}{c^4 k E(\varkappa)} \left[f_{20} x^4 + f_{21} k^2 y^2 x^2 + f_{22} k^4 y^4 \right] X$

where V is the free-stream velocity, $\varkappa^2 = 1 - \tan^2 \gamma / \tan^2 \mu$, μ is the Mach angle, $E(\varkappa)$ is the complete elliptic integral of the second kind of modulus $\varkappa$, and $f_{14}, f_{15}, \ldots f_{22}$, F_3 are functions of $\varkappa$ which are calculated in Appendix II of this report. The complete list of velocity potentials for $n = 1$ to 5 is given in Appendix IV, from which the pressure distributions can be calculated.

Henceforth all forces are normalised by dividing by $(\pi \rho V^2 c^2)/(k^2 E(\varkappa))$.

Formulae for the local surface slope, α_r, and the load per unit area, p_r, on the basic cambered and twisted surfaces, z_r, are given in Table 2 below:

TABLE 2

r	z_r	$\alpha_r = -\dfrac{\partial z_r}{\partial x}$	$\left(\dfrac{\pi c^2}{2k}\right) p_r$
1	$- \delta x$	δ	$\dfrac{\delta x}{X}$
2	$-\dfrac{\delta}{c} x^2$	$\dfrac{2\delta}{c} x$	$\dfrac{\delta}{c f_1} \left(\dfrac{x^2}{X} + X \right)$
3	$-\dfrac{\delta}{c^2} x^3$	$\dfrac{3\delta}{c^2} x^2$	$\dfrac{3\delta}{c^2} F_1 \left[f_5 \left(\dfrac{x^3}{X} + 2xX \right) - f_7 (3xX) \right]$
4	$-\dfrac{\delta}{c^3} x^4$	$\dfrac{4\delta}{c^3} x^3$	$\dfrac{4\delta}{c^3} F_2 \left[f_{11} \left(\dfrac{x^4}{X} + 3x^2 X \right) - f_{13} (4x^2 - k^2 y^2) X \right]$
5	$-\dfrac{\delta}{c^2} k^2 y^2 x$	$\dfrac{\delta}{c^2} k^2 y^2$	$\dfrac{3\delta}{c^2} F_1 \left[f_4 \left(\dfrac{x^3}{X} + 2xX \right) - f_6 (xX) \right]$
6	$-\dfrac{\delta}{c^3} k^2 y^2 x^2$	$\dfrac{2\delta}{c^3} k^2 y^2 x$	$\dfrac{2\delta}{c^3} F_2 \left[f_{10} \left(\dfrac{x^4}{X} + 3x^2 X \right) - f_{12} (4x^2 - k^2 y^2) X \right]$
7	$-\dfrac{\delta}{c^2} (f_4 x^3 - f_5 k^2 y^2 x)$ $\equiv f_4 z_3 - f_5 z_5$	$\dfrac{\delta}{c^2} (3 f_4 x^2 - \dot{f_5} k^2 y^2)$	$\dfrac{\delta}{c^2} (3xX)$
8	$-\dfrac{\delta}{c^4} x^5$	$\dfrac{5\delta}{c^4} x^4$	$\dfrac{\delta}{c^4} F_3 \left[f_{14} \left(\dfrac{x^5}{X} + 4x^3 X \right) + f_{15} k^2 y^2 \left(\dfrac{x^3}{X} + 2xX \right) + f_{16} k^4 y^4 \left(\dfrac{x}{X} \right) \right]$
9	$-\dfrac{\delta}{c^4} k^2 y^2 x^3$	$\dfrac{3\delta}{c^4} k^2 y^2 x^2$	$-\dfrac{\delta}{c^4} F_3 \left[f_{17} \left(\dfrac{x^5}{X} + 4x^3 X \right) + f_{18} k^2 y^2 \left(\dfrac{x^3}{X} + 2xX \right) + f_{19} k^4 y^4 \left(\dfrac{x}{X} \right) \right]$
10	$-\dfrac{\delta}{c^4} k^4 y^4 x$	$\dfrac{\delta}{c^4} k^4 y^4$	$\dfrac{\delta}{c^4} F_3 \left[f_{20} \left(\dfrac{x^5}{X} + 4x^3 X \right) + f_{21} k^2 y^2 \left(\dfrac{x^3}{X} + 2xX \right) + f_{22} k^4 y^4 \left(\dfrac{x}{X} \right) \right]$

The surface z_7, which is a combination of surfaces z_3, z_5, is the simplest surface of thsi type with no pressure singularities on the leading edges. Other such surfaces can be found by the combination of surfaces z_4, z_6 or of surfaces z_8, z_9, z_{10}.

The functions $f_1, f_4, \ldots f_{13}, F_1, F_2$ are functions of $\varkappa$, which are given in Appendix I. Some numerical values are given in Appendix III.

4. *The Lift, Drag and Interference Drags of the Basic Cambered and Twisted Surfaces.*—As stated in Section 2, for a surface given by z_r:

the lift is

$$L_r = \int p_r \, dS; \quad \cdots \quad \cdots \quad \cdots \quad \cdots \quad \cdots \quad \cdots \quad \cdots \tag{44}$$

the pressure integral is

$$D_r = \int p_r \alpha_r \, dS; \quad \cdots \quad \cdots \quad \cdots \quad \cdots \quad \cdots \quad \cdots \quad \cdots \tag{45}$$

and the suction force is

$$S_r = 2\pi \rho \varkappa \int_0^{x_1} P_r{}^2 \, dx. \quad \cdots \quad \cdots \quad \cdots \quad \cdots \quad \cdots \quad \cdots \tag{46}$$

The interference pressure integral of two surfaces given by z_r, z_s is

$$D_{r,s} = D_{s,r} = \int (p_r \alpha_s + p_s \alpha_r) \, dS; \quad \cdots \quad \cdots \quad \cdots \quad \cdots \tag{47}$$

and the 'interference' suction force is

$$S_{r,s} = S_{s,r} = 2\pi \rho \varkappa \int_0^{x_1} (2P_r P_s) \, dx. \quad \cdots \quad \cdots \quad \cdots \quad \cdots \tag{48}$$

Using the load distributions given in Section 3, it can be shown that the integrals in formulae (44) to (48) are the sum of integrals of the form

$$\int_0^{c/k} \int_{ky}^{c} \frac{k^{2m} y^{2m} x^n}{(x^2 - k^2 y^2)^{1/2}} \, dx \, dy \equiv \frac{c^{2m+n+1}}{k} T_{2m,n} \quad \text{for the triangular wing,}$$

and

$$\int_0^{c/(k-h)} \int_{ky}^{c+hy} \frac{k^{2m} y^{2m} x^n}{(x^2 - k^2 y^2)^{1/2}} \, dx \, dy \equiv I_{2m,n} \quad \text{for the swept-back wing,}$$

with straight supersonic or sonic trailing edges, where m, n are positive integers, and $\cot^{-1} h$ is the apex semi-angle of the trailing edge.

In Appendix V, it is shown that, for all values of m, n,

$$T_{2m,n} = \frac{\pi (2m)!}{2^{2m+1}(2m+n+1)(m!)^2}, \quad \cdots \quad \cdots \quad \cdots \quad \cdots \tag{49}$$

and a Table of numerical values is given.

In Appendix VI, it is shown that $I_{2m,n}{}^*$ is the sum of terms of the form

$$\int_0^{c/(k-h)} \frac{(c + hy)^M k^{2m} y^{2m}}{Z} \, dy \equiv J_{2m,n}, \quad \cdots \quad \cdots \quad \cdots \quad \cdots \tag{50}$$

and terms of the form

$$\int_0^{c/(k-h)} (ky)^{2N} \cosh^{-1} \frac{c + hy}{ky} \, dy \equiv H_{2N} = \frac{c}{2N+1} J_{2N,0}, \quad \cdots \quad \cdots \tag{51}$$

where m, M, N are integers, and $Z = \{(c + hy)^2 - k^2 y^2\}^{1/2}$. The integrated formulae for $J_{2m,M}(2m + M = 1, 2, \ldots 10)$, as functions of λ are also given, where $\lambda^2 = 1 - h^2/k^2$.

---

* Recurrence formulae for $I_{N,n}$, $J_{N,n}$, which have been programmed for an electronic computor, and some tables of values will be given in a later paper.

Formulae for L_r, D_r, S_r, $D_{r,s}$, $S_{r,s}$ for triangular wings, and for swept-back wings, are given in Tables 3 to 12 (at the end of the report).

Formulae in terms of $I_{2m,n}$ will be given in a later paper.

Some general formulae, and relations between lift and drag (which are useful for checking), are given in Appendix VII.

5. *The Pitching Moment and Position of the Centre of Pressure.*—The pitching moment, about an axis through the apex, of the wing given by $z = \sum_{r=1}^{n} (A_r z_r)$ is

$$\bar{M} = \sum_{r=1}^{n} (A_r M_r) , \qquad \qquad \qquad \qquad \qquad \qquad (28)$$

where M_r is the pitching moment for the surface given by z_r. The distance of the centre of pressure of the wing from the apex is given by

$$\frac{\bar{x}}{c} = \frac{\bar{M}}{cL} = \nu . \qquad \qquad \qquad \qquad \qquad \qquad (27)$$

The centre of pressure, G, of the flat triangular wing is at two-thirds the root chord from the apex. The pitching-moment coefficient, C_{M0}, about this chordwise position is given by

$$\frac{C_{M0}}{C_L} = 2 \left(\frac{2}{3} - \frac{\bar{M}}{cL} \right) = 2 \left(\frac{2}{3} - \nu \right) . \qquad \qquad \qquad (52)$$

The distance, $\bar{h}$, of the centre of pressure upstream of G is given by

$$\frac{\bar{h}}{c} = \frac{1}{2} \frac{C_{M0}}{C_L} = \frac{2}{3} - \frac{\bar{M}}{cL} . \qquad \qquad \qquad \qquad (53)$$

C_{M0} is unaltered by a change in C_L (and hence it is the pitching-moment coefficient at zero lift), but the centre of pressure moves towards or away from G for an increase or decrease respectively in C_L. It is shown in Section 2.2 that the centre of pressure can be fixed, for design lift, in any position. If fixed at G, it would (theoretically) remain fixed for all C_L. The same remarks apply to the swept-back wing if C_{M0} is taken about G, the centre of pressure of the corresponding flat wing.

Formulae for M_r for the triangular wing and for the swept-back wing, are given in Tables 13 and 14. General formulae are given in Appendix VII.

6. *Numerical Results.*—Some numerical results are given for triangular wings, and comparison is made with a few results for swept-back wings. Further results for swept-back wings will be published later.

It is shown in Section 2 that the minimum values of drag/(lift)^2, (d_{opt} or t_{opt}), and the corresponding coefficients a_r/L, for the combination of given cambered and twisted surfaces, are functions of the drag/(lift)^2 of the separate surfaces, ($\bar{d}_r$ or t_r), and the corresponding interference quantities, ($d_{r,s}$ or $t_{r,s}$). All forces were normalised by dividing by $\pi \rho V^2 c^2 / (k^2 E(\varkappa))$, but the percentage decrease in each case, when compared with the corresponding flat wing, with or without suction, is independent of the normalising factor.

11

The equation of the final surface is

$$z = \sum (A_r z_r) + F(y) = \frac{kE(\varkappa)}{2\pi} C_{L0} \sum \left\{ \frac{(a_r/L)}{L_r} z_r \right\} + F(y) , \qquad .. \qquad .. \qquad .. \quad (54)$$

where C_{L0} is the design lift coefficient, based on the area of the plan-form, and $F(y)$ is a small arbitrary function of y.

Numerical values of d_r, $d_{r,s}$; t_r, $t_{r,s}$, for $\tan \gamma / \tan \mu = 1$, $0\cdot7338$, $0\cdot7$, $0\cdot3577$, $0\cdot1184$, 0 are given in Appendix X, where the equations of the surfaces z_r $(r = 1, 2, \ldots 10)$ are also given.

In Table 15, which is given below, the maximum decrease in drag/(lift)^2, with or without suction, for different combinations of the basic surfaces, is expressed as a percentage of the corresponding quantity for the flat wing (*i.e.*, with or without suction respectively). Two examples of wings with centre of pressure fixed are given. It is found that twist (local surface slope a function of y only) is, on the whole, more effective in reducing drag for given lift for the larger values of $\tan \gamma / \tan \mu$, and that camber (local surface slope a function of x only), is more effective for the smaller values, though, in general, the best results are obtained by a combination of camber and twist.

In the limiting cases when:

    (i) <u>$\tan \gamma / \tan \mu = 1$</u>, that is, for a wing with sonic leading edges, there is no drag reduction for any combination of camber only, but there is a reduction (of not more than about 10 per cent) by the use of twist only, or certain combinations of camber and twist.

    (ii) <u>$\tan \gamma / \tan \mu \to 0$</u>, that is, the effective aspect ratio $\sqrt{(M^2 - 1)}A$ tends to zero, no drag reduction is possible if suction forces are included, but a reduction, arbitrarily near to 50 per cent can be obtained by the use of camber only, or a combination of camber and twist, if suction forces are ignored; that is, the lowest drag of a cambered wing is equal to the drag of the uncambered wing with full suction (in this case, the theoretical suction force on the cambered wing vanishes, whether or not it is included in the optimising process).

The relation between the drag on the flat triangular wing with suction, and without suction, is given by:

$$t_1 \equiv d_1 - s_1 = \left\{ 1 - \frac{\varkappa}{2E(\varkappa)} \right\} d_1 . \quad .. \qquad .. \qquad .. \qquad .. \qquad .. \quad (55)$$

The ratio s_1/d_1 varies from $\frac{1}{2}$ to 0 as $\tan \gamma / \tan \mu$ increases from 0 to 1.

Fig. 5b shows the estimated drag reductions due to camber and twist, with or without suction, and the theoretical drag reduction on the uncambered wing due to suction. In each case, the reduction is compared with the drag of the flat wing without suction.

Some of the results, the variation of C_D, C_{M0}, and the position of the centre of pressure are discussed after Table 15.

6.1. *Detailed Results.*—Some diagrams showing the maximum percentage drag reduction for triangular wings, with or without suction, for different surface combinations, are shown in Figs. 1 to 3.

Some of the best results for triangular wings shown in Table 15 are now discussed. The shapes of the wings are given, the variation of C_D, C_{M0}, and the position of the centre of pressure are shown. In the equation of the wing surface, all lengths are now measured in root-chord lengths, and a (small) function of y, which does not affect the load distribution and local surface slope, is added so that $z = 0$ on the leading edges. C_{M0} is the pitching-moment coefficient about the two-thirds chord position, G, and h is the distance of the centre of pressure from G, measured towards the apex.

12

TABLE 15

(The shapes of surfaces $r = 1, 2, \ldots 10$ are given in Table 3, and in Appendix IV.)

Optimum Results for Reduction of Drag on a Triangular Wing

$\Delta d \equiv d_1 - d$ (Suction omitted)				$\Delta t \equiv t_1 - t$ (Suction included)	

(1) tan γ/tan $\mu \to 0$ ('slender' wings)

	Surface combinations r	Optimum ($\Delta d/d_1$) (per cent)		Surface combinations r	Optimum ($\Delta t/t_1$) (per cent)
$n = 2$	1, 2	33·3			
$n = 3$	1, 3	37·5			
$n = 4$	1, 4	40·0	Camber (surface slope a function of x only)		
$n = 5$	1, 8	41·7			
$z_n = -\dfrac{\delta x^n}{c^{n-1}}$	1, n	$50n/(n+1)$ →50		1, n	0
$N = 1$	1, 5	0	Twist (surface slope a function of y only)	1, 5	0
$N = 2$	1, 6	2·7			
$N = 3$	1, 9	6·3			
$N = 11$	1, 11	12·0			
$Z_N = -\dfrac{\delta x^N k^2 y^2}{c^{N+1}}$	1, N	→25	Camber and twist	1, N	0
	1, 2, 3	41·7			
	1, n_1, n_2	→50		1, n_1, n_2	0
	1, N, n	→50			

(2) tan γ/tan $\mu = 0\cdot1184$

r	Optimum ($\Delta d/d_1$) (per cent)		r	Optimum ($\Delta t/t_1$) (per cent)
1, 2	27·8	Camber	1, 2	1·9
1, 3	29·4		1, 3	1·7
1, 4	29·4		1, 4	1·6
1, 5	0·3	Twist	1, 5	0·1
1, 6	0·6	Camber and twist	1, 6	0·2
1, 2, 3	29·6	Camber	1, 2, 3	2·0
			1, 2, 4	2·0
1, 2, 5	35·4		1, 2, 5	1·9
1, 3, 5	36·0			
1, 4, 5	35·0			
1, 2, 6	33·4	Camber and twist	1, 2, 6	1·9
1, 3, 6	35·0			
1, 4, 6	34·3			
1, 5, 6	32·8		1, 5, 6	1·2
1, 2, 5 (c.p. fixed at G)	20·6			

13

TABLE 15—*continued*

(3) $\tan \gamma / \tan \mu = 0\cdot2$

r	Optimum $(\Delta d/d_1)$ (per cent)	
1, 2	22·0	} Camber
1, 4	20·7	

(4) $\tan \gamma / \tan \mu = 0\cdot3577$

r	Optimum $(\Delta d/d_1)$ (per cent)		r	Optimum $(\Delta t/t_1)$ (per cent)
1, 2	12·1	}	1, 2	5·1
1, 3	10·7	} Camber	1, 3	4·2
1, 4	9·2	}	1, 4	3·6
1, 5	3·4	Twist	1, 5	1·2
1, 6	0·9	Camber and twist	1, 6	1·4
		Camber	1, 2, 3	6·1
			1, 2, 4	6·0
			1, 3, 4	5·5
1, 2, 5	21·7		1, 2, 5	5·2
1, 3, 5	19·7			
1, 2, 6	19·7			
1, 5, 6	21·6	} Camber and twist	1, 5, 6	2·1
1, 2, 5, 6	25·1		1, 2, 5, 6	5·3
1, 2, 3, 5	22·3		1, 2, 3, 6	6·3
1, 2, 5, 6 (c.p. fixed at G)	21·8			

(5) $\tan \gamma / \tan \mu = 0\cdot5$

r	Optimum $(\Delta d/d_1)$ (per cent)		r	Optimum $(\Delta t/t_1)$ (per cent)
1, 2	6·1	} Camber	1, 2	5·3
1, 4	4·1		1, 4	3·4
1, 5	4·9	Twist		

TABLE 15—*continued*

(6) $\tan \gamma / \tan \mu = 0 \cdot 7$

r	Optimum $(\Delta d / d_1)$ (per cent)			r	Optimum $(\Delta t / t_1)$ (per cent)
1, 2	1·7	} Camber		1, 2	3·9
1, 3	1·2			1, 3	2·9
1, 4	0·95			1, 4	2·4
1, 8	0·81			1, 8	1·9
1, 5	5·8	} Twist		1, 5	2·5
1, 10	5·1			1, 10	2·0
1, 6	3·4	} Camber and twist		1, 6	2·6
1, 9	2·2			1, 9	2·45
1, 2, 3	2·4	} Camber		1, 2, 3	5·5
1, 2, 4	2·3			1, 2, 4	5·4
1, 3, 4	2·0			1, 3, 4	6·7
1, 2, 5	10·9				
1, 3, 5	9·6			1, 3, 5	3·4
1, 4, 5	9·2			1, 4, 5	3·5
1, 2, 10	8·45				
1, 3, 10	8·1	} Camber and twist			
1, 2, 6	7·9			1, 2, 6	4·6
1, 3, 6	7·4			1, 3, 6	3·8
1, 4, 6	7·3			1, 4, 6	3·4
1, 5, 6	9·2			1, 5, 6	2·6
1, 5, 10	5·9	Twist			
1, 2, 5, 6	14·0	} Camber and twist			
1, 2, 5, 10	10·7				

(7) $\tan \gamma / \tan \mu = 0 \cdot 7338$

r	Optimum $(\Delta d / d_1)$ (per cent)			r	Optimum $(\Delta t / t_1)$ (per cent)
1, 2	1·3	} Camber		1, 2	3·6
1, 3	0·9			1, 3	2·7
1, 4	0·7			1, 4	2·2
1, 5	5·9	Twist		1, 5	2·6
1, 6	3·6	Camber and twist		1, 6	2·7
		Camber		1, 2, 3	4·9
				1, 2, 4	4·6
				1, 3, 4	3·9

TABLE 15—*continued*

(7) $\tan \gamma / \tan \mu = 0 \cdot 7338$—*continued*

r	Optimum $(\Delta d/d_1)$ (per cent)			r	Optimum $(\Delta t/t_1)$ (per cent)
1, 2, 5	9·4			1, 2, 5	4·6
1, 3, 5	9·0				
1, 2, 6	7·5	Camber and twist			
1, 3, 6	7·2				
1, 5, 6	13·1			1, 5, 6	2·7
1, 2, 5, 6	13·2			1, 2, 5, 6	4·8

(8) $\tan \gamma / \tan \mu = 1$. In this case $s_r = 0$, and thus $\Delta d/d_1 = \Delta t/t_1$

				r	Optimum $(\Delta t/t_1)$ (per cent)
$z_n = -\dfrac{\delta x^n}{c^{n-1}}$		Camber		1, n	0
				1, n_1, n_2	0
		Twist		1, 5	5·9
		Camber and twist		1, 6	4·1
				1, 5, 6	8·1

Examples 1: $\tan \gamma / \tan \mu = 0 \cdot 7338$.

(*a*) The surfaces given by $r = 1, 5, 6$ are combined to give optimum d. The percentage decrease in $d \ (= D/L^2)$, when compared with the corresponding flat wing (with suction omitted) is given by:

$$\left(\frac{\Delta d}{d_1}\right)_{\text{optimum}} = 13 \cdot 1 \text{ per cent.}$$

If full suction is realised, the corresponding $\Delta t/t_1 = -3 \cdot 0$ per cent.

If only half suction is realised, the corresponding $(\Delta t/t_1)_{1/2 \text{ suction}} = + 6 \cdot 2$ per cent.

The shape of the wing is given by

$$z = -\frac{kE(\varkappa)}{2\pi} C_{L0}, \{(1 \cdot 4225 - 10 \cdot 2017 k^2 y^2)(x - ky) + 4 \cdot 6640 k^2 y^2 (x^2 - k^2 y^2)\} .$$

At design C_{L0}, $C_{M0}/C_{L0} = 0 \cdot 0255$.

The variation of the position of the centre of pressure with C_L, for design $C_{L0} = 0 \cdot 12$, is given below:

C_L	0·08	0·10	0·12	0·14	0·16
$\bar{h}/c$	0·0191	0·0153	0·0127	0·0109	0·0096

Fig. 6 shows the shape of the wing for semi-apex-angle $\gamma = 18$ deg, $M = 2 \cdot 47$.

(b) The surfaces given by $r = 1, 2, 5, 6$ are combined to give optimum d.

$$\left(\frac{\Delta d}{d_1}\right)_{\text{optimum}} = 13 \cdot 2 \text{ per cent.}$$

If full suction is realised, the corresponding $\Delta t/t_1 = -4 \cdot 0$ per cent.

If only half suction is realised, the corresponding $(\Delta t/t_1)_{1/2 \text{ suction}} = +5 \cdot 8$ per cent.

The shape of the wing is given by

$$z = -\frac{kE(\varkappa)}{2\pi} C_{L0}\{(1 \cdot 3011x - 9 \cdot 5164k^2y^2)(x - ky) + (0 \cdot 0816 + 4 \cdot 2626k^2y^2)(x^2 - k^2y^2)\}.$$

At design C_{L0}, $C_{M0}/C_{L0} = 0 \cdot 0124$.

The variation of the position of the centre of pressure with C_L, for design $C_{L0} = 0 \cdot 12$, is given below:

C_L	0·08	0·10	0·12	0·14	0·16
$\bar{h}/c$	0·0093	0·0074	0·0062	0·0053	0·0046

Fig. 7a shows the shape of the wing for $\gamma = 18$ deg, $M = 2 \cdot 47$.

(c) Surfaces given by $r = 1, 2, 5, 6$ are combined, to give optimum t. The percentage decrease in $t \, (\equiv T/L^2)$, when compared with the corresponding flat wing (with suction), is given by:

$$\left(\frac{\Delta t}{t_1}\right)_{\text{optimum}} = 4 \cdot 8 \text{ per cent.}$$

The effect on the pressure integral is given by

$$\frac{\Delta d}{d_1} = -0 \cdot 4 \text{ per cent.}$$

The shape of the wing is given by

$$z = -\frac{kE(\varkappa)}{2\pi} C_{L0}\{(1 \cdot 7224 - 2 \cdot 8113k^2y^2)(x - ky) - (0 \cdot 3907 - 1 \cdot 1349k^2y^2)(x^2 - k^2y^2)\}.$$

At design C_{L0}, $C_{M0}/C_{L0} = 0 \cdot 1150$.

The variation of the position of the centre of pressure with C_L, for design $C_{L0} = 0 \cdot 12$, is given below:

C_L	0·08	0·10	0·12	0·14	0·16
$\bar{h}/c$	0·0863	0·0690	0·0575	0·0493	0·0431

Fig. 8 shows the shape of the wing for $\gamma = 18$ deg, $M = 2 \cdot 47$.

Examples 2: $\tan \gamma/\tan \mu = 0 \cdot 3577$.

(a) Surfaces given by $r = 1, 2, 5, 6$ are combined to give optimum d.

$$\left(\frac{\Delta d}{d_1}\right)_{\text{optimum}} = 25 \cdot 1 \text{ per cent.}$$

If full suction is realised, the corresponding $\Delta t/t_1 = -18 \cdot 1$ per cent.

If only half suction is realised, the corresponding $(\Delta t/t_1)_{1/2 \text{ suction}} = +9 \cdot 1$ per cent.

17

The shape of the wing is given by

$$z = -\frac{kE(\varkappa)}{2\pi} C_{L0}\{(0\cdot6456 - 10\cdot1298k^2y^2)(x - ky) + (0\cdot5079 + 4\cdot2681k^2y^2)(x^2 - k^2y^2)\}.$$

At design C_{L0}, $C_{M0}/C_{L0} = -0\cdot1049$.

The variation of the position of the centre of pressure with C_L, for design $C_{L0} = 0\cdot1$, is given below:

C_L	$0\cdot06$	$0\cdot08$	$0\cdot10$	$0\cdot12$	$0\cdot14$
$\hbar/c$	$-0\cdot0874$	$-0\cdot0656$	$-0\cdot0524$	$-0\cdot0437$	$-0\cdot0375$

Fig. 9a shows the shape of the wing for $\gamma = 9$ deg, $M = 2\cdot47$.

(b) Surfaces given by $r = 1, 2, 3, 5$ are combined to give optimum d.

$$\left(\frac{\Delta d}{d_1}\right)_{\text{optimum}} = 22\cdot3 \text{ per cent.}$$

If full suction is realised, the corresponding $\Delta t/t_1 = -18\cdot5$ per cent.

If only half suction is realised, the corresponding $(\Delta t/t_1)_{1/2\,\text{suction}} = +7\cdot2$ per cent.

The shape of the wing is given by

$$z = -\frac{kE(\varkappa)}{2\pi} C_{L0}\{-(0\cdot4517 + 2\cdot1406k^2y^2)(x - ky) + 1\cdot5910(x^2 - k^2y^2) - 0\cdot3864(x^3 - k^3y^3)\}.$$

The local incidence at the apex is negative in this case. At design C_{L0}, $C_{M0}/C_{L0} = -0\cdot1161$.

The variation of the position of the centre of pressure with C_L, for design $C_{L0} = 0\cdot1$ is given below:

C_L	$0\cdot06$	$0\cdot08$	$0\cdot10$	$0\cdot12$	$0\cdot14$
$\hbar/c$	$-0\cdot0967$	$-0\cdot0725$	$-0\cdot0580$	$-0\cdot0484$	$-0\cdot0415$

Fig. 10 shows the shape of the wing for $\gamma = 9$ deg, $M = 2\cdot47$.

(c) Surfaces given by $r = 1, 2, 3, 6$ are combined to give optimum t.

$$\left(\frac{\Delta t}{t_1}\right)_{\text{optimum}} = 6\cdot3 \text{ per cent.}$$

The effect on the pressure integral is given by

$$\frac{\Delta d}{d_1} = -5\cdot1 \text{ per cent.}$$

The shape of the wing is given by

$$z = -\frac{kE(\varkappa)}{2\pi} C_{L0}\{3\cdot1438(x - ky) - (2\cdot1233 + 0\cdot1427k^2y^2)(x^2 - k^2y^2) + 0\cdot6973(x^3 - k^3y^3)\}.$$

At design C_{L0}, $C_{M0}/C_{L0} = 0\cdot2132$.

The variation of the position of the centre of pressure with C_L, for design $C_{L0} = 0\cdot1$, is given below:

C_L	$0\cdot06$	$0\cdot08$	$0\cdot10$	$0\cdot12$	$0\cdot14$
$\hbar/c$	$0\cdot1777$	$0\cdot1332$	$0\cdot1066$	$0\cdot0888$	$0\cdot0761$

Fig. 11a shows the shape of the wing for $\gamma = 9$ deg, $M = 2\cdot47$.

18

(d) Surfaces given by $r = 1, 2, 5, 6$ are combined to give optimum d. The centre of pressure is fixed at the two-thirds chord position, G.

$$\left(\frac{\Delta d}{d_1}\right)_{\text{optimum}} = 21 \cdot 8 \text{ per cent.}$$

If full suction is realised, the corresponding $\Delta t/t_1 = -11 \cdot 4$ per cent.

If half suction is realised, the corresponding $(\Delta t/t_1)_{1/2 \text{ suction}} = +9 \cdot 5$ per cent.

The shape of the wing is given by

$$z = -\frac{kE(\varkappa)}{2\pi} C_{L0}\{(1 \cdot 3491 - 12 \cdot 3324 k^2 y^2)(x - ky) + (0 \cdot 1519 + 5 \cdot 2376 k^2 y^2)(x^2 - k^2 y^2)\}.$$

$C_{M0} = 0$, and the centre of pressure remains at G for all C_L (linear theory). Fig. 12 shows the shape of the wing for $\gamma = 9$ deg, $M = 2 \cdot 47$.

Examples 3: $\tan \gamma/\tan \mu = 0 \cdot 1184$

(a) Surfaces given by $r = 1, 3, 5$ are combined to give optimum d.

$$\left(\frac{\Delta d}{d_1}\right)_{\text{optimum}} = 36 \cdot 0 \text{ per cent.}$$

If full suction is realised, the corresponding $\Delta t/t_1 = -16 \cdot 4$ per cent.

If half suction is realised, the corresponding $(\Delta t/t_1)_{1/2 \text{ suction}} = +18 \cdot 2$ per cent.

The shape of the wing is given by

$$z = -\frac{kE(\varkappa)}{2\pi} C_{L0}\{-(0 \cdot 0600 + 1 \cdot 8726 k^2 y^2)(x - ky) + 0 \cdot 5390(x^3 - k^3 y^3)\}.$$

The local incidence at the apex is negative in this case. At design C_{L0}, $C_{M0}/C_{L0} = -0 \cdot 2827$.

The variation of the position of the centre of pressure with C_L, for design $C_{L0} = 0 \cdot 05$, is given below:

C_L	$0 \cdot 03$	$0 \cdot 04$	$0 \cdot 05$	$0 \cdot 06$	$0 \cdot 07$	$0 \cdot 10$
$\bar{h}/c$	$-0 \cdot 2356$	$-0 \cdot 1767$	$-0 \cdot 1413$	$-0 \cdot 1178$	$-0 \cdot 1010$	$-0 \cdot 0707$

Fig. 13a shows the shape of the wing for $\gamma = 3$ deg, $M = 2 \cdot 47$.

(b) Surfaces given by $r = 1, 2, 5$ are combined to give optimum d. The centre of pressure is fixed at G.

$$\left(\frac{\Delta d}{d_1}\right)_{\text{optimum}} = 20 \cdot 6 \text{ per cent.}$$

If full suction is realised, the corresponding $\Delta t/t_1 = -19 \cdot 9$ per cent.

If half suction is realised, the corresponding $(\Delta t/t_1)_{1/2 \text{ suction}} = +6 \cdot 9$ per cent.

The shape of the wing is given by

$$z = -\frac{kE(\varkappa)}{2\pi} C_{L0}\{(0 \cdot 5646 - 5 \cdot 1086 k^2 y^2)(x - ky) + 0 \cdot 6010(x^2 - k^2 y^2)\}.$$

$C_{M0} = 0$, and the centre of pressure remains at G for all C_L (linear theory). Fig. 14 shows the shape of the wing for $\gamma = 3$ deg, $M = 2 \cdot 47$.

For this low value of $\tan \gamma/\tan \mu$, very little drag reduction is possible if suction forces are included (*see* Table 15). But if suction forces are omitted, larger percentage decreases (< 50 per cent) can be obtained by combining four or more surfaces.

19

In the limiting case, when $\tan \gamma / \tan \mu \to 0$, that is for very slender wings, for which the effective aspect ratio $\sqrt{(M^2 - 1)}A \to 0$, it is shown in Appendix X that no drag reduction is possible if suction forces are included. This is in agreement with the results of slender wing theory[13, 14, 26, 27]. But if suction forces are omitted, a drag reduction arbitrarily near to 50 per cent can be obtained; that is, when the order of the camber is very large, the drag of the cambered wing without suction tends to that of the flat wing with suction, for the same lift. This result agrees with a similar result obtained by S. H. Tsien[33], using conical camber, which is a special combination of chordwise and spanwise camber and twist.

In Fig. 4, the maximum percentage drag reductions for triangular wings (with or without suction), are plotted against $\tan \gamma / \tan \mu$ for the simplest camber or twist combinations. The effect of adding camber to any combination is: to increase $(\Delta d / d_1)_{\mathrm{opt}}$ towards a limit of 50 per cent for $\tan \gamma / \tan \mu = 0$, and to decrease $(\Delta d / d_1)_{\mathrm{opt}}$ and $(\Delta t / t_1)_{\mathrm{opt}}$ towards zero for $\tan \gamma / \tan \mu = 1$, with corresponding changes for values of $\tan \gamma / \tan \mu < 1$. The effect of adding twist to any combination is: to decrease $(\Delta d / d_1)_{\mathrm{opt}}$ towards zero for $\tan \gamma / \tan \mu = 0$, and to increase $(\Delta d / d_1)_{\mathrm{opt}}$ and $(\Delta t / t_1)_{\mathrm{opt}}$ towards a limit of about 10 per cent for $\tan \gamma / \tan \mu = 1$, with corresponding changes for values of $\tan \gamma / \tan \mu < 1$. The estimated (probable) optimum results for the best combinations of both camber and twist are shown in Fig. 5.

The relation between the drag coefficient C_D and any C_L is given by equation (35) in Section 2. The variation of C_D and of C_{DP} (the coefficient for the pressure integral only), with C_L, for Examples 1(b), 2(a), 2(c), 3(a) is shown in Figs. 7b, 9b, 11b, 13b.

For a swept-back wing, with supersonic or sonic trailing edges, as the angle of sweepback $\pi/2 - \sigma$, of the trailing edges is increased:

(i) if suction forces are ignored, the maximum percentage reduction in drag for given lift, when compared with the corresponding flat wing, in general, increases, the greatest percentage reduction being 50 per cent (as for the triangular wing) for very slender wings;

(ii) if suction forces are included, the maximum percentage drag reduction, in general, decreases for the smaller values of $\tan \gamma / \tan \mu$, but increases for values of $\tan \gamma / \tan \mu$ near to one, with no reduction possible for very slender wings.

The possible reductions for a wing with sonic leading edges, for a few simple camber and twist combinations are compared with those for the corresponding triangular wing.

Swept-back wing				Triangular wing	
$\gamma = \mu$	$\sigma > \mu$			$\gamma = \mu$	
r	Optimum $(\Delta t / t_1)$ (per cent)			r	Optimum $(\Delta t / t_1)$ (per cent)
	as $\sigma \to \mu$				
1, 2	$\to 16 \cdot 7$	} Camber		1, 2	0
1, 3	$\to 15 \cdot 0$			1, 3	0
1, 4	$\to 13 \cdot 6$			1, 4	0
1, 5	$\to 1 \cdot 1$	Twist		1, 5	5·7
1, 6	$\to 0 \cdot 6$	} Camber and twist		1, 6	4·1
				1, 5, 6	8·1

Further calculations for the swept-back wing will be published later.

6.2. *Leading-Edge Suction.*—Graphs showing the variation of the suction force along the leading edges of some triangular wings ($1(a)$, $2(a)$; $1(c)$, $2(c)$) designed for $(\varDelta d/d_1)_{opt}$, or $(\varDelta t/t_1)_{opt}$, are shown in Fig. 15.

The suction force per unit length of leading edge is $2\pi\rho\varkappa P^2$, where P is the strength of the singularity in the perturbation velocity, u. Hence, writing

$$\text{(suction force per unit length of edge)}/(\tfrac{1}{2}\rho V^2 c) \equiv C_S ,$$

and measuring x, y in root-chord lengths,

for wing $1(a)$:
$$2\pi(C_S/C_{L_0}{}^2) = 0\cdot6793x(1\cdot4225 - 5\cdot1008x^2 + 5\cdot1706x^3)^2;$$

for wing $2(a)$:
$$2\pi(C_S/C_{L_0}{}^2) = 0\cdot9338x(0\cdot6456 + 0\cdot8652x - 4\cdot8021x^2 + 3\cdot8065x^3)^2;$$

for wing $1(c)$:
$$2\pi(C_S/C_{L_0}{}^2) = 0\cdot6793x(1\cdot7224 - 0\cdot5638x - 1\cdot4056x^2 + 1\cdot0148x^3)^2;$$

for wing $2(c)$:
$$2\pi(C_S/C_{L_0}{}^2) = 0\cdot9338x(3\cdot1438 - 3\cdot6172x + 1\cdot5425x^2 - 0\cdot1273x^3)^2 .$$

The suction force vanishes, with that on the corresponding flat plate, when $\tan\gamma/\tan\mu = 1$.

When $\tan\gamma/\tan\mu$ is small, the leading-edge suction force on the minimum-drag wing, designed for optimum d, is small, and tends to vanish as $(\varDelta d/d_1)_{opt} \to 0\cdot5$ for $\tan\gamma/\tan\mu \to 0$, so that, for small effective aspect ratio, the pressure integral tends to become the total lift-dependent drag, and is equal to the drag of the corresponding flat wing with suction forces included. The (theoretical) optimum shape of a very slender wing is given by $z = \{-2C_{L_0}/(\pi A)\}x^n$ (that is, camber near the tip), where n is large, A is the aspect ratio, C_{L_0} is the design lift coefficient, and x, z are measured in root-chord lengths.

7. *Discussion and Conclusion.*—It has been shown, using linear theory, how camber and twist can be used to reduce the drag due to incidence, on a triangular or swept-back wing, with subsonic leading edges and supersonic or sonic trailing edges. The percentage drag reduction, when compared with the drag of the corresponding flat wing having the same lift, depends only on the value of $\tan\gamma/\tan\mu$ (where γ is the semi-apex-angle, and μ is the Mach angle), for the triangular wing, and on $\tan\gamma/\tan\mu$ and $\tan\gamma/\tan\sigma$ (where σ is the trailing edge semi-apex angle), for the swept-back wing; but in each case, the wing must be designed for given plan-form, given Mach number, and given design lift coefficient.

It is found that, on the whole, twist (surface slope a function of y only), especially towards the wing tips, is more effective in reducing drag, for given lift, for the larger values of $\tan\gamma/\tan\mu$, and that camber (surface slope a function of x only) is more effective for the smaller values, though, in general, the best results are obtained by a combination of camber and twist. For the triangular wing, if suction forces are ignored, the maximum percentage drag reduction varies from about 10 per cent (for sonic leading edges) to 50 per cent (for very slender wings); and if suction forces are included, from zero (for very slender wings) to about 10 per cent (when the leading edges are sonic). Graphs showing the probable optimum results, with or without suction, are shown in Fig. 5.

The statements 'assuming no suction', 'assuming $\tfrac{1}{2}$-suction', etc. (also used by previous writers), may be misleading. It is known that linear theory works fairly well away from the leading edges, but that it breaks down at the leading edges, and that singularities, which appear because of the linear-theory approximations, do not really exist. Camber and twist may be chosen so that these singularities do not occur theoretically; it is plausible then to expect that linear theory will give good agreement over the whole aerofoil. Further work is in hand on optimisation of camber and twist with this restriction on their choice. In the present work, it has been assumed when necessary that, physically, the presence or absence of the leading-edge suction force, predicted theoretically, will not affect the remainder of the pressures.

21

In this report, camber and twist is chosen so that either 'part', or the whole of C_D is a minimum for given C_L. The statements 'minimum drag assuming (1) no suction, or (2) $\frac{1}{2}$-suction, or (3) some fraction of the suction, or (4) full suction', mean that suitable camber and twist is found which modifies the leading-edge singularities, and the whole pressure distribution, so that, for given C_L, (1) C_{Dp}, or (2) $C_{Dp} - \frac{1}{2}C_{DS}$, or (3) $C_{Dp} -$ (some fraction of C_{DS}), or (4) $C_D = C_{Dp} - C_{DS}$, is a minimum. The values of C_D, C_{Dp}, etc., so obtained can then be compared with the corresponding quantities for the flat wing, or with the total theoretical C_D (*i.e.*, with full suction), of the flat wing in each case.

The 'part' not 'optimised' could be considered as a partial guess at the part due to over-estimation of the effect of the singularities.

Experiments with different wings, of the same plan-form and section, should give some indication as to which kind of camber and twist will give the best results.

It has been shown that the centre of pressure can be fixed in any position, with a corresponding (slight, for larger values of $\tan \gamma / \tan \mu$) decrease in percentage drag reduction. If fixed at the centre of pressure of the corresponding flat wing, it remains fixed for all C_L (according to linear theory). The positions of the centre of pressure at design lift coefficient, C_{L0}, and of the centre of pressure, G, of the flat wing, are shown in Figs. 6 to 14. The variation of the positions of the centre of pressure with C_L are given in Section 6.

For a swept-back wing with supersonic or sonic trailing edges, as the angle of sweepback of the trailing edges is increased, the maximum percentage drag reduction, for given lift, when compared with the drag of the corresponding flat swept-back wing, increases when $\tan \gamma / \tan \mu$ is near to one (to at least 16 per cent when $\tan \gamma / \tan \mu = 1$), or when suction forces are omitted, but decreases for the smaller values of $\tan \gamma / \tan \mu$ when suction is included.

The same methods could be applied to a wing with swept-forward (supersonic or sonic) trailing edges, when the percentage drag reductions would be less than those for the triangular wing, except when full suction is included, when they would, in general, be greater for the smaller values of $\tan \gamma / \tan \mu$.

The optimum results for the triangular wing, obtained by superimposing 1, 2 or 3 types of camber and/or twist on the flat plate, are shown in Figs. 1 to 4. Further reductions could be obtained by combining a large number of surfaces, but, in most cases, the results seem to be converging. The combination of four surfaces with the flat plate, in a few cases, was found to give scarcely any improvement on the results already obtained with three surfaces and the flat plate.

If further results are required, it might be simpler to combine some of the 'optimum' surfaces already found rather than to start again with a larger number of basic surfaces.

The variation of the suction force along the leading edge, for wings designed for minimum drag, is shown in Fig. 15, and is compared with that for the corresponding flat wing. For wings designed with camber and twist to give no (theoretical) leading-edge singularities, the results will, in general, be less favourable than for designs with full freedom of camber and twist, but some calculations, which will be reported later, show that, by including some higher-order solutions, results more favourable than at first expected can be obtained.

Tsien[33] has made use of conical camber to reduce the drag, for given lift, of some triangular wings with subsonic leading edges. He obtained an appreciable reduction when suction forces were ignored, but scarcely any reduction when suction forces were included, except for values of $\tan \gamma / \tan \mu$ close to one.

Conical camber can be derived from the chordwise and spanwise camber and twist used in this report, with the restriction that the load distribution is that of a cone field. It thus seems that higher percentage drag reductions are likely to be predicted by the use of suitable chordwise and spanwise camber and twist than by the use of conical camber. This is certainly the case when full suction forces are included.

22

LIST OF SYMBOLS

A		Aspect ratio
A_1, A_2, A_3		Coefficients depending on $\varkappa$ (*see* Appendix II)
A_r		Constant coefficients (*cf.* equations (2), etc.)
a_m		Lamé function coefficient (*see* Appendix II)
a_r	$=$	$A_r L_r$
$a_{r,r}, a_{r,s}$		Constant coefficients (*cf.* equations (30) to (33))
a	$=$	h/k
B_1, B_2, B_3		Coefficients depending on $\varkappa$ (*see* Appendix II)
b_m		Lamé function coefficient (*see* Appendix II)
b_r	$=$	$\sum_r c_r \qquad (r = 0, 1, \ldots R/2;$ or $r = 0, 1, \ldots (R-1)/2)$
$\bar{C}_1, \bar{C}_2$		*cf.* equation (38)
C_1, C_2, C_3		Coefficients depending on $\varkappa$ (*see* Appendix II)
C_D		Drag coefficient (suction included)
C_{Dp}		Drag coefficient (suction ignored)
$\bar{C}_{D0}$		Drag coefficient at lift coefficient $\bar{C}_{L0}$ (*cf.* equation (38))
C_L		Lift coefficient
C_{L0}		Design lift coefficient
$\bar{C}_{L0}$		Any arbitrary lift coefficient (*cf.* equation (38))
C_{M0}		Pitching-moment coefficient (at zero lift)
C_p		Pressure coefficient
C_S		(suction force per unit length of leading edge)$/(\frac{1}{2}\rho V^2 c)$
c		Length of root chord
c_r		Coefficients in load distribution formula (*cf.* equation (VII.1))
D		(Normalised) pressure integral
D_r		(Normalised) pressure integral of surface z_r
$D_{r,s} = D_{s,r}$		(Normalised) 'interference' pressure integral of surfaces z_r, z_s
d	$=$	D/L^2
d_r	$=$	D_r/L^2
$d_{r,s}$	$=$	$D_{r,s}/(L_r L_s)$
$E(\varkappa)$		Complete elliptic integral of the second kind of modulus $\varkappa$
$\left.\begin{array}{c} f_1, f_4, \ldots f_{13} \\ F_1, F_2 \end{array}\right\}$		Functions of $\varkappa$, given in Appendix I
$\left.\begin{array}{c} f_{14}, \ldots f_{22} \\ F_3 \end{array}\right\}$		Functions of $\varkappa$, given in Appendix II
H_{2N}	$=$	$\displaystyle\int_0^{c/(k-h)} (ky)^{2N} \cosh^{-1} \frac{c+hy}{ky}\, dy$
h	$=$	$\cot \sigma$

23

$\bar{h}$		Distance of centre of pressure of triangular wing from the two-thirds chord position
$I_{2m,n}$		$\displaystyle\int_0^{c/(k-h)} \int_{ky}^{c+hy} \frac{(ky)^{2m}x^n}{(x^2-k^2y^2)^{1/2}}\,dx\,dy$
$J_{2m,M}$		$\displaystyle\int_0^{c/(k-h)} \frac{(c+hy)^M(ky)^{2m}}{Z}\,dy$
$K(\varkappa)$		Complete elliptic integral of the first kind of modulus $\varkappa$
k	$=$	$\cot\gamma$
L		(Normalised) lift
L_r		(Normalised) lift for surface z_r
$\bar{M}$		(Normalised) pitching moment about the apex
M_r		(Normalised) pitching moment of surface z_r about the apex
M		Free-stream Mach number
P		Strength of leading-edge pressure singularity
P_r		Strength of leading-edge pressure singularity of surface z_r
p		(Normalised) load per unit area
p_r		(Normalised) load per unit area of surface z_r
Q	$=$	$2M+N$ (in Appendix VII)
R	$=$	$2m+n$ (in Appendix VII)
S		(Normalised) suction force (*cf.* equation (1))
S_r		(Normalised) suction force for surface z_r
$S_{r,s}=S_{s,r}$		(Normalised) 'interference' suction force for surfaces z_r, z_s
s_r	$=$	S_r/L_r^2
$s_{r,s}$	$=$	$S_{r,s}/(L_rL_s)$
T		(Normalised) drag due to incidence, camber and twist $=D-S$
$T_{2m,n}$	$=$	$[kI_{2m,n}/c^{2m+n+1}]_{h=0}$
t	$=$	$T/L^2=(D-S)/L^2$
t_r	$=$	$d_r-s_r=(D_r-S_r)/L_r^2$
$t_{r,s}$	$=$	$d_{r,s}-s_{r,s}=(D_{r,s}-S_{r,s})/L_rL_s$
u		Perturbation velocity in the free-stream direction
V		Free-stream velocity
X	$=$	$(x^2-k^2y^2)^{1/2}$
$\bar{x}$		Distance of centre of pressure from apex of wing
x		Chordwise co-ordinate (measured downstream from the apex)
y		Spanwise co-ordinate (positive to starboard)
z		Normal co-ordinate (positive upwards)

$$Z \quad = \quad [(c + hy)^2 - k^2 y^2]^{1/2}$$

$\alpha \qquad$ Local surface slope $\left(= - \dfrac{\partial z}{\partial x} \right)$ (measured in radians)

$\alpha_r \qquad$ Local surface slope of surface z_r

$\beta \quad = \quad (M^2 - 1)^{1/2}$

$\gamma \qquad$ Apex semi-angle

$\Delta \qquad$ *See* Appendix II

$\Delta_{\mathrm{III}}, \Delta_{\mathrm{IV}} \qquad$ *cf.* equations (20) and (24)

$\Delta_r \qquad$ *cf.* equations (26) and (31)

$\Delta_N \qquad$ *cf.* equation (26)

$\Delta_{N-1} \qquad$ *cf.* equation (31)

$\Delta d \quad = \quad d_1 - d$

$\Delta t \quad = \quad t_1 - t$

$\delta \qquad$ Small dimensionless constant

$(\theta) \quad = \quad (\pi/2) + \cos^{-1} \lambda$

$\varkappa \quad = \quad (1 - \tan^2 \gamma / \tan^2 \mu)^{1/2}$

$\lambda \quad = \quad (1 - h^2/k^2)^{1/2}$

$\lambda_m \qquad$ Coefficients depending on $\varkappa$ (*see* Appendix II)

$\mu \qquad$ Mach angle

$\nu \quad = \quad \bar{M}/(cL)$

$\nu_r \quad = \quad M_r/(cL_r)$

$\rho \qquad$ Free-stream density

$\sigma \qquad$ Apex semi-angle of the trailing edge (of a swept-back wing)

$\phi \qquad$ Velocity potential

REFERENCES

No.	Author	Title, etc.
1	G. M. Roper	Calculation of the effect of camber and twist on the pressure distribution and drag on some curved plates at supersonic speeds. R. & M. 2794. September, 1950.
2	G. M. Roper	Some applications of the Lamé function solutions of the linearised supersonic-flow equations. R. & M. 2865. August, 1951.
3	A. Robinson	Aerofoil theory of a flat delta wing at supersonic speeds. R. & M. 2548. September, 1946.
4	A. Robinson	Rotary derivatives of a delta wing at supersonic speeds. *J.R.Ae. Soc.* November, 1948.
5	E. W. Hobson	*Spherical and Ellipsoidal Harmonics.* Cambridge University Press.
6	M. M. Munk	The minimum induced drag of aerofoils. N.A.C.A. Report 121. 1921.
7	R. T. Jones	The minimum drag of thin wings in frictionless flow. *J. Ae. Sci.* Vol. 18. 2. February, 1951.
8	R. T. Jones	Theoretical determination of the minimum drag of airfoils at supersonic speeds. *J. Ae. Sci.* Vol. 19. 12. December, 1952.
9	E. W. Graham	A drag-reduction method for wings of fixed plan-form. Douglas Report S.M.14441. July, 1952. *J. Ae. Sci.* Vol. 19. 12. December, 1952.
10	K. Walker	Examples of drag reduction for rectangular wings. Douglas Report S.M.14446. January, 1953.
11	Beverly J. Beane	Examples of drag reduction for delta wings. Douglas Report S.M.14447. January, 1953.
12	A. M. Rodriguez, P. A. Lagerstrom and E. W. Graham	Theorems concerning the drag reduction of wings of fixed plan-form. Douglas Report S.M.14445. March, 1953. *J. Ae. Sci.* Vol. 21. 1. January, 1954.
13	Mac C. Adams and W. R. Sears	On an extension of slender-wing theory. *J. Ae. Sci.* Vol. 19. 6. June, 1952.
14	Mac C. Adams and W. R. Sears	Slender-body theory: Reviews and extensions. *J. Ae. Sci.* Vol. 20. 2. February, 1953.
15	B. S. Baldwin, Jr.	Triangular wings cambered and twisted to support specified distribution of lift at supersonic speeds. N.A.C.A. Tech. Note 1816. February, 1949.
16	Beverly J. Beane	The effect of plan-form on the lift to drag ratio of wing-body combinations at supersonic speeds. Douglas Report S.M.14454. July, 1952.
17	Beverly J. Beane	Drag reduction due to wing incidence on twist for wing-body combinations. Douglas Report S.M.14740. March, 1953.
18	Clinton E. Brown	The reversibility theorem for thin airfoils in subsonic and supersonic flow. N.A.C.A. Tech. Note 1944. September, 1949.
19	A. Busemann	Infinitesimal conical supersonic flow. N.A.C.A. Tech. Memo. 1100. 1947.
20	A. H. Flax	Relations between the characteristics of a wing and its reverse in supersonic flow. *J. Ae. Sci.* Vol. 16. 8. August, 1949.
21	A. H. Flax	General reverse flow and variational theorems in lifting-surface theory. *J. Ae. Sci.* Vol. 19. 6. June, 1952.
22	P. Germain	General theory of conical flows and its application to supersonic aerodynamics. N.A.C.A. Tech. Memo. 1354. January, 1955. O.N.E.R.A. Rap. 1/1155A, 1948.

REFERENCES—*continued*

No.	Author	Title, etc.
23	M. E. Graham	Effect of linear symmetric twist on drag of rectangular wing in supersonic flow. Douglas Report S.M.13303. June, 1948.
24	S. Harmon	Theoretical relations between the stability derivatives of a wing in direct and in reverse supersonic flow. N.A.C.A. Tech. Note 1943. September, 1949.
25	W. D. Hayes	Reversed-flow theorems in supersonic aerodynamics. North American Aviation Inc. Report AL.755. August, 1948.
26	R. T. Jones	Properties of low-aspect-ratio pointed wings at speeds below and above the speed of sound. N.A.C.A. Report 835. 1946.
27	R. T. Jones	Estimated lift-drag ratios at supersonic speeds. N.A.C.A. Tech. Note. 1350. July, 1947
28	Th. von Kármán	Supersonic aerodynamics—Principles and applications. *J. Ae. Sci.* Vol. 14. 7. July, 1947.
29	R. T. Jones	Theory of wing-body drag at supersonic speeds. N.A.C.A. Research Memo. A53H18a. TIB 3890. September, 1953.
30	H. Lomax and M. A. Heaslet	Generalised conical-flow fields in supersonic wing theory. N.A.C.A. Tech. Note 2497. September, 1951.
31	M. M. Munk	The reversal theorem of linearised supersonic airfoil theory. *J. App. Phys.* Vol. 21. 2. February, 1950.
32	R. Sedney	On Jones's criterion for thin wings of minimum drag. *J. Ae. Sci.* Vol. 21. 9. September, 1954.
33	S. H. Tsien	The supersonic conical wing of minimum drag. Grad. Sch. of Aero. Eng., Cornell University, June, 1953.
34	F. Ursell and G. N. Ward	On some general theorems in the linearised theory of compressible flow. *Quart. J. Mech. App. Math.* Vol. III. Part 3. September, 1950.
35	M. D. Van Dyke	Subsonic edges in thin-wing and slender-body theory. N.A.C.A. Tech. Note 3343. November, 1954.
36	G. N. Ward	Supersonic flow past slender pointed bodies. *Quart. J. Mech. App. Math.* Vol. 2. 1. March, 1949.
37	C. F. Hall	Lift, drag and pitching moment of low-aspect-ratio wings at subsonic and supersonic speeds. N.A.C.A. Research Memo. A53A30. NACA/TIB/3646. April, 1953.
38	L. H. Jorgensen	Nose shapes for minimum pressure drag at supersonic Mach numbers. *J. Ae. Sci.* Vol. 21. 4. April, 1954.
39	K. W. Mangler	Calculation of the load distribution over a wing with arbitrary camber and twist at sonic speed. A.R.C. 17262. April, 1954.
40	N. Rott	Minimum-drag cambered rectangular wing for supersonic speeds. *J. Ae. Sci.* Vol. 20. 9. September, 1953.
41	M. D. Van Dyke	The second-order compressibility rule for airfoils. *J. Ae. Sci.* Vol. 21. 9. September, 1954.
42	M. D. Van Dyke	Second-order subsonic airfoil-section theory and its practical application. N.A.C.A. Tech. Note 3390. March, 1955.
43	K. W. Mangler	Applications of slender-wing theory in wing design. A.R.C. 18504. November, 1955.

APPENDIX I

The Functions $f_1, f_4, \ldots f_{13}, F_1, F_2$

$$f_1 = f_4 = \{(2\varkappa^2 - 1)E(\varkappa) + (1 - \varkappa^2)K(\varkappa)\}/(2\varkappa^2 E(\varkappa))$$

$$f_5 = 3\{(1 + \varkappa^2)E(\varkappa) - (1 - \varkappa^2)K(\varkappa)\}/(2\varkappa^2 E(\varkappa))$$

$$f_6 = \{(2 + \varkappa^2 - 3\varkappa^4)K(\varkappa) - (2 + 2\varkappa^2 - 6\varkappa^4)E(\varkappa)\}/(2\varkappa^4 E(\varkappa))$$

$$f_7 = \{(2 - 3\varkappa^2 + \varkappa^4)E(\varkappa) - (2 - 4\varkappa^2 + 2\varkappa^4)K(\varkappa)\}/(2\varkappa^4 E(\varkappa))$$

$$f_{10} = \{(2 + 2\varkappa^2 - 4\varkappa^4)K(\varkappa) - (2 + 3\varkappa^2 - 8\varkappa^4)E(\varkappa)\}/(2\varkappa^4 E(\varkappa))$$

$$f_{11} = 3\{(2 - 2\varkappa^2 + 2\varkappa^4)E(\varkappa) - (2 - 3\varkappa^2 + \varkappa^4)K(\varkappa)\}/(2\varkappa^4 E(\varkappa))$$

$$f_{12} = \{(8 - \varkappa^2 + 5\varkappa^4 - 12\varkappa^6)K(\varkappa) - (8 + 3\varkappa^4 + 7\varkappa^4 - 24\varkappa^6)E(\varkappa)\}/(6\varkappa^6 E(\varkappa))$$

$$f_{13} = \{(8 - 11\varkappa^2 + \varkappa^4 + 2\varkappa^6)E(\varkappa) - (8 - 15\varkappa^2 + 6\varkappa^4 + \varkappa^6)K(\varkappa)\}/(2\varkappa^6 E(\varkappa))$$

$$F_1 = 1/(f_5 f_6 - 3f_4 f_7)$$

$$F_2 = 1/(f_{11} f_{12} - f_{10} f_{13}) \, .$$

Calculation of the Functions $f_{14}, f_{15}, \ldots f_{22}, F_3$

Solutions of the linearised supersonic-flow equation, in terms of the Lamé functions of the 'M' class of degree $n = 5$, are given in Ref. 2, Part II, Appendix III.

It is shown that there are three solutions for the velocity potential, and that the shapes of the corresponding surfaces are given by: ($m = 1, 2, 3$)

$$z_m = \frac{\delta(1 - \varkappa^2)}{E(\varkappa)}(1 - a_m + b_m)(k^{11}I_m)\left[\tfrac{1}{5}(\varkappa^4 - a_m\varkappa^2 + b_m)x^5\right.$$

$$\left. + \tfrac{1}{3}(1 - \varkappa^2)(a_m\varkappa^2 - 2b_m)k^2y^2x^3 + (1 - \varkappa^2)^2b_mk^4y^4x\right] + f(y), \quad \cdots \quad \cdots \quad (II.1)$$

all lengths being measured in root-chord lengths. δ is a small arbitrary constant, $f(y)$ is a (small) arbitrary function of y, and

$$k^{11}I_m = \frac{1}{a_m^2 - 4b_m}\left[\frac{1}{2}\left\{\frac{a_m}{\varkappa^2 b_m} + \frac{2\varkappa^2 - a_m}{(1 - \varkappa^2)^2\varkappa^2(\varkappa^4 - a_m\varkappa^2 + b_m)} - 3\left(\frac{2 - 2a_m + a_m^2 - 2b_m}{(1 - \varkappa^2)(1 - a_m + b_m)^2}\right)\right.\right.$$

$$\left. + \frac{\varkappa^2 - 2}{(1 - \varkappa^2)^2}\left(\frac{2 - a_m}{1 - a_m + b_m}\right) + \frac{4}{(1 - \varkappa^2)(1 - a_m + b_m)}\right\}E(\varkappa) - \left\{2\left(\frac{a_m - 1}{b_m(1 - a_m + b_m)}\right)\right.$$

$$\left.\left. + \frac{\tfrac{1}{2}[a_m^2 - 2b_m - 2a_m(a_m^2 - b_m) + a_m^4 + 4a_m^2b_m - 14b_m^2 - 4a_mb_m(a_m^2 - 3b_m)]}{b_m^2(1 - a_m + b_m)^2}\right\}K(\varkappa)\right], \quad (II.2)$$

where a_m are the roots of the equation

$$27a_m^3 - (60\varkappa^2 + 42)a_m^2 + (32\varkappa^4 + 68\varkappa^2 + 16)a_m - 2\varkappa^2(12\varkappa^2 + 8) = 0, \quad \cdots \quad (II.3)$$

$$b_m = \varkappa^2 a_m/(12\varkappa^2 + 8 - 9a_m), \quad \cdots \quad \cdots \quad \cdots \quad \cdots \quad \cdots \quad \cdots \quad \cdots \quad (II.4)$$

$\varkappa^2 = 1 - \tan^2\gamma/\tan^2\mu$, and $E(\varkappa)$, $K(\varkappa)$ are complete elliptic integrals of the second and first kind respectively, of modulus $\varkappa$.

The shapes of the surfaces corresponding to velocity potentials proportional to x^4X, $k^2y^2x^2X$, k^4y^4X are given by:

$$z' = \sum_{m=1}^{3}[k^4\lambda_m'(1 - a_m + b_m)z_m] \equiv -\delta(A_1x^5 - B_1k^2y^2x^3 + C_1k^4y^4x), \quad \cdots \quad (II.5)$$

$$z'' = \sum_{m=1}^{3}[k^6\lambda_m''(1 - a_m + b_m)z_m] \equiv \delta(A_2x^5 - B_2k^2y^2x^3 + C_2k^4y^4x), \quad \cdots \quad \cdots \quad (II.6)$$

$$z''' = \sum_{m=1}^{3}[k^8\lambda_m'''(1 - a_m + b_m)z_m] \equiv -\delta(A_3x^5 - B_3k^2y^2x^3 + C_3k^4y^4x), \quad \cdots \quad (II.7)$$

respectively, where (writing $a_2b_3 - a_3b_2 + a_3b_1 - a_1b_3 + a_1b_2 - a_2b_1 \equiv \Delta$),

$$k^4\lambda_1' = \frac{1}{\varkappa^4\Delta}(a_2b_3 - a_3b_2),$$

$$k^4\lambda_2' = \frac{1}{\varkappa^4\Delta}(a_3b_1 - a_1b_3),$$

$$k^4\lambda_3' = \frac{1}{\varkappa^4\Delta}(a_1b_2 - a_2b_1);$$

$$k^6\lambda_1'' = \frac{1}{\varkappa^2(1-\varkappa^2)\varDelta}\left[b_2 - b_3 + \frac{1}{\varkappa^2}(a_2b_3 - a_3b_2)\right],$$

$$k^6\lambda_2'' = \frac{1}{\varkappa^2(1-\varkappa^2)\varDelta}\left[b_3 - b_1 + \frac{1}{\varkappa^2}(a_3b_1 - a_1b_3)\right],$$

$$k^6\lambda_3'' = \frac{1}{\varkappa^2(1-\varkappa^2)\varDelta}\left[b_1 - b_2 + \frac{1}{\varkappa^2}(a_1b_2 - a_2b_1)\right];$$

$$k^8\lambda_1''' = \frac{1}{(1-\varkappa^2)^2\varDelta}\left[\frac{1}{\varkappa^4}(a_2b_3 - a_3b_2) + \frac{2}{\varkappa^2}(b_2 - b_3) - (a_2 - a_3)\right],$$

$$k^8\lambda_2''' = \frac{1}{(1-\varkappa^2)^2\varDelta}\left[\frac{1}{\varkappa^4}(a_3b_1 - a_1b_3) + \frac{2}{\varkappa^2}(b_3 - b_1) - (a_3 - a_1)\right],$$

$$k^8\lambda_3''' = \frac{1}{(1-\varkappa^2)^2\varDelta}\left[\frac{1}{\varkappa^4}(a_1b_2 - a_2b_1) + \frac{2}{\varkappa^2}(b_1 - b_2) - (a_1 - a_2)\right].$$

Hence the three basic camber and twist solutions are obtained:

$$z = -\,\delta x^5 \equiv \delta F_3(f_{14}z' + f_{15}z'' + f_{16}z''')\,, \qquad \qquad \qquad \qquad \text{(II.8)}$$

$$z = -\,\delta k^2 y^2 x^3 \equiv -\,\delta F_3(f_{17}z' + f_{18}z'' + f_{19}z''')\,, \qquad \qquad \qquad \text{(II.9)}$$

$$z = -\,\delta k^4 y^4 x \equiv \delta F_3(f_{20}z' + f_{21}z'' + f_{22}z''')\,, \qquad \qquad \qquad \text{(II.10)}$$

where

$$f_{14} = B_2C_3 - B_3C_2\,, \qquad f_{15} = B_1C_3 - B_3C_1\,, \qquad f_{16} = B_1C_2 - B_2C_1\,;$$

$$f_{17} = C_2A_3 - C_3A_2\,, \qquad f_{18} = C_1A_3 - C_3A_1\,, \qquad f_{19} = C_1A_2 - C_2A_1\,;$$

$$f_{20} = A_2B_3 - A_3B_2\,, \qquad f_{21} = A_1B_3 - A_3B_1\,, \qquad f_{22} = A_1B_2 - A_2B_1\,;$$

$$F_3 = 1/(A_1f_{14} - A_2f_{15} + A_3f_{16})$$

$$= 1/(B_1f_{17} - B_2f_{18} + B_3f_{19})$$

$$= 1/(C_1f_{20} - C_2f_{21} + C_3f_{22})\,.$$

Numerical values of a_m; λ_m', λ_m'', λ_m''' are given in Appendices VIII and IX. Some numerical values of $f_{14}, \ldots f_{22}$, F_3 are given in Appendix III.

Numerical Values of the Functions $f_1, f_4, \ldots f_{13}; f_{14}, \ldots f_{22}; F_1, F_2, F_3$

$\dfrac{\tan \gamma}{\tan \mu}$	$\varkappa^2$	$f_1 = f_4$	f_5	f_6	f_7	f_{10}	f_{11}	f_{12}	f_{13}
0	1	0·5	3·0	1·0	0	1·5	3·0	1·0	0
0·1	0·99	0·5135	2·9600	1·0624	0·0048	1·5751	2·9744	1·1040	0·0142
0·1184	0·9860	0·5176	2·9470	1·0816	0·0066	1·5993	2·9669	1·1370	0·0194
0·2	0·96	0·5390	2·8831	1·1774	0·0176	1·7163	2·9358	1·2929	0·0508
0·3	0·91	0·5690	2·7929	1·3093	0·0359	1·8786	2·9002	1·5044	0·1010
0·3577	0·8721	0·5870	2·7391	1·3870	0·0478	1·9740	2·8826	1·6267	0·1333
0·4	0·84	0·6000	2·6999	1·4429	0·0571	2·0430	2·8713	1·7143	0·1578
0·5	0·75	0·6300	2·6097	1·5703	0·0799	2·2007	2·8495	1·9123	0·2163
0·6	0·64	0·6585	2·5247	1·6894	0·1030	2·3476	2·8338	2·0944	0·2735
0·6140	0·6231	0·6622	2·5134	1·7048	0·1062	2·3670	2·8321	2·1182	0·2813
0·6873	0·5276	0·6814	2·4558	1·7842	0·1228	2·4656	2·8243	2·2390	0·3212
0·7	0·51	0·6845	2·4463	1·7969	0·1257	2·4817	2·8235	2·2583	0·3284
0·7112	0·4942	0·6874	2·4378	1·8086	0·1282	2·4960	2·8225	2·2757	0·3342
0·7141	0·49	0·6881	2·4357	1·8116	0·1289	2·4997	2·8223	2·2802	0·3358
0·7338	0·4615	0·6930	2·4211	1·8317	0·1331	2·5246	2·8205	2·3109	0·3453
0·8	0·36	0·7085	2·3743	1·8952	0·1473	2·6038	2·8167	2·4066	0·3786
0·9	0·19	0·7300	2·3093	1·9820	0·1685	2·7125	2·8146	2·5365	0·4306
1·0	0	0·7500	2·2500	2·0625	0·1875	2·8125	2·8125	2·65625	0·46875

$\dfrac{\tan \gamma}{\tan \mu}$	f_{14}	f_{15}	f_{16}	f_{17}	f_{18}	f_{19}	f_{20}	f_{21}	f_{22}
0·6140	3·4980	0·6358	0·0156	−0·1688	−1·9562	−0·0340	0·0229	0·1688	0·4616
0·7	3·4050	0·7320	0·0224	−0·1495	−2·0586	−0·4520	0·0195	0·1844	0·4914

$\dfrac{\tan \gamma}{\tan \mu}$	F_1	F_2	F_3
0·1184	0·3147	0·2992	
0·3577	0·2692	0·2259	
0·5	0·2534	0·2011	
0·6140	0·2455	0·1875	0·5687
0·7	0·2417	0·1798	0·5454
0·7338	0·2405	0·1771	

APPENDIX IV

Velocity Potentials of the Basic Cambered and Twisted Surfaces

$$X \equiv (x^2 - k^2y^2)^{1/2}$$

r	z_r	$(\varkappa E(\varkappa)/V)\phi_r$	
1	$-\delta x$	δX	⎫
2	$-\dfrac{\delta}{c}x^2$	$\dfrac{\delta}{cf_1}xX$	
3	$-\dfrac{\delta}{c^2}x^3$	$3F_1\dfrac{\delta}{c^2}[f_5 x^2 - f_7(x^2 - k^2y^2)]X$	⎬ Camber
4	$-\dfrac{\delta}{c^3}x^4$	$3F_2\dfrac{\delta}{c^3}[f_{11}x^3 - f_{13}(x^3 - k^2y^2 x)]X$	⎭
5	$-\dfrac{\delta}{c^2}k^2y^2x$	$F_1\dfrac{\delta}{c^2}[3f_4 x^2 - f_6(x^2 - k^2y^2)]X$	Twist
6	$-\dfrac{\delta}{c^3}k^2y^2x^2$	$2F_2\dfrac{\delta}{c^3}[f_{10}x^3 - f_{12}(x^3 - k^2y^2 x)]X$	⎫ Camber and twist
7	$f_4z_3 - f_5z_5$	$\dfrac{\delta}{c^2}(x^2 - k^2y^2)X$	⎭
8	$-\dfrac{\delta}{c^4}x^5$	$\dfrac{\delta}{c^4}F_3(f_{14}x^4 + f_{15}k^2y^2x^2 + f_{16}k^4y^4)X$	Camber
9	$-\dfrac{\delta}{c^4}k^2y^2x^3$	$-\dfrac{\delta}{c^4}F_3(f_{17}x^4 + f_{18}k^2y^2x^2 + f_{19}k^4y^4)X$	Camber and twist
10	$-\dfrac{\delta}{c^4}k^4y^4x$	$\dfrac{\delta}{c^4}F_3(f_{20}x^4 + f_{21}k^2y^2x^2 + f_{22}k^4y^4)X$	Twist

$$\text{Evaluation of the Integral } \int_0^{c/k} \int_{ky}^{c} \frac{k^{2m}y^{2m}x^n}{(x^2 - k^2y^2)^{1/2}} \, dx \, dy \equiv \frac{c^{2m+n+1}}{k} \, T_{2m,n} ,$$

Where m, n are Positive Integers

It can be shown that

$$\int_{ky}^{c} \frac{x^n}{(x^2 - k^2y^2)^{1/2}} \, dx = \frac{1}{n} (c^2 - k^2y^2)^{1/2} \left[c^{n-1} + \frac{n-1}{n-2} c^{n-3}k^2y^2 \right.$$

$$\left. + \frac{(n-1)(n-3)}{(n-2)(n-4)} c^{n-5}k^4y^4 + \dots + \frac{(n-1)(n-3)\dots 2}{(n-2)(n-4)\dots 1} (ky)^{n-1} \right]$$

if n is odd, ... (V.1)

$$= \frac{1}{n} (c^2 - k^2y^2)^{1/2} \left[c^{n-1} + \frac{n-1}{n-2} c^{n-3}k^2y^2 \right.$$

$$\left. + \frac{(n-1)(n-3)}{(n-2)(n-4)} c^{n-5}k^4y^4 + \dots + \frac{(n-1)(n-3)\dots 3}{(n-2)(n-4)\dots 2} c(ky)^{n-2} \right]$$

$$+ \frac{(n-1)(n-3)\dots 1}{n(n-2)\dots 2} (ky)^n \cosh^{-1} \frac{c}{ky}$$

if n is even, ... (V.2)

$$\int_0^{c/k} k^{2n}y^{2n}(c^2 - k^2y^2)^{1/2} \, dy = \frac{\pi c^{2n+2}}{k} \left(\frac{(2n)!}{2^{2n+2}n!(n+1)!} \right) \quad .. \quad .. \quad .. \quad \text{(V.3)}$$

$$\int_0^{c/k} k^{2n}y^{2n} \cosh^{-1} \frac{c}{ky} \, dy = \frac{\pi c^{2n+1}}{k} \left(\frac{(2n)!}{2^{2n+1}(2n+1)(n!)^2} \right) \, . \, .. \quad .. \quad .. \quad \text{(V.4)}$$

Hence

$$T_{2m,n} = \frac{k}{c^{2m+n+1}} \int_0^{c/k} \int_{ky}^{c} \frac{k^{2m}y^{2m}x^n}{(x^2 - k^2y^2)^{1/2}} \, dx \, dy$$

$$= \frac{\pi(2m)!}{2^{2m+1}(2m+n+1)(m!)^2} \quad .. \quad .. \quad .. \quad .. \quad .. \quad \text{(V.5)}$$

for all values of m, n.

If $m = 0$,

$$T_{0,n} = \frac{\pi}{2(n+1)} .$$

If $n = 0$,

$$T_{2m,0} = \frac{\pi(2m)!}{2^{2m+1}(2m+1)(m!)^2} .$$

A table of values of $T_{2m,n}$ used in the numerical calculations is given:

Values of $T_{2m,n}$

n	$\frac{1}{\pi} T_{0,n}$	$\frac{1}{\pi} T_{2,n}$	$\frac{1}{\pi} T_{4,n}$	$\frac{1}{\pi} T_{6,n}$	$\frac{1}{\pi} T_{8,n}$
0	1/2	1/12	3/80	5/224	35/2304
1	1/4	1/16	1/32	5/256	7/512
2	1/6	1/20	3/112	5/288	35/2816
3	1/8	1/24	3/128	1/64	35/3072
4	1/10	1/28	1/48	5/352	35/3328
5	1/12	1/32	3/160	5/384	5/512
6	1/14	1/36	3/176	5/416	7/768
7	1/16	1/40	1/64	5/448	35/4096
8	1/18	1/44	3/208	1/96	35/4352
9	1/20	1/48	3/224	5/512	35/4608

33

Evaluation of the Integral $\displaystyle\int_0^{c/(k-h)} \int_{ky}^{c+hy} \frac{k^{2m}y^{2m}x^n}{(x^2 - k^2y^2)^{1/2}} \, dx \, dy \equiv I_{2m,\,n}$,

Where m, n are Positive Integers

Writing $\{(c + hy)^2 - k^2y^2\}^{1/2} \equiv Z$, it can be shown that:

$$\int_{ky}^{c+hy} \frac{x^n}{(x^2 - k^2y^2)^{1/2}} \, dx = \frac{1}{nZ} \Bigg[(c + hy)^{n+1} + \frac{1}{n-2}(c+hy)^{n-1}k^2y^2$$

$$+ \frac{n-1}{(n-2)(n-4)}(c+hy)^{n-3}k^4y^4$$

$$+ \ldots + \frac{(n-1)(n-3)\ldots 4}{(n-2)(n-4)\ldots 1}(c+hy)^2(ky)^{n-1}$$

$$- \frac{(n-1)(n-3)\ldots 2}{(n-2)(n-4)\ldots 1}(ky)^{n+1}\Bigg]$$

if n is odd; .. .. (VI.1)

$$\int_{ky}^{c+hy} \frac{x^n}{(x^2 - k^2y^2)^{1/2}} \, dx = \frac{1}{nZ} \Bigg[(c + hy)^{n+1} + \frac{1}{n-2}(c+hy)^{n-1}k^2y^2$$

$$+ \ldots + \frac{(n-1)(n-3)\ldots 5}{(n-2)(n-4)\ldots 2}(c+hy)^3(ky)^{n-2}$$

$$- \frac{(n-1)(n-3)\ldots 3}{(n-2)(n-4)\ldots 2}(c+hy)(ky)^{n}\Bigg]$$

$$+ \frac{(n-1)(n-3)\ldots 1}{n(n-2)\ldots 2}(ky)^n \cosh^{-1}\frac{c+hy}{ky}$$

if n is even. .. .. (VI.2)

Hence, if n is odd,

$$I_{2m,\,n} \equiv \int_0^{c/(k-h)} \int_{ky}^{c+hy} \frac{k^{2m}y^{2m}x^n}{(x^2 - k^2y^2)^{1/2}} \, dx \, dy$$

is the sum of integrals of the form

$$\int_0^{c/(k-h)} \frac{(c + hy)^M k^{2m}y^{2m}}{Z} \, dy \equiv J_{2m,\,M} \, . \quad .. \quad .. \quad .. \quad .. \text{(VI.3)}$$

If n is even, there are also terms of the form

$$\int_0^{c/(k-h)} (ky)^{2N} \cosh^{-1}\frac{c+hy}{ky} \, dy \equiv H_{2N} \, . \, .. \quad .. \quad .. \quad .. \text{(VI.4)}$$

It can be shown that

$$H_{2N} = \frac{c}{2N+1} J_{2N,\,0} \, . \quad .. \quad .. \quad .. \quad .. \quad .. \quad .. \quad .. \text{(VI.5)}$$

Putting $\qquad y = \frac{c}{k^2 - h^2}(h + k \sin \theta)$,

$$J_{2m,\,M} = \frac{c^{2m+M}}{k\lambda^{4m+2M+1}} \int_{-\cos^{-1}\lambda}^{\pi/2} (1 + a \sin \theta)^M (a + \sin \theta)^{2m} \, d\theta \, ,$$

where $\lambda^2 = 1 - h^2/k^2$, and $a = h/k$*.

* Recurrence formulae for $I_{N,\,n}, J_{N,\,n}$, which have been programmed for an electronic computor, and some tables of values will be given in a later paper.

Formulae for the integrated values of $J_{2m,M}(2m + M = 1, 2, \ldots 10)$ are given below ($\frac{1}{2}\pi + \cos^{-1}\lambda$ is written as (θ)):

$2m, M$	$(k/c^2)J_{2m,M}$
$0, 0$	$\dfrac{1}{c^2\lambda}(\theta)$
$0, 1$	$\dfrac{1}{c\lambda^3}\{(\theta) + \lambda a\}$
$0, 2$	$\dfrac{1}{\lambda^5}\{\frac{1}{2}(3 - \lambda^2)(\theta) + \frac{1}{2}\lambda a(3 + \lambda^2)\}$
$2, 0$	$\dfrac{1}{\lambda^5}\{\frac{1}{2}(3 - 2\lambda^2)(\theta) + \frac{3}{2}\lambda a\}$
$0, 3$	$\dfrac{c}{\lambda^7}\{\frac{1}{2}(5 - 3\lambda^2)(\theta) + \frac{1}{6}\lambda a(15 + \lambda^2 + 2\lambda^4)\}$
$2, 1$	$\dfrac{c}{\lambda^7}\{\frac{1}{2}(5 - 4\lambda^2)(\theta) + \frac{1}{6}\lambda a(15 - 2\lambda^2)\}$
$0, 4$	$\dfrac{c^2}{\lambda^9}\{\frac{1}{8}(35 - 30\lambda^2 + 3\lambda^4)(\theta) + \frac{1}{24}\lambda a(105 - 20\lambda^2 + 5\lambda^4 + 6\lambda^6)\}$
$2, 2$	$\dfrac{c^2}{\lambda^9}\{\frac{1}{8}(35 - 35\lambda^2 + 4\lambda^4)(\theta) + \frac{1}{24}\lambda a(105 - 35\lambda^2 - 2\lambda^4)\}$
$4, 0$	$\dfrac{c^2}{\lambda^9}\{\frac{1}{8}(35 - 40\lambda^2 + 8\lambda^4)(\theta) + \frac{1}{24}\lambda a(105 - 50\lambda^2)\}$
$0, 5$	$\dfrac{c^3}{\lambda^{11}}\{\frac{1}{8}(63 - 70\lambda^2 + 15\lambda^4)(\theta) + \frac{1}{120}\lambda a(945 - 420\lambda^2 + 29\lambda^4 + 22\lambda^6 + 24\lambda^8)\}$
$2, 3$	$\dfrac{c^3}{\lambda^{11}}\{\frac{1}{8}(63 - 77\lambda^2 + 18\lambda^4)(\theta) + \frac{1}{120}\lambda a(945 - 525\lambda^2 + 4\lambda^4 - 4\lambda^6)\}$
$4, 1$	$\dfrac{c^3}{\lambda^{11}}\{\frac{1}{8}(63 - 84\lambda^2 + 24\lambda^4)(\theta) + \frac{1}{120}\lambda a(945 - 630\lambda^2 + 24\lambda^4)\}$
$0, 6$	$\dfrac{c^4}{\lambda^{13}}\{\frac{1}{16}(231 - 315\lambda^2 + 105\lambda^4 - 5\lambda^6)(\theta) + \frac{1}{240}\lambda a(3465 - 2415\lambda^2 + 273\lambda^4 + 39\lambda^6 + 38\lambda^8 + 40\lambda^{10})\}$
$2, 4$	$\dfrac{c^4}{\lambda^{13}}\{\frac{1}{16}(231 - 336\lambda^2 + 119\lambda^4 - 6\lambda^6)(\theta) + \frac{1}{240}\lambda a(3465 - 2730\lambda^2 + 273\lambda^4 - 4\lambda^6 - 4\lambda^8)\}$
$4, 2$	$\dfrac{c^4}{\lambda^{13}}\{\frac{1}{16}(231 - 357\lambda^2 + 140\lambda^4 - 8\lambda^6)(\theta) + \frac{1}{240}\lambda a(3465 - 3045\lambda^2 + 378\lambda^4 + 8\lambda^6)\}$
$6, 0$	$\dfrac{c^4}{\lambda^{13}}\{\frac{1}{16}(231 - 378\lambda^2 + 168\lambda^4 - 16\lambda^6)(\theta) + \frac{1}{240}\lambda a(3465 - 3360\lambda^2 + 588\lambda^4)\}$
$0, 7$	$\dfrac{c^5}{\lambda^{15}}\{\frac{1}{16}(429 - 693\lambda^2 + 315\lambda^4 - 35\lambda^6)(\theta) + \lambda a(\frac{429}{16} - \frac{407}{16}\lambda^2 + \frac{409}{80}\lambda^4 + \frac{53}{560}\lambda^6 + \frac{23}{168}\lambda^8 + \frac{29}{210}\lambda^{10} + \frac{1}{7}\lambda^{12})\}$
$2, 5$	$\dfrac{c^5}{\lambda^{15}}\{\frac{1}{16}(429 - 726\lambda^2 + 345\lambda^4 - 40\lambda^6)(\theta) + \lambda a(\frac{429}{16} - \frac{55}{2}\lambda^2 + \frac{449}{80}\lambda^4 - \frac{19}{280}\lambda^6 - \frac{1}{70}\lambda^8 - \frac{1}{105}\lambda^{10})\}$

$2m, M$	$(k/c^2)J_{2m,M}$
$4, 3$	$\dfrac{c^5}{\lambda^{15}}\left\{\frac{1}{16}(429 - 759\lambda^2 + 384\lambda^4 - 48\lambda^6)(\theta) + \lambda a\left(\frac{429}{16} - \frac{473}{16}\lambda^2 + \frac{267}{40}\lambda^4 - \frac{3}{70}\lambda^6 + \frac{1}{105}\lambda^8\right)\right\}$
$6, 1$	$\dfrac{c^5}{\lambda^{15}}\left\{\frac{1}{16}(429 - 792\lambda^2 + 432\lambda^4 - 64\lambda^6)(\theta) + \lambda a\left(\frac{429}{16} - \frac{253}{8}\lambda^2 + \frac{83}{10}\lambda^4 - \frac{1}{7}\lambda^6\right)\right\}$
$0, 8$	$\dfrac{c^6}{\lambda^{17}}\left\{\frac{1}{128}(6435 - 12012\lambda^2 + 6930\lambda^4 - 1260\lambda^6 + 35\lambda^8)(\theta)\right.$ $\left. + \lambda a\left(\frac{6435}{128} - \frac{3861}{64}\lambda^2 + \frac{1177}{64}\lambda^4 - \frac{229}{280}\lambda^6 + \frac{513}{4480}\lambda^8 + \frac{809}{6720}\lambda^{10} + \frac{41}{336}\lambda^{12} + \frac{1}{8}\lambda^{14}\right)\right\}$
$2, 6$	$\dfrac{c^6}{\lambda^{17}}\left\{\frac{1}{128}(6435 - 12441\lambda^2 + 7425\lambda^4 - 1395\lambda^6 + 40\lambda^8)(\theta)\right.$ $\left. + \lambda a\left(\frac{6435}{128} - \frac{8151}{128}\lambda^2 + \frac{2563}{128}\lambda^4 - \frac{4847}{4480}\lambda^6 - \frac{43}{2240}\lambda^8 - \frac{17}{1680}\lambda^{10} - \frac{1}{168}\lambda^{12}\right)\right\}$
$4, 4$	$\dfrac{c^6}{\lambda^{17}}\left\{\frac{1}{128}(6435 - 12870\lambda^2 + 8019\lambda^4 - 1584\lambda^6 + 48\lambda^8)(\theta)\right.$ $\left. + \frac{1}{8}\lambda a\left(\frac{6435}{16} - \frac{2145}{4}\lambda^2 + \frac{2871}{16}\lambda^4 - \frac{561}{56}\lambda^6 + \frac{1}{70}\lambda^8 + \frac{1}{35}\lambda^{10}\right)\right\}$
$6, 2$	$\dfrac{c^6}{\lambda^{17}}\left\{\frac{1}{128}(6435 - 13299\lambda^2 + 8712\lambda^4 - 1872\lambda^6 + 64\lambda^8)(\theta)\right.$ $\left. + \frac{1}{8}\lambda a\left(\frac{6435}{16} - \frac{9009}{16}\lambda^2 + \frac{1639}{8}\lambda^4 - \frac{941}{70}\lambda^6 - \frac{1}{7}\lambda^8\right)\right\}$
$8, 0$	$\dfrac{c^6}{\lambda^{17}}\left\{\frac{1}{128}(6435 - 13728\lambda^2 + 9504\lambda^4 - 2304\lambda^6 + 128\lambda^8)(\theta) + \frac{1}{8}\lambda a\left(\frac{6435}{16} - \frac{4719}{8}\lambda^2 + \frac{473}{2}\lambda^4 - \frac{761}{35}\lambda^6\right)\right\}$
$0, 9$	$\dfrac{c^7}{\lambda^{19}}\left\{\frac{1}{128}(12155 - 25740\lambda^2 + 18018\lambda^4 - 4620\lambda^6 + 315\lambda^8)(\theta)\right.$ $\left. + \frac{1}{8}\lambda a\left(\frac{12155}{16} - \frac{26455}{24}\lambda^2 + \frac{11011}{24}\lambda^4 - \frac{341}{7}\lambda^6 + \frac{5329}{5040}\lambda^8 + \frac{2131}{2520}\lambda^{10} + \frac{181}{210}\lambda^{12} + \frac{55}{63}\lambda^{14} + \frac{8}{9}\lambda^{16}\right)\right\}$
$2, 7$	$\dfrac{c^7}{\lambda^{19}}\left\{\frac{1}{128}(12155 - 26455\lambda^2 + 19019\lambda^4 - 5005\lambda^6 + 350\lambda^8)(\theta)\right.$ $\left. + \frac{1}{8}\lambda a\left(\frac{12155}{16} - \frac{55055}{48}\lambda^2 + \frac{7865}{16}\lambda^4 - \frac{6149}{112}\lambda^6 + \frac{89}{630}\lambda^8 - \frac{37}{420}\lambda^{10} - \frac{2}{35}\lambda^{12} - \frac{2}{63}\lambda^{14}\right)\right\}$
$4, 5$	$\dfrac{c^7}{\lambda^{19}}\left\{\frac{1}{128}(12155 - 27170\lambda^2 + 20163\lambda^4 - 5500\lambda^6 + 400\lambda^8)(\theta)\right.$ $\left. + \frac{1}{8}\lambda a\left(\frac{12155}{16} - \frac{3575}{3}\lambda^2 + \frac{25597}{48}\lambda^4 - \frac{10417}{168}\lambda^6 + \frac{109}{315}\lambda^8 + \frac{1}{45}\lambda^{10} + \frac{4}{315}\lambda^{12}\right)\right\}$
$6, 3$	$\dfrac{c^7}{\lambda^{19}}\left\{\frac{1}{128}(12155 - 27885\lambda^2 + 21450\lambda^4 - 6160\lambda^6 + 480\lambda^8)(\theta)\right.$ $\left. + \frac{1}{8}\lambda a\left(\frac{12155}{16} - \frac{59345}{48}\lambda^2 + \frac{7007}{12}\lambda^4 - \frac{2057}{28}\lambda^6 + \frac{20}{63}\lambda^8 - \frac{2}{63}\lambda^{10}\right)\right\}$
$8, 1$	$\dfrac{c^7}{\lambda^{19}}\left\{\frac{1}{128}(12155 - 28600\lambda^2 + 22880\lambda^4 - 7040\lambda^6 + 640\lambda^8)(\theta)\right.$ $\left. + \frac{1}{8}\lambda a\left(\frac{12155}{16} - \frac{30745}{24}\lambda^2 + \frac{3861}{6}\lambda^4 - \frac{649}{7}\lambda^6 + \frac{8}{9}\lambda^8\right)\right\}$
$0, 10$	$\dfrac{c^8}{\lambda^{21}}\left\{\frac{1}{256}(46189 - 109395\lambda^2 + 90090\lambda^4 - 30030\lambda^6 + 3465\lambda^8 - 63\lambda^{10})(\theta)\right.$ $\left. + \frac{1}{8}\lambda a\left(\frac{46189}{32} - \frac{235807}{96}\lambda^2 + \frac{19591}{15}\lambda^4 - \frac{125983}{560}\lambda^6 + \frac{79607}{10080}\lambda^8 + \frac{1577}{2016}\lambda^{10} + \frac{37}{48}\lambda^{12} + \frac{983}{1260}\lambda^{14} + \frac{71}{90}\lambda^{16} + \frac{4}{5}\lambda^{18}\right)\right\}$
$2, 8$	$\dfrac{c^8}{\lambda^{21}}\left\{\frac{1}{256}(46189 - 111826\lambda^2 + 94094\lambda^4 - 32032\lambda^6 + 3773\lambda^8 - 70\lambda^{10})(\theta)\right.$ $\left. + \frac{1}{8}\lambda a\left(\frac{46189}{32} - \frac{60775}{24}\lambda^2 + \frac{331331}{240}\lambda^4 - \frac{68497}{280}\lambda^6 + \frac{15763}{2016}\lambda^8 - \frac{71}{1260}\lambda^{10} - \frac{17}{280}\lambda^{12} - \frac{13}{315}\lambda^{14} - \frac{1}{45}\lambda^{16}\right)\right\}$
$4, 6$	$\dfrac{c^8}{\lambda^{21}}\left\{\frac{1}{256}(46189 - 114257\lambda^2 + 98527\lambda^4 - 34463\lambda^6 + 4180\lambda^8 - 80\lambda^{10})(\theta)\right.$ $\left. + \frac{1}{8}\lambda a\left(\frac{46189}{32} - \frac{250393}{96}\lambda^2 + \frac{234949}{160}\lambda^4 - \frac{60203}{224}\lambda^6 - \frac{9119}{1008}\lambda^8 + \frac{11}{210}\lambda^{10} + \frac{1}{70}\lambda^{12} + \frac{2}{315}\lambda^{14}\right)\right\}$

$2m, M$	$(k/c^2)J_{2m, M}$
6, 4	$\dfrac{c^8}{\lambda^{21}}\{\tfrac{1}{256}(46189 - 116688\lambda^2 + 103389\lambda^4 - 37466\lambda^6 + 4752\lambda^8 - 96\lambda^{10})(\theta)$ $\quad + \tfrac{1}{8}\lambda a(\tfrac{46189}{32} - \tfrac{128843}{48}\lambda^2 + \tfrac{753467}{480}\lambda^4 - \tfrac{84513}{280}\lambda^6 + \tfrac{3839}{360}\lambda^8 + \tfrac{2}{315}\lambda^{10} - \tfrac{2}{105}\lambda^{12})$
8, 2	$\dfrac{c^8}{\lambda^{21}}\{\tfrac{1}{256}(46189 - 119119\lambda^2 + 108680\lambda^4 - 41184\lambda^6 + 5632\lambda^8 - 128\lambda^{10})(\theta)$ $\quad + \tfrac{1}{8}\lambda a(\tfrac{46189}{32} - \tfrac{264979}{96}\lambda^2 + \tfrac{404261}{240}\lambda^4 - \tfrac{48763}{140}\lambda^6 + \tfrac{8921}{630}\lambda^8 + \tfrac{4}{45}\lambda^{10})\}$
10, 0	$\dfrac{c^8}{\lambda^{21}}\{\tfrac{1}{8}(\tfrac{46189}{32} - \tfrac{60775}{16}\lambda^2 + 3575\lambda^4 - 1430\lambda^6 + 220\lambda^8 - 8\lambda^{10})(\theta)$ $\quad + \tfrac{1}{8}\lambda a(\tfrac{46189}{32} - \tfrac{17017}{6}\lambda^2 + \tfrac{72501}{40}\lambda^4 - \tfrac{14443}{35}\lambda^6 + \tfrac{7381}{315}\lambda^8)\}$

When $\lambda = 1$, the swept-back wing becomes triangular. It has been verified for all the values $2m + M = 1, 2, \ldots 10$ that, in this case $\,'I_{2m, n} = \dfrac{c^{2m+n+1}}{k}\, T_{2m, n}$ (*see* Appendix V).

When the trailing edges of the swept-back wing are sonic, $\lambda = \varkappa$.

APPENDIX VII

Some General Formulae for the Lift, Drag, 'Interference' Drag, and Pitching Moments
of Cambered and Twisted Surfaces

All forces are normalised by dividing by $(\pi \rho V^2 c^2)/(k^2 E(\varkappa))$.

For the surface given by $z = -\delta x^n (ky)^{2m}/c^{R-1}$, where $R = 2m + n$, the load distribution can be put in the forms

$$p_r = \frac{2k}{\pi c^{R+1}} \sum_r \frac{c_r(ky)^{2r}x^{R-2r}}{X}, \quad \text{.. \quad .. \quad .. \quad .. \quad .. \quad .. \quad (VII.1)}$$

or

$$p_r = \frac{2k}{\pi c^{R+1}} \left[\frac{b_r x^R}{X} + X f(x, k^2 y^2) \right]. \quad \text{.. \quad .. \quad .. \quad .. \quad .. \quad (VII.2)}$$

(*See* Table 2), where the c_r are functions of $\varkappa$, and $b_r = \sum_r c_r$; and the incidence is

$$\alpha_r = \delta n x^{n-1}(ky)^{2m}/c^{R-1}. \quad \text{.. \quad .. \quad .. \quad .. \quad .. \quad (VII.3)}$$

In this Appendix, each summation $\sum_r$ is for $r = 0, 1, \ldots R/2$ if R is even, and $r = 0, 1, \ldots (R-\ )/2$ if R is odd.

Therefore, for a triangular surface:

the lift is

$$L_r = \int p_r \, dS = \frac{4\delta}{\pi} \sum_r (c_r T_{2r, R-2r})$$

$$= \frac{\delta}{R+1} \sum_r \left\{ \frac{c_r(2r)!}{2^{2r-1}(r!)^2} \right\}; \quad \text{.. \quad .. \quad .. \quad .. \quad (VII.4)}$$

the pressure integral is

$$D_r = \int p_r \alpha_r \, dS = \frac{4n}{\pi} \delta^2 \sum_r (c_r T_{2(m+r), R-2r+n-1})$$

$$= \frac{n\delta^2}{R} \sum_r \left\{ \frac{c_r[2(m+r)]!}{2^{2(m+r)}[(m+r)!]^2} \right\}; \quad \text{.. \quad .. \quad (VII.5)}$$

and the suction force is

$$S_r = 2\pi \rho \varkappa \int_0^c P_r^2 \, dx = \frac{\varkappa \delta^2}{E(\varkappa)} b_r^2 \frac{1}{2R}. \quad \text{.. \quad .. \quad .. \quad .. \quad (VII.6)}$$

The interference pressure integral for two surfaces given by $z_r = -\delta x^n (ky)^{2m}/c^{R-1}$, $z_s = -\delta x^N (ky)^{2M}/c^{Q-1}$, where $Q = 2M + N$, is: (Values of s in $\sum_s$ are the same as for r, with Q in place of R)

$$D_{r,s} = \int (p_r \alpha_s + p_s \alpha_r) \, dS$$

$$= \frac{4n\delta^2}{\pi} \sum_s \left(c_s T_{2(m+s), Q-2s+n-1} \right) + \frac{4N\delta^2}{\pi} \sum_r \left(c_r T_{2(M+r), R-2r+N-1} \right)$$

$$= \frac{\delta^2}{R+Q} \left[n \sum_s \left(\frac{c_s[2(m+s)]!}{2^{2m+2s-1}[(m+s)!]^2} \right) + N \sum_r \left(\frac{c_r[2(M+r)]!}{2^{2M+2r-1}[(M+r)!]^2} \right) \right]; \quad \text{.. \quad (VII.7)}$$

and the interference suction force is

$$S_{r,s} = 2\pi \rho \varkappa \int_0^c (2P_r P_s) \, dx = \frac{2\varkappa \delta^2}{E(\varkappa)} \frac{b_r b_s}{R+Q}. \cdot \text{.. \quad .. \quad .. \quad .. \quad (VII.8)}$$

The pitching moment, about the apex, for surface z_r is

$$M_r = \int p_r x \, dS = \frac{4\delta c}{\pi} \sum_r \left(c_r T_{2r,\, R-2r+1} \right)$$

$$= \frac{c\delta}{R+2} \sum_r \left(\frac{c_r (2r)!}{2^{2r-1}(r!)^2} \right) = \left(\frac{R+1}{R+2} \right) cL_r . \qquad \cdots \qquad \cdots \qquad \cdots \quad \text{(VII.9)}$$

The corresponding formulae for a swept-back surface with straight supersonic, or sonic, trailing edges are:

$$L_r = \frac{4\delta k}{\pi c^{R+1}} \sum_r \left(c_r I_{2r,\, R-2r} \right); \qquad \cdots \qquad \cdots \qquad \cdots \qquad \cdots \qquad \cdots \qquad \cdots \quad \text{(VII.10)}$$

$$D_r = \frac{4\delta^2 k}{\pi c^{2R}} \sum_r c_r I_{2(m+r),\, R-2r+n-1} \bigg); \qquad \cdots \qquad \cdots \qquad \cdots \qquad \cdots \qquad \cdots \quad \text{(VII.11)}$$

$$S_r = \frac{\varkappa \delta^2}{E(\varkappa)} \frac{1}{(1-a)^{2R}} b_r^{\,2} \frac{1}{2R}, \qquad \cdots \qquad \cdots \qquad \cdots \qquad \cdots \qquad \cdots \quad \text{(VII.12)}$$

where $a = h/k$;

$$D_{r,\,s} = \frac{4\delta^2 k}{\pi c^{R+Q}} \left[n \sum_s \left(c_s I_{2(m+s),\, Q-2s+n-1} \right) + N \sum_r \left(c_r I_{2(M+r),\, R-2r+N-1} \right) \right], \quad \text{(VII.13)}$$

$$S_{r,\,s} = \frac{2\varkappa \delta^2}{E(\varkappa)} \frac{1}{(1-a)^{R+Q}} \frac{b_r b_s}{R+Q}, \qquad \cdots \qquad \cdots \qquad \cdots \qquad \cdots \qquad \cdots \quad \text{(VII.14)}$$

$$M_r = \frac{4\delta k}{\pi c^{R+1}} \sum_r \left(c_r I_{2r,\, R-2r+1} \right) . \, \cdots \qquad \cdots \qquad \cdots \qquad \cdots \qquad \cdots \qquad \cdots \quad \text{(VII.15)}$$

For cambered triangular surfaces of the form $z = -\delta x^n / c^{n-1}$, $m = 0$, $R = n$, and it can be shown that

$$D_r = \frac{(n+1)\delta}{2} L_r \qquad \cdots \qquad \cdots \qquad \cdots \qquad \cdots \qquad \cdots \qquad \cdots \qquad \cdots \quad \text{(VII.16)}$$

$$D_{r,\,s} = \frac{\delta}{n+N} \left[n(N+1)L_s + N(n+1)L_r \right]$$

$$= \frac{2}{n+N} \left(n D_s + N D_r \right); \qquad \cdots \qquad \cdots \qquad \cdots \qquad \cdots \qquad \cdots \quad \text{(VII.17)}$$

$$d_r = \frac{(n+1)\delta}{2L_r}\,;$$

$$d_{r,\,s} = \frac{\delta}{n+N} \left[\frac{n(N+1)}{L_r} + \frac{N(n+1)}{L_s} \right]$$

$$= \frac{2}{n+N} \left[\frac{n(N+1)}{n+1} d_r + \frac{N(n+1)}{N+1} d_s \right]; \qquad \cdots \qquad \cdots \qquad \cdots \quad \text{(VII.18)}$$

$$S_r = \frac{\varkappa \delta^2}{E(\varkappa)} \frac{b_r^{\,2}}{2n}\,; \qquad \cdots \qquad \cdots \qquad \cdots \qquad \cdots \qquad \cdots \qquad \cdots \quad \text{(VII.19)}$$

$$S_{r,\,s} = \frac{2\varkappa \delta^2}{E(\varkappa)} \frac{b_r b_s}{n+N} . \qquad \cdots \qquad \cdots \qquad \cdots \qquad \cdots \qquad \cdots \qquad \cdots \quad \text{(VII.20)}$$

39

For triangular cambered (surface slope a function of x only) surfaces with sonic leading edges, $\varkappa = 0$, and

$$D_r = n\delta^2; \qquad\qquad d_r = \frac{(n+1)^2}{4n} = t_r; \qquad .. \qquad .. \qquad .. \quad (VII.21)$$

$$d_{r,s} = \frac{(n+1)(N+1)}{n+N} = t_{r,s}. \qquad .. \qquad .. \qquad .. \qquad .. \quad (VII.22)$$

In the limiting case, when $\varkappa \to 1$, i.e., $\tan\gamma/\tan\mu = (M^2-1)^{1/2}\tan\gamma \to 0$, for the cambered surfaces $z_r = -\delta x^n/c^{n-1}$, $z_s = -\delta x^N/c^{N-1}$, $b_r = n$, $L_r = n$, and hence $(n, N \geqslant 1)$

$$\left.\begin{aligned} d_r &= \frac{n+1}{2n} \\[4pt] s_r &= \frac{1}{2n} \end{aligned}\right\} t_r = \tfrac{1}{2} = t_s; \qquad\qquad \left.\begin{aligned} d_{r,s} &= \frac{n+N+2}{n+N} \\[4pt] s_{r,s} &= \frac{2}{n+N} \end{aligned}\right\} t_{r,s} = 1,$$

and therefore $t_r + t_s = t_{r,s}$, and $t_{r,s} = 2t_r = 2t_s$.

Also
$$t_{r,s} = 1 \text{ for all } n, N(\geqslant 1) \text{ for surfaces } z_r = -\frac{\delta x^n}{c^{n-1}}, z_s = -\frac{\delta x^N k^2 y^2}{c^{N+1}}$$

$$= \frac{4}{3} \text{ for all } n, N(\geqslant 1) \text{ for surfaces } z_r = -\frac{\delta x^n k^2 y^2}{c^{n+1}}, z_s = -\frac{\delta x^N k^2 y^2}{c^{N+1}}$$

$$t_r = \frac{2}{3} \text{ for all } n \geqslant 1 \text{ for cambered and twisted surfaces } z_r = -\frac{\delta x^n k^2 y^2}{c^{n+1}}.$$

There are indications that similar results hold for higher powers of $k^2 y^2$ in z_r and z_s.

APPENDIX VIII

Numerical Values of a_m, b_m

$\dfrac{\tan \gamma}{\tan \mu}$	a_1	b_1	a_2	b_2	a_3	b_3	$\varkappa^2$
0	0·666667	0·047619	1·111111	0·111111	2	1	1
0·1	0·664970	0·047377	1·103081	0·109729	1·987504	0·987535	0·99
0·2	0·659505	0·046607	1·079320	0·105663	1·950064	0·950562	0·96
0·3	0·648970	0·045153	1·040976	0·099180	1·887832	0·890340	0·91
0·4	0·630543	0·042697	0·990590	0·090794	1·801089	0·808960	0·84
0·5	0·598776	0·038677	0·933138	0·081362	1·690307	0·709326	0·75
0·6	0·544852	0·032358	0·876653	0·072022	1·556272	0·595150	0·64
0·7	0·459468	0·023469	0·829013	0·063494	1·400408	0·471012	0·51
0·7211	0·436934	0·021341	0·820339	0·061748	1·364949	0·444048	0·48
0·8	0·338897	0·013161	0·790825	0·054722	1·225834	0·342758	0·36
0·9	0·184935	0·004078	0·750701	0·040478	1·042142	0·219831	0·19
1·0	0	0	0·666667	0	0·888889	0·126984	0

41

APPENDIX IX

Numerical Values of λ_m', λ_m'', λ_m'''

tan γ/tan μ	$k^4\lambda_1'$	$k^4\lambda_2'$	$k^4\lambda_3'$	$k^6\lambda_1''$	$k^6\lambda_2''$	$k^6\lambda_3''$	$k^8\lambda_1'''$	$k^8\lambda_2'''$	$k^8\lambda_3'''$	$\varkappa^2$
0	2·62500	−1·68750	0·06250							1
0·1	2·69840	−1·74222	0·06413	0·68660	114·06225	−12·70684	0·32045	86·20341	10177·588	0·9
0·2	2·93344	−1·91772	0·06934	0·78825	29·67611	− 3·33745	0·40779	22·81665	654·9521	0·96
0·3	3·37805	−2·24977	0·07930	0·99635	14·03547	− 1·61400	0·53905	11·15200	137·3924	0·91
0·4	4·11647	−2·79575	0·09651	1·39406	8·49012	− 1·02646	0·80435	7·10968	47·44718	0·84
0·5	5·24759	−3·59616	0·12636	2·13750	5·74962	− 0·93854	1·33448	5·22539	21·88458	0·75
0·6	6·82132	−4·56100	0·18108	3·46218	3·99047	− 0·67115	2·36691	4·13520	12·33554	0·64
0·7	9·07704	−5·52492	0·29250	5·75745	2·74579	− 0·65701	4·32642	3·53619	8·15027	0·51
0·7112	9·42255	−5·63968	0·31157	6·11835	2·63678	− 0·66066	4·64624	3·28446	7·85596	0·4942
0·7211	9·75534	−5·74514	0·33006	6·46478	2·54675	− 0·66486	4·95533	3·49116	7·60481	0·48
0·8	14·04160	−6·88558	0·56013	10·78680	2·00364	− 0·73407	8·90245	3·75386	6·18168	0·36
0·9	23·96306	−8·93885	0·97539	20·41064	1·77704	− 0·85380	17·92285	3·06294	5·45887	0·19

42

APPENDIX X

Triangular Wing—Numerical Values of d_r, $d_{r,s}$; t_r, $t_{r,s}$, $\tan\gamma/\tan\mu = 0\cdot7338$, $(d_{r,r} \equiv 2d_r;\ t_{r,r} \equiv 2t_r)$ $\varkappa^2 = 0\cdot4615$

	r	z_r	d_r	$d_{1,r}$	$d_{2,r}$	$d_{3,r}$	$d_{4,r}$	$d_{5,r}$	$d_{6,r}$
Camber	1	$-\delta x$	1	2	1·923941	1·895608	1·881686	2·474180	2·426818
	2	$-\dfrac{\delta}{c}x^2$	1·039434	1·923941	2·078867	2·183459	2·257038	2·582909	2·641195
	3	$-\dfrac{\delta}{c^2}x^3$	1·194144	1·895608	2·183459	2·388288	2·538991	2·689460	2·830092
	4	$-\dfrac{\delta}{c^3}x^4$	1·377634	1·881686	2·257034	2·538991	2·755268	2·783406	2·990803
Twist	5	$-\dfrac{\delta}{c^2}k^2y^2x$	2·431522	2·474180	2·582909	2·689460	2·783406	4·863045	5·071779
Camber and twist	6	$-\dfrac{\delta}{c^3}k^2y^2x^2$	2·699749	2·426818	2·641195	2·830092	2·990803	5·071779	5·399497

r		t_r	$t_{1,r}$	$t_{2,r}$	$t_{3,r}$	$t_{4,r}$	$t_{5,r}$	$t_{6,r}$
1		0·752024	1·504048	1·593306	1·636966	1·663251	1·743092	1·794006
2		0·915446	1·593306	1·830891	1·976545	2·075004	1·998040	2·113852
3		1·104222	1·636966	1·976545	2·208444	2·376255	2·181104	2·358642
4		1·302473	1·663251	2·075004	2·376255	2·604945	2·323410	2·555314
5		1·713052	1·743092	1·998039	2·181104	2·323410	3·426106	3·739158
6		2·068936	1·794006	2·113852	2·358642	2·555314	3·739158	4·137873

43

Triangular Wing—Numerical Values of d_r, $d_{r,s}$, $\tan \gamma/\tan \mu = 0\cdot7$, $\kappa^2 = 0\cdot51$

r	z_r	d_r	$d_{1,r}$	$d_{2,r}$	$d_{3,r}$	$d_{4,r}$	$d_{8,r}$	$d_{5,r}$	$d_{6,r}$	$d_{9,r}$	$d_{10,r}$
1	$-\delta x$	1	$(2d_1 = 2)$	$1\cdot9127$	$1\cdot8796$	$1\cdot8643$	$1\cdot8511$	$2\cdot4656$	$2\cdot4115$	$2\cdot3688$	$2\cdot8037$
2	$-\dfrac{\delta}{c}x^2$	$1\cdot0267$	$1\cdot9127$	$(2d_2=2\cdot0534)$	$2\cdot1506$	$2\cdot2215$	$2\cdot2677$	$2\cdot5609$	$2\cdot6112$	$2\cdot6400$	$2\cdot9771$
3	$-\dfrac{\delta}{c^2}x^3$	$1\cdot1728$	$1\cdot8796$	$2\cdot1506$	$(2d_3=2\cdot3456)$	$2\cdot4908$	$2\cdot5960$	$2\cdot6577$	$2\cdot7885$	$2\cdot8798$	$3\cdot1575$
4	$-\dfrac{\delta}{c^3}x^4$	$1\cdot3508$	$1\cdot8643$	$2\cdot2215$	$2\cdot4908$	$(2d_4=2\cdot7016)$	$2\cdot8593$	$2\cdot7498$	$2\cdot9451$	$3\cdot0912$	$3\cdot3337$
8	$-\dfrac{\delta}{c^4}x^5$	$1\cdot5320$	$1\cdot8511$	$2\cdot2677$	$2\cdot5960$	$2\cdot8593$	$(2d_8=3\cdot0640)$	$2\cdot8186$	$3\cdot0686$	$3\cdot2602$	$3\cdot4771$
5	$-\dfrac{\delta}{c^2}k^2y^2x$	$2\cdot3983$	$2\cdot4656$	$2\cdot5609$	$2\cdot6577$	$2\cdot7498$	$2\cdot8186$	$(2d_5=4\cdot7966)$	$4\cdot9905$	$5\cdot1302$	$6\cdot5855$
6	$-\dfrac{\delta}{c^3}k^2y^2x^2$	$2\cdot6500$	$2\cdot4115$	$2\cdot6112$	$2\cdot7885$	$2\cdot9451$	$3\cdot0686$	$4\cdot9905$	$(2d_6=5\cdot3000)$	$5\cdot5345$	$7\cdot0168$
9	$-\dfrac{\delta}{c^4}k^2y^2x^3$	$2\cdot9255$	$2\cdot3688$	$2\cdot6400$	$2\cdot8798$	$3\cdot0912$	$3\cdot2602$	$5\cdot1302$	$5\cdot5345$	$(2d_9=5\cdot8510)$	$7\cdot3501$
10	$-\dfrac{\delta}{c^4}k^4y^4x$	$4\cdot9649$	$2\cdot8037$	$2\cdot9771$	$3\cdot1575$	$3\cdot3337$	$3\cdot4771$	$6\cdot5855$	$7\cdot0168$	$7\cdot3501$	$(2d_{10}=9\cdot9298)$

Triangular Wing—Numerical Values of t_r, $t_{r,s}$, $\tan \gamma / \tan \mu = 0\cdot7$, $\varkappa^2 = 0\cdot51$

r	z_r	t_r	$t_{1,r}$	$t_{2,r}$	$t_{3,r}$	$t_{4,r}$	$t_{8,r}$	$t_{5,r}$	$t_{6,r}$	$t_{9,r}$	$t_{10,r}$
1	$-\delta x$	0·7346	$(2t_1 = 1\cdot4692)$	1·5589	1·6036	1·6314	1·6462	1·6935	1·7420	1·7737	1·8357
2	$-\dfrac{\delta}{c} x^2$	0·8940	1·5589	$(2t_2 = 1\cdot7880)$	1·9298	2·0274	2·0921	1·9432	2·0543	2·1299	2·1474
3	$-\dfrac{\delta}{c^2} x^3$	1·0771	1·6036	1·9298	$(2t_3 = 2\cdot1542)$	2·3177	2·4366	2·1222	2·2919	2·4156	2·4024
4	$-\dfrac{\delta}{c^3} x^4$	1·2709	1·6314	2·0274	2·3177	$(2t_4 = 2\cdot5418)$	2·7094	2·2659	2·4868	2·6558	2·6256
8	$-\dfrac{\delta}{c^4} x^5$	1·4608	1·6462	2·0921	2·4366	2·7094	$(2t_8 = 2\cdot9216)$	2·3715	2·6383	2·8466	2·8043
5	$-\dfrac{\delta}{c^2} k^2 y^2 x$	1·6495	1·6935	1·9432	2·1222	2·2659	2·3715	$(2t_5 = 3\cdot2990)$	3·6018	3·8316	4·4732
6	$-\dfrac{\delta}{c^3} k^2 y^2 x^2$	1·9922	1·7420	2·0543	2·2919	2·4868	2·6383	3·6018	$(2t_6 = 3\cdot9844)$	4·2849	4·9843
9	$-\dfrac{\delta}{c^4} k^2 y^2 x^3$	2·3249	1·7737	2·1299	2·4156	2·6558	2·8466	3·8316	4·2849	$(2t_9 = 4\cdot6498)$	5·3961
10	$-\dfrac{\delta}{c^4} k^4 y^4 x$	3·3758	1·8357	2·1474	2·4024	2·6256	2·8043	4·4732	4·9843	5·3961	$(2t_{10} = 6\cdot7516)$

Triangular Wing—Numerical Values of d_r, $d_{r,s}$; t_r, $t_{r,s}$, $\tan\gamma/\tan\mu = 0.3577$, $x^2 = 0.87205$

r	z_r	d_r	$d_{1,r}$	$d_{2,r}$	$d_{3,r}$	$d_{4,r}$	$d_{5,r}$	$d_{6,r}$
1	$-\delta x$	1	2	1·782636	1·687146	1·636244	2·288764	2·174058
2	$-\dfrac{\delta}{c}x^2$	0·880465	1·782636	1·760930	1·763738	1·773600	2·227927	2·201272
3	$-\dfrac{\delta}{c^2}x^3$	0·916195	1·687146	1·763738	1·832389	1·890558	2·210661	2·245122
4	$-\dfrac{\delta}{c^3}x^4$	0·994132	1·636244	1·773600	1·890558	1·988264	2·213120	2·293638
5	$-\dfrac{\delta}{c^2}k^2y^2x$	1·908894	2·288764	2·227927	2·210661	2·213120	3·817787	3·847113
6	$-\dfrac{\delta}{c^3}k^2y^2x^2$	1·976767	2·174058	2·201272	2·245122	2·293638	3·847113	3·953534

r		t_r	$t_{1,r}$	$t_{2,r}$	$t_{3,r}$	$t_{4,r}$	$t_{5,r}$	$t_{6,r}$
1		0·585662	1·171324	1·230185	1·267308	1·292864	1·276311	1·306216
2		0·673296	1·230185	1·346592	1·427868	1·487450	1·417965	1·478070
3		0·774391	1·267308	1·427868	1·548783	1·642031	1·526734	1·617007
4		0·882970	1·292864	1·487450	1·642031	1·765940	1·613788	1·731748
5		1·084236	1·276311	1·417965	1·526734	1·613788	2·168472	2·332391
6		1·266720	1·306216	1·478070	1·617007	1·731748	2·332391	2·533439

Triangular Wing—Numerical Values of d_r, $d_{r,s}$; t_r, $t_{r,s}$, $\tan\gamma/\tan\mu = 0\cdot1184$, $\varkappa^2 = 0\cdot9860$

r	z_r	d_r	$d_{1,r}$	$d_{2,r}$	$d_{3,r}$	$d_{4,r}$	$d_{5,r}$	$d_{6,r}$
1	$-\delta x$	1	2	$1\cdot690196$	$1\cdot539986$	$1\cdot452816$	$2\cdot070965$	$1\cdot895328$
2	$-\dfrac{\delta}{c} x^2$	$0\cdot776470$	$1\cdot690196$	$1\cdot552940$	$1\cdot476218$	$1\cdot428765$	$1\cdot899199$	$1\cdot795377$
3	$-\dfrac{\delta}{c^2} x^3$	$0\cdot719981$	$1\cdot539986$	$1\cdot476218$	$1\cdot439962$	$1\cdot418289$	$1\cdot791546$	$1\cdot731226$
4	$-\dfrac{\delta}{c^3} x^4$	$0\cdot707526$	$1\cdot452816$	$1\cdot428765$	$1\cdot418289$	$1\cdot415051$	$1\cdot719606$	$1\cdot688400$
5	$-\dfrac{\delta}{c^2} k^2 y^2 x$	$1\cdot461410$	$2\cdot070965$	$1\cdot899199$	$1\cdot791546$	$1\cdot719606$	$2\cdot922819$	$2\cdot787716$
6	$-\dfrac{\delta}{c^3} k^2 y^2 x^2$	$1\cdot352096$	$1\cdot895328$	$1\cdot795377$	$1\cdot731226$	$1\cdot688400$	$2\cdot787716$	$2\cdot704192$

r		t_r	$t_{1,r}$	$t_{2,r}$	$t_{3,r}$	$t_{4,r}$	$t_{5,r}$	$t_{6,r}$
1		$0\cdot513743$	$1\cdot027486$	$1\cdot041853$	$1\cdot052911$	$1\cdot061892$	$1\cdot052880$	$1\cdot062009$
2		$0\cdot533342$	$1\cdot041853$	$1\cdot066683$	$1\cdot086558$	$1\cdot102995$	$1\cdot084731$	$1\cdot100945$
3		$0\cdot557350$	$1\cdot052911$	$1\cdot086558$	$1\cdot114700$	$1\cdot138588$	$1\cdot111681$	$1\cdot134997$
4		$0\cdot584759$	$1\cdot061892$	$1\cdot102995$	$1\cdot138588$	$1\cdot169518$	$1\cdot134974$	$1\cdot165007$
5		$0\cdot750881$	$1\cdot052880$	$1\cdot084731$	$1\cdot111681$	$1\cdot134974$	$1\cdot501763$	$1\cdot541476$
6		$0\cdot794247$	$1\cdot062009$	$1\cdot100945$	$1\cdot134997$	$1\cdot165007$	$1\cdot541476$	$1\cdot588494$

47

APPENDIX X—*continued*

Triangular Wing (Sonic Leading Edges)—Numerical Values of $d_r = t_r$, $d_{r,s} = t_{r,s}$, $\tan \gamma/\tan \mu = 1$, $\varkappa = 0$

r	z_r	t_r	$t_{1,r}$	$t_{2,r}$	$t_{3,r}$	$t_{4,r}$	$t_{8,r}$	$t_{5,r}$	$t_{6,r}$
1	$-\delta x$	1	2	2	2	2	2	5/2	5/2
2	$-\dfrac{\delta x^2}{c}$	9/8	2	9/4	12/5	5/2	18/7	27/10	45/16
3	$-\dfrac{\delta}{c^2}x^3$	4/3	2	12/5	8/3	20/7	3	43/15	43/14
4	$-\dfrac{\delta}{c^3}x^4$	25/16	2	5/2	20/7	25/8	10/3	3	105/32
8	$-\dfrac{\delta}{c^4}x^5$	9/5	2	18/7	3	10/3	18/5		
	$-\dfrac{\delta}{c^{n-1}}x^n$	$\dfrac{(n+1)^2}{4n} \to \dfrac{n}{4}$	2	$\dfrac{3(n+1)}{n+2}$	$\dfrac{4(n+1)}{n+3}$	$\dfrac{5(n+1)}{n+4}$	$\dfrac{6(n+1)}{n+5}$		
5	$-\dfrac{\delta}{c^2}xk^2y^2$	13/5	5/2	27/10	43/15	3		26/5	11/2
6	$-\dfrac{\delta}{c^3}x^2k^2y^2$	95/32	5/2	45/16	43/14	105/32		11/2	95/16

Triangular Wing—Numerical Values of d_r, $d_{r,s}$; t_r, $t_{r,s}$, $\tan\gamma/\tan\mu = 0$, $\varkappa = 1$

r	z_r	d_r	$d_{1,r}$	$d_{2,r}$	$d_{3,r}$	$d_{4,r}$	$d_{8,r}$	$d_{5,r}$	$d_{6,r}$	t_1	$t_{1,r}$	$t_{2,r}$	$t_{3,r}$	$t_{4,r}$	$t_{8,r}$	$t_{5,r}$	$t_{6,r}$
1	$-\delta x$	1	2	5/3	3/2	7/5	4/3	2	9/5	1/2	1	1	1	1	1	1	1
2	$-\dfrac{\delta}{c}x^2$	3/4	5/3	3/2	7/5	4/3	9/7	9/5	5/3	1/2	1	1	1	1	1	1	1
3	$-\dfrac{\delta}{c^2}x^3$	2/3	3/2	7/5	4/3	9/7	5/4	5/3	11/7	1/2	1	1	1	1	1	1	1
4	$-\dfrac{\delta}{c^3}x^4$	5/8	7/5	4/3	9/7	5/4	11/9	11/7	3/2	1/2	1	1	1	1	1	1	1
8	$-\dfrac{\delta}{c^4}x^5$	3/5	4/3	9/7	5/4	11/9	6/5	3/2	13/9	1/2	1	1	1	1	1	1	1
n	$-\dfrac{\delta}{c^{n-1}}x^n$	$\dfrac{n+1}{2n}\to\tfrac12$	$\dfrac{n+3}{n+1}$	$\dfrac{n+4}{n+2}$	$\dfrac{n+5}{n+3}$	$\dfrac{n+6}{n+4}$	$\dfrac{n+7}{n+5}$										
5	$-\dfrac{\delta}{c^2}xk^2y^2$	4/3	2	9/5	5/3	11/7	3/2	8/3	52/21	2/3	1	1	1	1	1	4/3	4/3
6	$-\dfrac{\delta}{c^3}x^2k^2y^2$	7/6	9/5	5/3	11/7	3/2	13/9	52/21	7/3	2/3	1	1	1	1	1	4/3	4/3
N	$-\dfrac{\delta}{c^{N+1}}x^Nk^2y^2$	$\dfrac{3N+1}{3N}\to 1$	$\dfrac{N+7}{N+3}$	$\dfrac{N+8}{N+4}$	$\dfrac{N+9}{N+5}$	$\dfrac{N+10}{N+6}$	$\dfrac{N+11}{N+7}$										

All forces and moments are normalised by dividing by $(\pi \rho V^2 c^2)/(k^2 E(\varkappa))$.

TABLE 3

Formulae for the Total Lift on Triangular Surfaces

r	z_r	L_r	
1	$-\delta x$	δ	
2	$-\dfrac{\delta}{c} x^2$	$\dfrac{\delta}{f_1}$	
3	$-\dfrac{\delta}{c^2} x^3$	$\tfrac{3}{4}\delta F_1(4f_5 - 3f_7)$	Camber
4	$-\dfrac{\delta}{c^3} x^4$	$\delta F_2(4f_{11} - 3f_{13})$	
5	$-\dfrac{\delta}{c^2} k^2 y^2 x$	$\tfrac{3}{4}\delta F_1(4f_4 - f_6)$	Twist
6	$-\dfrac{\delta}{c^3} k^2 y^2 x^2$	$\tfrac{1}{2}\delta F_2(4f_{10} - 3f_{12})$	Camber and twist
7	$f_4 z_3 - f_5 z_5$	$\tfrac{3}{4}\delta$	
8	$-\dfrac{\delta}{c^4} x^5$	$\dfrac{\delta}{8} F_3(8f_{14} + 2f_{15} + f_{16})$	Camber
9	$-\dfrac{\delta}{c^4} k^2 y^2 x^3$	$-\dfrac{\delta}{8} F_3(8f_{17} + 2f_{18} + f_{19})$	Camber and twist
10	$-\dfrac{\delta}{c^4} k^4 y^4 x$	$\dfrac{\delta}{8} F_3(8f_{20} + 2f_{21} + f_{22})$	Twist

TABLE 4

Formulae for the Pressure Integral for Triangular Surfaces

r	D_r
1	δ^2
2	$\frac{3}{2}\delta^2/f_1$
3	$\frac{3}{2}\delta^2 F_1(4f_5 - 3f_7)$
4	$\frac{5}{2}\delta^2 F_2(4f_{11} - 3f_{13})$
5	$\frac{1}{8}\delta^2 F_1(6f_4 - f_6)$
6	$\frac{7}{16}\delta^2 F_2(2f_{10} - f_{12})$
7	$\frac{1}{8}\delta^2(12f_4 - f_5)$
8	$\frac{3}{8}\delta^2 F_3(8f_{14} + 2f_{15} + f_{16})$
9	$-\frac{3}{80}\delta^2 F_3(16f_{17} + 8f_{18} + 5f_{19})$
10	$\dfrac{\delta^2}{128}F_3(16f_{20} + 10f_{21} + 7f_{22})$

TABLE 5

Formulae for the Suction Force on Triangular Surfaces

r	$(E(\varkappa)/\varkappa)S_r$
1	$\frac{1}{2}\delta^2$
2	$\frac{1}{4}(\delta/f_1)^2$
3	$\frac{3}{2}\delta^2(F_1 f_5)^2$
4	$2\delta^2(F_2 f_{11})^2$
5	$\frac{3}{2}\delta^2(F_1 f_4)^2$
6	$\frac{1}{2}\delta^2(F_2 f_{10})^2$
7	0
8	$\frac{1}{10}\delta^2 F_3{}^2(f_{14} + f_{15} + f_{16})^2$
9	$\frac{1}{10}\delta^2 F_3{}^2(f_{17} + f_{18} + f_{19})^2$
10	$\frac{1}{10}\delta^2 F_3{}^2(f_{20} + f_{21} + f_{22})^2$

TABLE 6

Formulae for the 'Interference' Pressure Integral for Triangular Surfaces

$(D_{r,s} - D_{s,r}$ is the interference pressure integral for the two surfaces given by z_r, $z_s)$

r, s	$D_{r,s}$
1, 2	$\frac{1}{3}\frac{\delta^2}{f_1}(4f_1 + 3)$
1, 3	$\frac{3}{4}\delta^2\{2 + F_1(4f_5 - 3f_7)\}$
1, 4	$\frac{1}{5}\delta^2\{8 + 5F_2(4f_{11} - 3f_{13})\}$
1, 5	$\frac{1}{4}\delta^2[1 + 3F_1(4f_4 - f_6)]$
1, 6	$\frac{1}{10}\delta^2\{4 + 5F_2(4f_{10} - 3f_{12})]$
1, 8	$\frac{1}{24}\delta^2[40 + 3F_3(8f_{14} + 2f_{15} + f_{16})]$
1, 9	$\frac{1}{8}\delta^2\{4 - F_3(8f_{17} + 2f_{18} + f_{19})]$
1, 10	$\frac{1}{8}\delta^2[1 + F_3(8f_{20} + 2f_{21} + f_{22})]$
2, 3	$\frac{3}{5}\delta^2\left[\frac{3}{f_1} + F_1(8f_5 - 6f_7)\right]$
2, 4	$\frac{1}{8}\delta^2\left[\frac{6}{f_1} + 5F_2(4f_{11} - 3f_{13})\right]$
2, 5	$\frac{1}{5}\delta^2\left[\frac{5}{4f_1} + 6F_1(4f_4 - f_6)\right]$
2, 6	$\frac{1}{12}\delta^2\left[\frac{5}{f_1} + 10F_2(4f_{10} - 3f_{12})\right]$
2, 8	$\frac{3}{14}\delta^2\left[\frac{10}{f_1} + F_3(8f_{14} + 2f_{15} + f_{16})\right]$
2, 9	$\frac{3}{14}\delta^2\left[\frac{5}{2f_1} - F_3(8f_{17} + 2f_{18} + f_{19})\right]$
2, 10	$\frac{1}{14}\delta^2\left[\frac{7}{4f_1} + 3F_3(8f_{20} + 2f_{21} + f_{22})\right]$
3, 4	$\frac{3}{7}\delta^2[4F_1(4f_5 - 3f_7) + 5F_2(4f_{11} - 3f_{13})]$
3, 5	$\frac{3}{8}\delta^2 F_1[16f_4 - 4f_6 + 2f_5 - f_7]$
3, 6	$\frac{3}{14}\delta^2[5F_2(4f_{10} - 3f_{12}) + 3F_1(2f_5 - f_7)]$
3, 8	$\frac{3}{32}\delta^2[20F_1(4f_5 - 3f_7) + 3F_3(8f_{14} + 2f_{15} + f_{16})]$
3, 9	$\frac{9}{32}\delta^2[3F_1(2f_5 - f_7) - F_3(8f_{17} + 2f_{18} + f_{19})]$
3, 10	$\frac{3}{64}\delta^2[F_1(8f_5 - 3f_7) + 6F_3(8f_{20} + 2f_{21} + f_{22})]$
4, 5	$\frac{1}{14}\delta^2[24F_1(4f_4 - f_6) + 7F_2(2f_{11} - f_{13})]$

52

TABLE 6—*continued*

r, s	$D_{r,s}$
4, 6	$\frac{1}{8}\delta^2 F_2[10(4f_{10} - 3f_{12}) + 7(2f_{11} - f_{13})]$
4, 8	$\frac{1}{9}\delta^2[25F_2(4f_{11} - 3f_{13}) + 3F_3(8f_{14} + 2f_{15} + f_{16})]$
4, 9	$\frac{1}{6}\delta^2[7F_2(2f_{11} - f_{13}) - 2F_3(8f_{17} + 2f_{18} + f_{19})]$
4, 10	$\frac{1}{48}\delta^2[3F_2(8f_{11} - 3f_{13}) + 16F_3(8f_{20} + 2f_{21} + f_{22})]$
5, 6	$\frac{1}{28}\delta^2[6F_1(6f_4 - f_6) + 7F_2(2f_{10} - f_{12})]$
5, 8	$\frac{1}{64}\delta^2[120F_1(4f_4 - f_6) + F_3(16f_{14} + 8f_{15} + 5f_{16})]$
5, 9	$\frac{1}{64}\delta^2[18F_1(6f_4 - f_6) - F_3(16f_{17} + 8f_{18} + 5f_{19})]$
5, 10	$\frac{1}{64}\delta^2[3F_1(8f_4 - f_6) + F_3(16f_{20} + 8f_{21} + 5f_{22})]$
6, 8	$\frac{1}{36}\delta^2[50F_2(4f_{10} - 3f_{12}) + F_3(16f_{14} + 8f_{15} + 5f_{16})]$
6, 9	$\frac{1}{36}\delta^2[21F_2(2f_{10} - f_{12}) - F_3(16f_{17} + 8f_{18} + 5f_{19})]$
6, 10	$\frac{1}{288}\delta^2[9F_2(8f_{10} - 3f_{12}) + 8F_3(16f_{20} + 8f_{21} + 5f_{22})]$
8, 9	$\frac{3}{80}\delta^2 F_3[16f_{14} + 8f_{15} + 5f_{16} - 10(8f_{17} + 2f_{18} + f_{19})]$
8, 10	$\frac{1}{128}\delta^2 F_3[16f_{14} + 10f_{15} + 7f_{16} + 48(8f_{20} + 2f_{21} + f_{22})]$
9, 10	$\frac{1}{640}\delta^2 F_3[24(16f_{20} + 8f_{21} + 5f_{22}) - 5(16f_{17} + 10f_{18} + 7f_{19})]$

TABLE 7

Formulae for the 'Interference' Suction Force for Triangular Surfaces

$(S_{r,s} = S_{s,r}$ is the interference suction force for surfaces given by z_r, z_s)

r, s	$(E(x)/x)S_{r,s}$
1, 2	$2\delta^2/(3f_1)$
1, 3	$\frac{3}{2}\delta^2(F_1 f_5)$
1, 4	$\frac{9}{5}\delta^2(F_2 f_{11})$
1, 5	$\frac{3}{2}\delta^2(F_1 f_4)$
1, 6	$\frac{4}{3}\delta^2(F_2 f_{10})$
1, 8	$\frac{1}{3}\delta^2 F_3(f_{14}+f_{15}+f_{16})$
1, 9	$-\frac{1}{3}\delta^2 F_3(f_{17}+f_{18}+f_{19})$
1, 10	$\frac{1}{3}\delta^2 F_3(f_{20}+f_{21}+f_{22})$
2, 3	$\frac{6}{5}\delta^2(F_1 f_5/f_1)$
2, 4	$\frac{4}{3}\delta^2(F_2 f_{11}/f_1)$
2, 5	$\frac{9}{5}\delta^2(F_1 f_4/f_1)$
2, 6	$\frac{8}{3}\delta^2(F_2 f_{10}/f_1)$
2, 8	$\frac{2}{7}\delta^2(F_3/f_1)(f_{14}+f_{15}+f_{16})$
2, 9	$-\frac{2}{7}\delta^2(F_3/f_1)(f_{17}+f_{18}+f_{19})$
2, 10	$\frac{2}{7}\delta^2(F_3/f_1)(f_{20}+f_{21}+f_{22})$
3, 4	$\frac{24}{7}\delta^2(F_1 f_5)(F_2 f_{11})$
3, 5	$3\delta^2(F_1 f_5)(F_1 f_4)$
3, 6	$\frac{12}{7}\delta^2(F_1 f_5)(F_2 f_{10})$
3, 8	$\frac{3}{4}\delta^2(F_1 f_5)F_3(f_{14}+f_{15}+f_{16})$
3, 9	$-\frac{3}{4}\delta^2(F_1 f_5)F_3(f_{17}+f_{18}+f_{19})$
3, 10	$\frac{3}{4}\delta^2(F_1 f_5)F_3(f_{20}+f_{21}+f_{22})$
4, 5	$\frac{24}{7}\delta^2(F_2 f_{11})(F_1 f_4)$
4, 6	$2\delta^2(F_2 f_{11})(F_2 f_{10})$
4, 8	$\frac{8}{5}\delta^2(F_2 f_{11})F_3(f_{14}+f_{15}+f_{16})$
4, 9	$-\frac{8}{5}\delta^2(F_2 f_{11})F_3(f_{17}+f_{18}+f_{19})$
4, 10	$\frac{8}{5}\delta^2(F_2 f_{11})F_3(f_{20}+f_{21}+f_{22})$
5, 6	$\frac{12}{7}\delta^2(F_1 f_4)(F_2 f_{10})$
5, 8	$\frac{3}{4}\delta^2(F_1 f_4)F_3(f_{14}+f_{15}+f_{16})$
5, 9	$-\frac{3}{4}\delta^2(F_1 f_4)F_3(f_{17}+f_{18}+f_{19})$
5, 10	$\frac{3}{4}\delta^2(F_1 f_4)F_3(f_{20}+f_{21}+f_{22})$
6, 8	$\frac{4}{5}\delta^2(F_2 f_{10})F_3(f_{14}+f_{15}+f_{16})$
6, 9	$-\frac{4}{5}\delta^2(F_2 f_{10})F_3(f_{17}+f_{18}+f_{19})$
6, 10	$\frac{4}{3}\delta^2(F_2 f_{10})F_3(f_{20}+f_{21}+f_{22})$
8, 9	$-\frac{1}{5}\delta^2 F_3^2(f_{14}+f_{15}+f_{16})(f_{17}+f_{18}+f_{19})$
8, 10	$\frac{1}{5}\delta^2 F_3^2(f_{14}+f_{15}+f_{16})(f_{20}+f_{21}+f_{22})$
9, 10	$-\frac{1}{5}\delta^2 F_3^2(f_{17}+f_{18}+f_{19})(f_{20}+f_{21}+f_{22})$

TABLE 8

Formulae for the Total Lift on Swept-back Surfaces

r	$(\pi c^2/k)L_r$
1	$4\delta(J_{0,2} - J_{2,0})$
2	$\dfrac{4\delta}{cf_1}(J_{0\,3} - J_{2,1})$
3	$12\,\dfrac{\delta F_1}{c^2}[(f_5 - f_7)J_{0,4} + (2f_7 - f_5)J_{2,2} - f_7 J_{4,0}]$
4	$16\,\dfrac{\delta F_2}{c^3}[(f_{11} - f_{13})J_{0,5} - (f_{11} - 2f_{13})J_{2,3} - f_{13}J_{4,1}]$
5	$4\,\dfrac{\delta F_1}{c^2}[(3f_4 - f_6)J_{0,4} - (3f_4 - 2f_6)J_{2,2} - f_6 J_{4,0}]$
6	$8\,\dfrac{\delta F_2}{c^3}[(f_{10} - f_{12})J_{0,5} - (f_{10} - 2f_{12})J_{2,3} - f_{12}J_{4,1}]$
8	$4\,\dfrac{\delta F_3}{c^4}[f_{14}J_{0,6} - (f_{14} - f_{15})J_{2,4} - (f_{15} - f_{16})J_{4,2} - f_{16}J_{6,0}]$
9	$-4\,\dfrac{\delta F_3}{c^4}[f_{17}J_{0,6} - (f_{17} - f_{18})J_{2,4} - (f_{18} - f_{19})J_{4,2} - f_{19}J_{6,0}]$
10	$4\,\dfrac{\delta F_3}{c^4}[f_{20}J_{0,6} - (f_{20} - f_{21})J_{2,4} - (f_{21} - f_{22})J_{4,2} - f_{22}J_{6,0}]$

TABLE 9

Formulae for the Pressure Integral for Swept-back Surfaces

r	$(\pi c^2/k)D_r$
1	$4\delta^2(J_{0,2} - J_{2,0})$
2	$\dfrac{8\delta^2}{3c^2 f_1}(2J_{0,4} - J_{2,2} - J_{4,0})$
3	$36\dfrac{\delta^2 F_1}{c^4}\left[\tfrac{3}{8}(f_5 - f_7)J_{0,6} - \tfrac{1}{15}(7f_5 - 12f_7)J_{2,4} + \tfrac{1}{15}(2f_5 + 3f_7)J_{4,2} - \tfrac{1}{15}(4f_5 + 6f_7)J_{6,0}\right]$
4	$64\dfrac{\delta^2 F_2}{c^6}\left[\tfrac{1}{7}(f_{11} - f_{13})J_{0,8} - \tfrac{1}{35}(17f_{11} - 31f_{13})J_{2,6} + \tfrac{1}{35}(f_{11} - 8f_{13})J_{4,4} + \tfrac{1}{35}(4f_{11} + 3f_{13})J_{6,2}\right.$ $\left. - \tfrac{1}{35}(8f_{11} + 6f_{13})J_{8,0}\right]$
5	$4\dfrac{\delta^2 F_1}{c^4}\left[(3f_4 - f_6)J_{2,4} - (3f_4 - 2f_6)J_{4,2} - f_6 J_{6,0}\right]$
6	$\dfrac{16\delta^4 F_2}{15c^6}\left[12(f_{10} - f_{12})J_{2,6} - (11f_{10} - 21f_{12})J_{4,4} + (f_{10} - 6f_{12})J_{6,2} - (2f_{10} + 3f_{12})J_{8,0}\right]$
8	$\dfrac{4\delta^2 F_3}{63c^8}\left[175f_{14}J_{0,10} + 5(27f_{15} - 31f_{14})J_{2,8} + (4f_{14} - 99f_{15} + 63f_{16})J_{4,6} + (8f_{14} + 12f_{15} + 21f_{16})J_{6,4}\right.$ $\left. + (32f_{14} + 48f_{15} + 84f_{16})J_{8,2} - (64f_{14} + 96f_{15} + 168f_{16})J_{10,0}\right]$
9	$-\dfrac{4\delta^2 F_3}{35c^8}\left[75f_{17}J_{2,8} + 3(21f_{18} - 23f_{17})J_{4,6} + (2f_{17} - 49f_{18} + 35f_{19})J_{6,4} + (8f_{17} + 14f_{18} + 35f_{19})J_{8,2}\right.$ $\left. - (16f_{17} + 28f_{18} + 70f_{19})J_{10,0}\right]$
10	$\dfrac{4\delta^2 F_3}{c^8}\left[f_{20}J_{4,6} - (f_{20} - f_{21})J_{6,4} - (f_{21} - f_{22})J_{8,2} - f_{22}J_{10,0}\right]$

TABLE 10

Formulae for the Suction Force on Swept-back Surfaces

$$a = h/k = (1 - \lambda^2)^{1/2}$$

r	$(E(\varkappa)/\varkappa)S_r$
1	$\dfrac{\delta^2}{2(1-a)^2}$
2	$\dfrac{\delta^2}{4f_1{}^2(1-a)^4}$
3	$\dfrac{3\delta^2}{2(1-a)^6}(F_1 f_5)^2$
4	$\dfrac{2\delta^2}{(1-a)^8}(F_2 f_{11})^2$
5	$\dfrac{3\delta^2}{2(1-a)^6}(F_1 f_4)^2$
6	$\dfrac{\delta^2}{2(1-a)^8}(F_2 f_{10})^2$
8	$\dfrac{\delta^2}{10(1-a)^{10}}[F_3(f_{14}+f_{15}+f_{16})]^2$
9	$\dfrac{\delta^2}{10(1-a)^{10}}[F_3(f_{17}+f_{18}+f_{19})]^2$
10	$\dfrac{\delta^2}{10(1-a)^{10}}[F_3(f_{20}+f_{21}+f_{22})]^2$

TABLE 11

Formulae for the 'Interference' Pressure Integral for Swept-back Surfaces

r, s	$(\pi c^2/k)D_{r,s}$
1, 2	$\frac{4\delta^2}{3cf_1}[f_1cJ_{2,0} + 3(f_1 + 1)(J_{0,3} - J_{2,1})]$
1, 3	$\frac{4\delta^2}{c^2}[\{1 + 3F_1(f_5 - f_7)\}J_{0,4} + \{1 - 3F_1(f_5 - 2f_7)\}J_{2,2} - (2 + 3F_1f_7)J_{4,0}]$
1, 4	$\frac{2\delta^2}{c^3}[3H_4 + 2\{1 + 4F_2(f_{11} - f_{13})\}J_{0,5} + \{1 - 8F_2(f_{11} - 2f_{13})\}J_{2,3} - (3 + 8F_2f_{13})J_{4,1}]$
1, 5	$\frac{4\delta^2}{c^2}[F_1(3f_4 - f_6)J_{0,4} + \{1 - F_1(3f_4 - 2f_6)\}J_{2,2} - (1 + F_1f_6)J_{4,0}]$
1, 6	$\frac{4\delta^2}{c^3}[H_4 + 2F_2(f_{10} - f_{12})J_{0,5} + \{1 - 2F_2(f_{10} - 2f_{12})\}J_{2,3} - (1 + 2F_2f_{12})J_{4,1}]$
1, 8	$\frac{4\delta^2}{3c^4}[3J_{0,6} + J_{2,4} + 4J_{4,2} - 8J_{6,0} + 3F_3\{f_{14}J_{0,6} - (f_{14} - f_{15})J_{2,4} - (f_{15} - f_{16})J_{4,2} - f_{16}J_{6,0}\}]$
1, 9	$\frac{4\delta^2}{c^4}[- F_3f_{17}J_{0,6} + \{1 + F_3(f_{17} - f_{18})\}J_{2,4} + \{1 + F_3(f_{18} - f_{19})\}J_{4,2} - \{2 - F_3f_{19}\}J_{6,0}]$
1, 10	$\frac{4\delta^2}{c^4}[F_3f_{20}J_{0,6} - F_3(f_{20} - f_{21})J_{2,4} + \{1 - F_3(f_{21} - f_{22})\}J_{4,2} - \{1 + F_3f_{22}\}J_{6,0}]$
2, 3	$\frac{3\delta^2}{c^3}\left[\left\{\frac{1}{f_1} + F_1(f_5 + 3f_7)\right\}H_4 + 2\left\{\frac{1}{f_1} + 3F_1(f_5 - f_7)\right\}J_{0,5} - \left\{\frac{1}{f_1} + F_1(5f_5 - 9f_7)\right\}J_{2,3}\right.$ $\left. - \left\{\frac{1}{f_1} + F_1(f_5 + 3f_7)\right\}J_{4,1}\right]$
2, 4	$\frac{16\delta^2}{15c^4}\left[6\left\{\frac{1}{f_1} + 4F_2(f_{11} - f_{13})\right\}J_{0,6} - \left\{\frac{3}{f_1} + 2F_2(11f_{11} - 21f_{13})\right\}J_{2,4} + \left\{\frac{3}{f_1} + 2F_2(f_{11} - 6f_{13})\right\}J_{4,2}\right.$ $\left. - 2\left\{\frac{3}{f_1} + F_2(2f_{11} + 3f_{13})\right\}J_{6,0}\right]$
2, 5	$\frac{\delta^2}{c^3}\left[3F_1(f_4 + f_6)H_4 + 6F_1(3f_4 - f_6)J_{0,5} + \left\{\frac{4}{f_1} - 3F_1(5f_4 - 3f_6)\right\}J_{2,3} - \left\{\frac{4}{f_1} + 3F_1(f_4 + f_6)\right\}J_{4,1}\right]$
2, 6	$\frac{8\delta^2}{15c^4}\left[24F_2(f_{10} - f_{12})J_{0,6} + \left\{\frac{10}{f_1} - 2F_2(11f_{10} - 21f_{12})\right\}J_{2,4} - \left\{\frac{5}{f_1} - 2F_2(f_{10} - 6f_{12})\right\}J_{4,2}\right.$ $\left. - \left\{\frac{5}{f_1} + 2F_2(2f_{10} + 3f_{12})\right\}J_{6,0}\right]$
2, 8	$\frac{\delta^2}{6c^5}\left[\left\{\frac{30}{f_1} + 3F_3(f_{14} + 2f_{15} + 8f_{16})\right\}H_6 + 40\left(\frac{1}{f_1} + F_3f_{14}\right)J_{0,7} - 2\left\{\frac{10}{f_1} + F_3(19f_{14} - 18f_{15})\right\}J_{2,5}\right.$ $\left. + \left\{\frac{10}{f_1} + F_3(f_{14} - 30f_{15} + 24f_{16})\right\}J_{4,3} - 3\left\{\frac{10}{f_1} + F_3(f_{14} + 2f_{15} + 8f_{16})\right\}J_{6,1}\right]$
2, 9	$\frac{\delta^2}{c^5}\left[\frac{1}{2}\left\{\frac{6}{f_1} - F_3(f_{17} + 2f_{18} + 8f_{19})\right\}H_6 - \frac{20}{3}F_3f_{17}J_{0,7} + \frac{1}{3}\left\{\frac{18}{f_1} + F_3(19f_{17} - 18f_{18})\right\}J_{2,5}\right.$ $\left. - \frac{1}{6}\left\{\frac{18}{f_1} + F_3(f_{17} - 30f_{18} + 24f_{19})\right\}J_{4,3} - \frac{1}{2}\left\{\frac{6}{f_1} - F_3(f_{17} + 2f_{18} + 8f_{19})\right\}J_{6,1}\right]$

TABLE 11—*continued*

r, s	$(\pi c^2/k)D_{r,s}$
2, 10	$\dfrac{\delta^2}{c^5}\Big[\tfrac{1}{2}F_3(f_{20}+2f_{21}+8f_{22})H_6 + \tfrac{20}{3}F_3 f_{20}J_{0,7} - \tfrac{1}{3}F_3(19f_{20}-18f_{21})J_{2,5} + \tfrac{1}{6}\Big\{\dfrac{24}{f_1}+F_3(f_{20}-30f_{21}+24f_{22})\Big\}J_{4,3}$ $\qquad -\tfrac{1}{2}F_3\Big\{\dfrac{8}{f_1}+F_3(f_{20}+2f_{21}+8f_{22})\Big\}J_{6,1}\Big]$
3, 4	$\dfrac{\delta^2}{c^5}[8\{3F_1(f_5-f_7)+4F_2(f_{11}-f_{13})\}J_{0,7} - 2\{3F_1(3f_5-5f_7) + 2F_2(7f_{11}-13f_{13})\}J_{2,5}$ $\qquad + \{3F_1(f_5+f_7)+2F_2(f_{11}-7f_{13})\}J_{4,3} - 3\{3F_1(f_5+f_7)+2F_2(f_{11}+f_{13})\}(J_{6,1}-H_6)]$
3, 5	$\dfrac{12\delta^2}{5c^4}F_1[3(3f_4-f_6)J_{0,6} - (7f_4-4f_6-5f_5+5f_7)J_{2,4}$ $\qquad + (2f_4+f_6+10f_7-5f_5)J_{4,2} - (4f_4+2f_6+5f_7)J_{6,0}]$
3, 6	$\dfrac{\delta^2}{c^5}[16F_2(f_{10}-f_{12})J_{0,7} + 2\{9F_1(f_5-f_7)-F_2(7f_{10}-13f_{12})\}J_{2,5} + \{F_2(f_{10}-7f_{12})-F_1(15f_5-27f_7)\}J_{4,3}$ $\qquad - 3\{F_2(f_{10}+f_{12})+F_1(f_5+3f_7)\}(J_{6,1}-H_6)]$
3, 8	$\dfrac{4\delta^2}{35c^6}[75\{3F_1(f_5-f_7)+f_{14}F_3\}J_{0,8} - 3\{5F_1(11f_5-18f_7)+F_3(23f_{14}-21f_{15})\}J_{2,6}$ $\qquad + \{5F_1(4f_5+3f_7)+F_3(2f_{14}-49f_{15}+35f_{16})\}J_{4,4}$ $\qquad + \{20F_1(4f_5+3f_7)+F_3(8f_{14}+14f_{15}+35f_{16})\}(J_{6,2}-2J_{8,0})]$
3, 9	$\dfrac{4\delta^2}{c^6}[-\tfrac{5}{7}F_3 f_{17}J_{0,8} + \tfrac{1}{35}\{189F_1(f_5-f_7)+F_3(23f_{17}-21f_{18})\}J_{2,6}$ $\qquad + \tfrac{1}{105}\{63F_1(12f_7-7f_5)-F_3(2f_{17}-49f_{18}+35f_{19})\}J_{4,4}$ $\qquad + \tfrac{1}{105}\{63F_1(2f_5+3f_7)-F_3(8f_{17}+14f_{18}+35f_{19})\}(J_{6,2}-2J_{8,0})]$
3, 10	$\dfrac{4\delta^2}{c^6}[\tfrac{5}{7}F_3 f_{20}J_{0,8} - \tfrac{1}{35}F_3(23f_{20}-21f_{21})J_{2,6} + \{3F_1(f_5-f_7)+\tfrac{1}{105}F_3(2f_{20}-49f_{21}+35f_{22})\}J_{4,4}$ $\qquad - 3F_1\{(f_5-2f_7)J_{6,2}+f_7 J_{8,0}\} + \tfrac{1}{105}F_3(8f_{20}+14f_{21}+35f_{22})(J_{6,2}-2J_{8,0})]$
4, 5	$\dfrac{\delta^2}{c^5}[8F_1(3f_4-f_6)J_{0,7} - 2\{F_1(9f_4-5f_6)-8F_2(f_{11}-f_{13})\}J_{2,5}$ $\qquad + \{F_1(3f_4+f_6)-16F_2(f_{11}-2f_{13})\}J_{4,3} - \{3F_1(3f_4+f_6)+16F_2 f_{13}\}J_{6,1}+3F_1(3f_4+f_6)H_6]$
4, 6	$\dfrac{32\delta^2}{c^6}F_2[\tfrac{4}{7}(f_{10}-f_{12})J_{0,8} - \tfrac{1}{35}(17f_{10}-31f_{12}-28f_{11}+28f_{13})J_{2,6} + \tfrac{1}{105}(3f_{10}-24f_{12}-77f_{11}+147f_{13})J_{4,4}$ $\qquad + \tfrac{1}{105}(12f_{10}+9f_{12}+7f_{11}-42f_{13})J_{6,2} - \tfrac{1}{105}(24f_{10}+18f_{12}+14f_{11}+21f_{13})J_{8,0}]$
4, 8	$\dfrac{\delta^2}{c^7}[10\{4F_2(f_{11}-f_{13})+F_3 f_{14}\}J_{0,9} - \{\tfrac{20}{3}F_2(5f_{11}-9f_{13})+F_3(9f_{14}-8f_{15})\}J_{2,7}$ $\qquad + \{\tfrac{5}{3}F_2(f_{11}-9f_{13})+\tfrac{1}{4}F_3(f_{14}-24f_{15}+16f_{16})\}J_{4,5}$ $\qquad + \{\tfrac{5}{6}F_2(5f_{11}+3f_{13})+\tfrac{1}{8}F_3(5f_{14}+8f_{15}+16f_{16})\}(J_{6,3}-3J_{8,1}+3H_8)]$
4, 9	$\dfrac{\delta^2}{c^7}[-10F_3 f_{17}J_{0,9} + \{32F_2(f_{11}-f_{13})+F_3(9f_{17}-8f_{18})\}J_{2,7}$ $\qquad - \{4F_2(7f_{11}-13f_{13})+\tfrac{1}{4}F_3(f_{17}-24f_{18}+16f_{19})\}J_{4,5}$ $\qquad + \{2F_2(f_{11}-7f_{13})-\tfrac{1}{8}F_3(5f_{17}+8f_{18}+16f_{19})\}J_{6,3}$ $\qquad - \{6F_2(f_{11}+f_{13})-\tfrac{3}{8}F_3(5f_{17}+8f_{18}+16f_{19})\}(J_{8,1}-H_8)]$

TABLE 11—*continued*

r, s	$(\pi c^2/k)D_{r,s}$
4, 10	$\dfrac{\delta^2}{c^7}[10F_3f_{20}J_{0,9} - F_3(9f_{20} - 8f_{21})J_{2,7} + \{16F_2(f_{11} - f_{13}) + \tfrac{1}{4}F_3(f_{20} - 24f_{21} + 16f_{22})\}J_{4,5}$ $\qquad - 16F_2\{(f_{11} - 2f_{13})J_{6,3} + f_{13}J_{8,1}\} + \tfrac{1}{8}F_3(5f_{20} + 8f_{21} + 16f_{22})(J_{6,3} - 3J_{8,1} + 3H_8)]$
5, 6	$\dfrac{\delta^2}{c^5}[3F_1(f_4 + f_6)H_6 + 2\{4F_2(f_{10} - f_{12}) + 3F_1(3f_4 - f_6)\}J_{2,5}$ $\qquad - \{8F_2(f_{10} - 2f_{12}) + 3F_1(5f_4 - 3f_6)\}J_{4,3} - \{8F_2f_{12} + 3F_1(f_4 + f_6)\}J_{6,1}]$
5, 8	$\dfrac{4\delta^2}{7c^6}[15F_1(3f_4 - f_6)J_{0,8} - \{3F_1(11f_4 - 6f_6) - 7F_3f_{14}\}J_{2,6} + \{F_1(4f_4 + f_6) - 7F_3(f_{14} - f_{15})\}J_{4,4}$ $\qquad + \{4F_1(4f_4 + f_6) - 7F_3(f_{15} - f_{16})\}J_{6,2} - \{8F_1(4f_4 + f_6) + 7F_3f_{16}\}J_{8,0}]$
5, 9	$\dfrac{4\delta^2}{5c^6}[\{9F_1(3f_4 - f_6) - 5F_3f_{17}\}J_{2,6} - \{3F_1(7f_4 - 4f_6) - 5F_3(f_{17} - f_{18})\}J_{4,4}$ $\qquad + \{3F_1(2f_4 + f_6) + 5F_3(f_{18} - f_{19})\}J_{6,2} - \{6F_1(2f_4 + f_6) - 5F_3f_{19}\}J_{8,0}]$
5, 10	$\dfrac{4\delta^2}{c^6}[F_3f_{20}J_{2,6} + \{F_1(3f_4 - f_6) - F_3(f_{20} - f_{21})\}J_{4,4} - \{F_1(3f_4 - 2f_6) + F_3(f_{21} - f_{22})\}J_{6,2} - (F_1f_6 + F_3f_{22})J_{8,0}]$
6, 8	$\dfrac{\delta^2}{c^7}[20F_2(f_{10} - f_{12})J_{0,9} - \tfrac{10}{3}\{F_2(5f_{10} - 9f_{12}) - 2F_3f_{14}\}J_{2,7} + \tfrac{1}{6}\{5F_2(f_{10} - 9f_{12}) - 2F_3(19f_{14} - 18f_{15})\}J_{4,5}$ $\qquad + \tfrac{1}{12}\{5F_2(5f_{10} + 3f_{12}) + 2F_3(f_{14} - 30f_{15} + 24f_{16})\}J_{6,3}$ $\qquad - \tfrac{1}{4}\{5F_2(5f_{10} + 3f_{12}) + 2F_3(f_{14} + 2f_{15} + 8f_{16})\}(J_{8,1} - H_8)]$
6, 9	$\dfrac{\delta^2}{c^7}[\tfrac{4}{3}\{12F_2(f_{10} - f_{12}) - 5F_3f_{17}\}J_{2,7} - \tfrac{1}{3}\{6F_2(7f_{10} - 13f_{12}) - F_3(19f_{17} - 18f_{18})\}J_{4,5}$ $\qquad + \tfrac{1}{6}\{6F_2(f_{10} - 7f_{12}) - F_3(f_{17} - 30f_{18} + 24f_{19})\}J_{6,3}$ $\qquad + \tfrac{1}{2}\{6F_2(f_{10} + f_{12}) - F_3(f_{17} + 2f_{18} + 8f_{19})\}(J_{8,1} - H_8)]$
6, 10	$\dfrac{\delta^2}{c^7}[\tfrac{20}{3}F_3f_{20}J_{2,7} + \{8F_2(f_{10} - f_{12}) - \tfrac{1}{3}F_3(19f_{20} - 18f_{21})\}J_{4,5}$ $\qquad - \{8F_2(f_{10} - 2f_{12}) - \tfrac{1}{6}F_3(f_{20} - 30f_{21} + 24f_{22})\}J_{6,3} - 8F_2f_{12}J_{8,1}$ $\qquad - \tfrac{1}{2}F_3(f_{20} + 2f_{21} + 8f_{22})(J_{8,1} - H_8)]$
8, 9	$\dfrac{4\delta^2}{9c^8}F_3[-25f_{17}J_{0,10} + \tfrac{5}{7}(27f_{14} + 31f_{17} - 27f_{18})J_{2,8}$ $\qquad - \tfrac{1}{35}\{27(23f_{14} - 21f_{15}) + 5(4f_{17} - 99f_{18} + 63f_{19})\}J_{4,6}$ $\qquad + \tfrac{1}{35}\{9(2f_{14} - 49f_{15} + 35f_{16}) - 5(8f_{17} + 12f_{18} + 21f_{19})\}J_{6,4}$ $\qquad + \tfrac{1}{35}\{9(8f_{14} + 14f_{15} + 35f_{16}) - 5(32f_{17} + 48f_{18} + 84f_{19})\}(J_{8,2} - 2J_{10,0})]$
8, 10	$\dfrac{4\delta^2}{63c^8}F_3[175f_{20}J_{0,10} - 5(31f_{20} - 27f_{21})J_{2,8} + (63f_{14} + 4f_{20} - 99f_{21} + 63f_{22})J_{4,6}$ $\qquad - (63f_{14} - 63f_{15} - 8f_{20} - 12f_{21} - 21f_{22})J_{6,4} - (63f_{15} - 63f_{16} - 32f_{20} - 48f_{21} - 84f_{22})J_{8,2}$ $\qquad - (63f_{16} + 64f_{20} + 96f_{21} + 168f_{22})J_{10,0}]$
9, 10	$\dfrac{4\delta^2}{35c^8}F_3[75f_{20}J_{2,8} - (69f_{20} - 63f_{21} + 35f_{17})J_{4,6} + (2f_{20} - 49f_{21} + 35f_{22} + 35f_{17} - 35f_{18})J_{6,4}$ $\qquad + (8f_{20} + 14f_{21} + 35f_{22} + 35f_{18} - 35f_{19})J_{8,2} - (16f_{20} + 28f_{21} + 70f_{22} - 35f_{19})J_{10,0}]$

TABLE 12

Formulae for the 'Interference' Suction Force for Swept-back Surfaces

r, s	$(E(\varkappa)/\varkappa)S_{r,s}$
$1, 2$	$\dfrac{\delta^2}{(1-a)^3}\dfrac{2}{3f_1}$
$1, 3$	$\dfrac{\delta^2}{(1-a)^4}\,\tfrac{3}{2}F_1 f_5$
$1, 4$	$\dfrac{\delta^2}{(1-a)^5}\,\tfrac{8}{5}F_2 f_{11}$
$1, 5$	$\dfrac{\delta^2}{(1-a)^4}\,\tfrac{3}{2}F_1 f_4$
$1, 6$	$\dfrac{\delta^2}{(1-a)^5}\,\tfrac{4}{5}F_2 f_{10}$
$1, 8$	$\dfrac{\delta^2}{(1-a)^6}\,\tfrac{1}{3}F_3(f_{14}+f_{15}+f_{16})$
$1, 9$	$\dfrac{-\,\delta^2}{(1-a)^6}\,\tfrac{1}{3}F_3(f_{17}+f_{18}+f_{19})$
$1, 10$	$\dfrac{\delta^2}{(1-a)^6}\,\tfrac{1}{3}F_3(f_{20}+f_{21}+f_{22})$
$2, 3$	$\dfrac{\delta^2}{(1-a)^5}\,\tfrac{6}{5}\dfrac{F_1 f_5}{f_1}$
$2, 4$	$\dfrac{\delta^2}{(1-a)^6}\,\tfrac{4}{3}\dfrac{F_2 f_{11}}{f_1}$
$2, 5$	$\dfrac{\delta^2}{(1-a)^5}\,\tfrac{6}{5}\dfrac{F_1 f_4}{f_1}$
$2, 6$	$\dfrac{\delta^2}{(1-a)^6}\,\tfrac{2}{3}\dfrac{F_2 f_{10}}{f_1}$
$2, 8$	$\dfrac{\delta^2}{(1-a)^7}\,\tfrac{2}{7}\dfrac{F_3}{f_1}\,(f_{14}+f_{15}+f_{16})$
$2, 9$	$\dfrac{-\,\delta^2}{(1-a)^7}\,\tfrac{2}{7}\dfrac{F_3}{f_1}\,(f_{17}+f_{18}+f_{19})$
$2, 10$	$\dfrac{\delta^2}{(1-a)^7}\,\tfrac{2}{7}\dfrac{F_3}{f_1}\,(f_{20}+f_{21}+f_{22})$
$3, 4$	$\dfrac{\delta^2}{(1-a)^7}\,\tfrac{24}{7}\,F_1 f_5 \cdot F_2 f_{11}$
$3, 5$	$\dfrac{\delta^2}{(1-a)^6}\,3F_1 f_5 \cdot F_1 f_4$
$3, 6$	$\dfrac{\delta^2}{(1-a)^7}\,\tfrac{12}{7}\,F_1 f_5 \cdot F_2 f_{10}$

TABLE 12—*continued*

r, s	$(E(\varkappa)/\varkappa)S_{r,s}$
3, 8	$\dfrac{\delta^2}{(1-a)^8}\,\tfrac{3}{4}F_1 f_5\,.\,F_3(f_{14}+f_{15}+f_{16})$
3, 9	$\dfrac{-\,\delta^2}{(1-a)^8}\,\tfrac{3}{4}F_1 f_5\,.\,F_3(f_{17}+f_{18}+f_{19})$
3, 10	$\dfrac{\delta^2}{(1-a)^8}\,\tfrac{3}{4}F_1 f_5\,.\,F_3(f_{20}+f_{21}+f_{22})$
4, 5	$\dfrac{\delta^2}{(1-a)^7}\,\tfrac{24}{7}F_2 f_{11}\,.\,F_1 f_4$
4, 6	$\dfrac{\delta^2}{(1-a)^8}\,2F_2 f_{11}\,.\,F_2 f_{10}$
4, 8	$\dfrac{\delta^2}{(1-a)^9}\,\tfrac{8}{9}F_2 f_{11}\,.\,F_3(f_{14}+f_{15}+f_{16})$
4, 9	$\dfrac{-\,\delta^2}{(1-a)^9}\,\tfrac{8}{9}F_2 f_{11}\,.\,F_3(f_{17}+f_{18}+f_{19})$
4, 10	$\dfrac{\delta^2}{(1-a)^9}\,\tfrac{8}{9}F_2 f_{11}\,.\,F_3(f_{20}+f_{21}+f_{22})$
5, 6	$\dfrac{\delta^2}{(1-a)^7}\,\tfrac{12}{7}F_1 f_4\,.\,F_2 f_{10}$
5, 8	$\dfrac{\delta^2}{(1-a)^8}\,\tfrac{3}{4}F_1 f_4\,.\,F_3(f_{14}+f_{15}+f_{16})$
5, 9	$\dfrac{-\,\delta^2}{(1-a)^8}\,\tfrac{3}{4}F_1 f_4\,.\,F_3(f_{17}+f_{18}+f_{19})$
5, 10	$\dfrac{\delta^2}{(1-a)^8}\,\tfrac{3}{4}F_1 f_4\,.\,F_3(f_{20}+f_{21}+f_{22})$
6, 8	$\dfrac{\delta^2}{(1-a)^9}\,\tfrac{4}{9}F_2 f_{10}\,.\,F_3(f_{14}+f_{15}+f_{16})$
6, 9	$\dfrac{-\,\delta^2}{(1-a)^9}\,\tfrac{4}{9}F_2 f_{10}\,.\,F_3(f_{17}+f_{18}+f_{19})$
6, 10	$\dfrac{\delta^2}{(1-a)^9}\,\tfrac{4}{9}F_2 f_{10}\,.\,F_3(f_{20}+f_{21}+f_{22})$
8, 9	$\dfrac{-\,\delta^2}{(1-a)^{10}}\,\tfrac{1}{5}F_3{}^2(f_{14}+f_{15}+f_{16})(f_{17}+f_{18}+f_{19})$
8, 10	$\dfrac{\delta^2}{(1-a)^{10}}\,\tfrac{1}{5}F_3{}^2(f_{14}+f_{15}+f_{16})(f_{20}+f_{21}+f_{22})$
9, 10	$\dfrac{-\,\delta^2}{(1-a)^{10}}\,\tfrac{1}{5}F_3{}^2(f_{17}+f_{18}+f_{19})(f_{20}+f_{21}+f_{22})$

TABLE 13

Formulae for the Pitching Moments of Triangular Surfaces

r	M_r
1	$\frac{2}{3}c\delta$
2	$\dfrac{3}{4f_1}c\delta$
3	$\frac{3}{5}c\delta F_1(4f_5 - 3f_7)$
4	$\frac{5}{6}c\delta F_2(4f_{11} - 3f_{13})$
5	$\frac{3}{5}c\delta F_1(4f_4 - f_6)$
6	$\frac{5}{12}c\delta F_2(4f_{10} - 3f_{12})$
8	$\frac{3}{28}c\delta F_3(8f_{14} + 2f_{15} + f_{16})$
9	$-\frac{3}{28}c\delta F_3(8f_{17} + 2f_{18} + f_{19})$
10	$\frac{3}{28}c\delta F_3(8f_{20} + 2f_{21} + f_{22})$

TABLE 14

Formulae for the Pitching Moments of Swept-back Surfaces

r	$(\pi c^2/k)M_r$
1	$2\delta(H_2 + J_{0,3} - J_{2,1})$
2	$\dfrac{4\delta}{3cf_1}(2J_{0,4} - J_{2,2} - J_{4,0})$
3	$\dfrac{3\delta}{2c^2}F_1[(f_5 + 3f_7)H_4 + 6(f_5 - f_7)J_{0,5} - (5f_5 - 9f_7)J_{2,3} - (f_5 + 3f_7)J_{4,1}]$
4	$\dfrac{16\delta}{15c^3}F_2[12(f_{11} - f_{13})J_{0,6} - (11f_{11} - 21f_{13})J_{2,4} + (f_{11} - 6f_{13})J_{4,2} - (2f_{11} + 3f_{13})J_{6,0}]$
5	$\dfrac{3\delta}{2c^2}F_1[(f_4 + f_6)H_4 + 2(3f_4 - f_6)J_{0,5} - (5f_4 - 3f_6)J_{2,3} - (f_4 + f_6)J_{4,1}]$
6	$\dfrac{8\delta}{15c^3}F_2[12(f_{10} - f_{12})J_{0,6} - (11f_{10} - 21f_{12})J_{2,4} + (f_{10} - 6f_{12})J_{4,2} - (2f_{10} + 3f_{12})J_{6,0}]$
8	$\dfrac{\delta}{12c^4}F_3[3(f_{14} + 2f_{15} + 8f_{16})H_6 + 40f_{14}J_{0,7} - 2(19f_{14} - 18f_{15})J_{2,5} + (f_{14} - 30f_{15} + 24f_{16})J_{4,3}$ $- 3(f_{14} + 2f_{15} + 8f_{16})J_{6,1}]$
9	$\dfrac{-\delta}{12c^4}F_3[3(f_{17} + 2f_{18} + 8f_{19})H_6 + 40f_{17}J_{0,7} - 2(19f_{17} - 18f_{18})J_{2,5} + (f_{17} - 30f_{18} + 24f_{19})J_{4,3}$ $- 3(f_{17} + 2f_{18} + 8f_{19})J_{6,1}]$
10	$\dfrac{\delta}{12c^4}F_3[3(f_{20} + 2f_{21} + 8f_{22})H_6 + 40f_{20}J_{0,7} - 2(19f_{20} - 18f_{21})J_{2,5} + (f_{20} - 30f_{21} + 24f_{22})J_{4,3}$ $- 3(f_{20} + 2f_{21} + 8f_{22})J_{6,1}]$

64

$\left(\dfrac{\Delta d}{d_1}\right)_{opt}$ %

E

F

G

H

A

B

C

D

SURFACES $\tau = 1$ 2 3 4 5 6 8 9 10

SUCTION FORCES IGNORED.
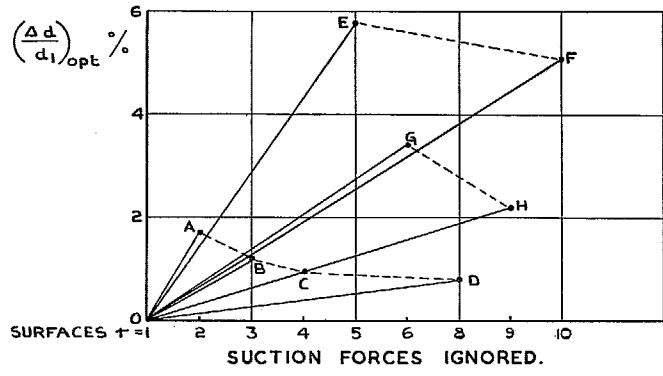
EXPLANATION :-
PTS. A,B,--F GIVE $(\Delta d/d_1)_{opt}$ FOR
SURFACE COMBINATIONS, $\tau=1,2$; $1,3$; ---, 10;
PTS. a,b,--f GIVE $(\Delta t/t_1)_{opt}$
FOR $\tau=1, 2$; $1,3$; ---, 10

SURFACES. (SEE APPENDIX IV)
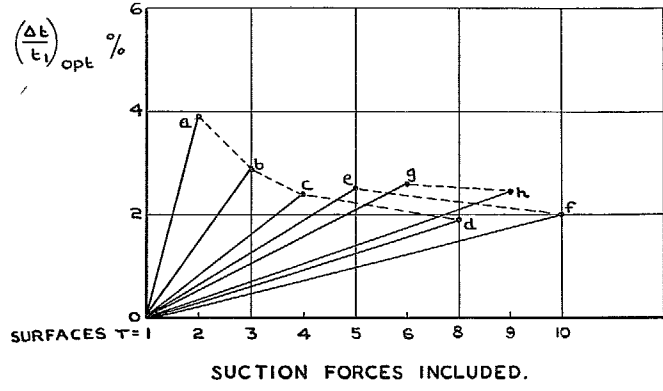
r	r
1	5] TWIST
2] CAMBER.	10
3	
4	6] CAMBER
8]	9] & TWIST.

$\left(\dfrac{\Delta t}{t_1}\right)_{opt}$ %

a

b

c e

g

h

d

f

SURFACES $\tau = 1$ 2 3 4 5 6 8 9 10

SUCTION FORCES INCLUDED.

FIG. 1a.   Maximum drag reduction on triangular wings for ' two-surface ' combinations, tan γ/tan $\mu = 0 \cdot 7$.

12

$\left(\dfrac{\Delta d}{d_1}\right)_{opt}$ %

10

G

8

H
J

6

4

A

2

B

C

SURFACES $\tau = 1$ 2 3 4 5 6 8 9 10

SUCTION FORCES IGNORED.
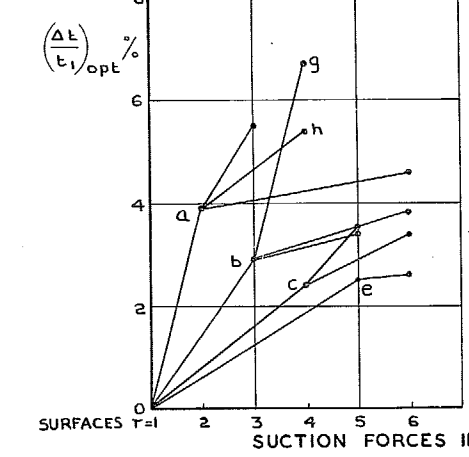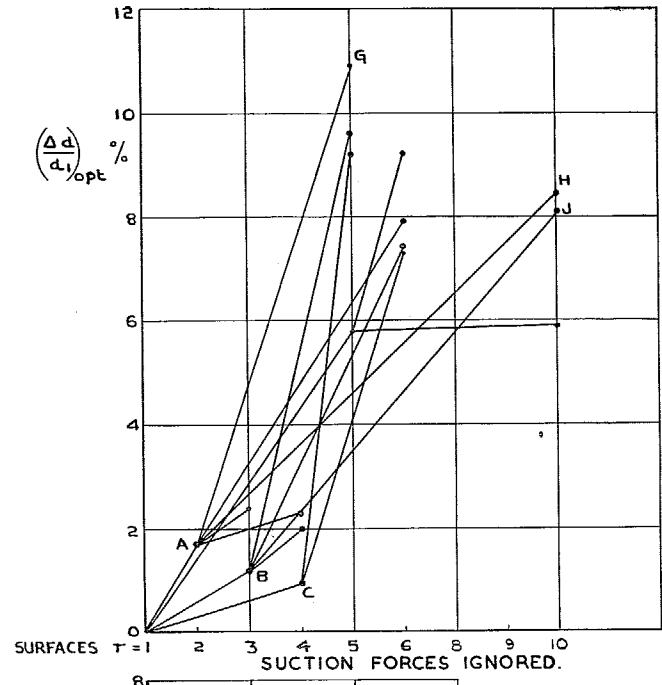
EXPLANATION :-
PTS. A,B,C; a,b,c AS IN
FIG 1(a)
PTS. G, H, J, ETC. GIVE
$(\Delta d/d_1)_{opt}$ FOR SURFACE
COMBINATIONS: $\tau=1,2,5$;
$\tau=1,2,10$; $\tau=1,3,10$; ETC.
PTS. g, h, ETC. GIVE
$(\Delta t/t_1)_{opt}$ FOR $\tau=1,3,4$;
$\tau=1,2,4$; ETC.

8

$\left(\dfrac{\Delta t}{t_1}\right)_{opt}$ %

6

g

h

a

b

c e

d

2

SURFACES $\tau = 1$ 2 3 4 5 6

SUCTION FORCES INCLUDED.

FIG. 1b.   Maximum drag reduction on triangular wings for ' three-surface ' combinations tan γ/tan $\mu = 0 \cdot 7$.
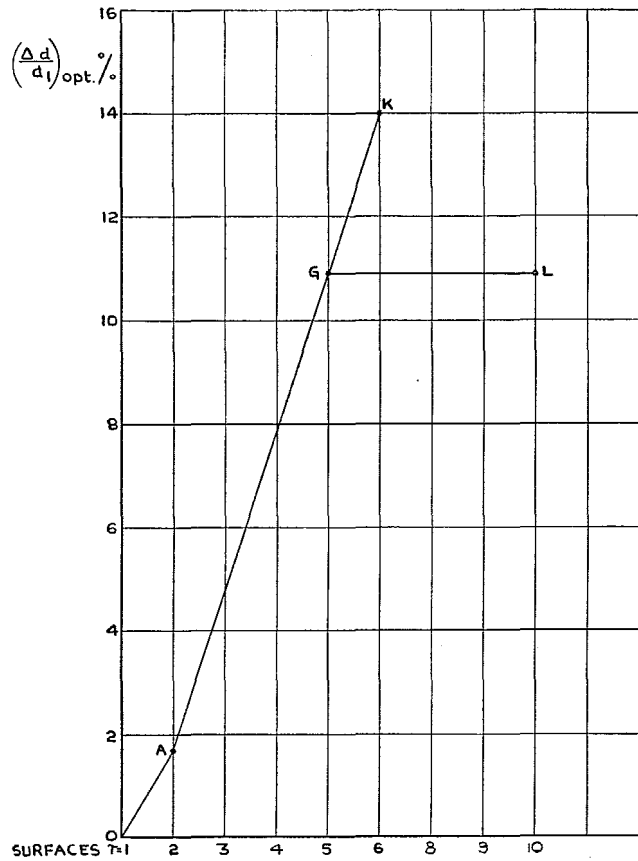
EXPLANATION:- POINTS A,G IN FIG. I(b)
POINTS K, L GIVE $\left(\Delta d/d_1\right)_{opt.}$ FOR SURFACE
COMBINATIONS $\tau=1,2,5,6$; $\tau=1,2,5,10$

FIG. 1c. Maximum drag reduction (suction ignored) on triangular wings for 'four-surface' combinations, $\tan \gamma/\tan \mu = 0\cdot 7$.

SUCTION FORCES IGNORED
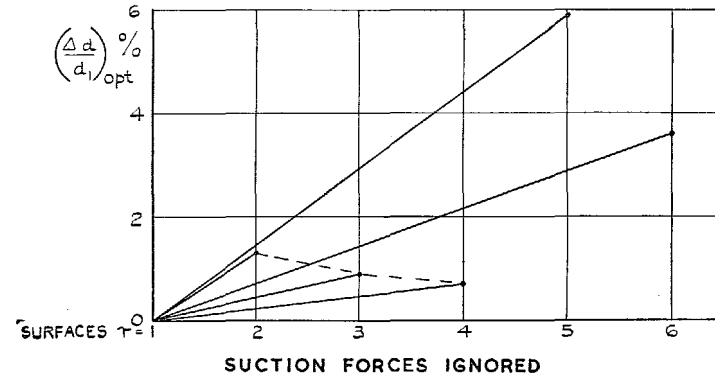
(EXPLANATION ON FIGS. 1)

SUCTION FORCES INCLUDED
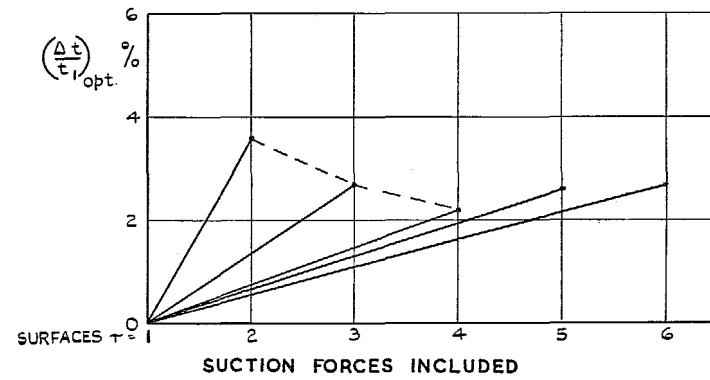
$\tau = 1$	FLAT TRIANGULAR WING
$\tau = 2,3,4$	CAMBER
$\tau = 5$	TWIST
$\tau = 6$	CAMBER AND TWIST

FIG. 2a. Maximum drag reduction on triangular wings for 'two-surface' combinations, $\tan \gamma/\tan \mu = 0\cdot 7338$.
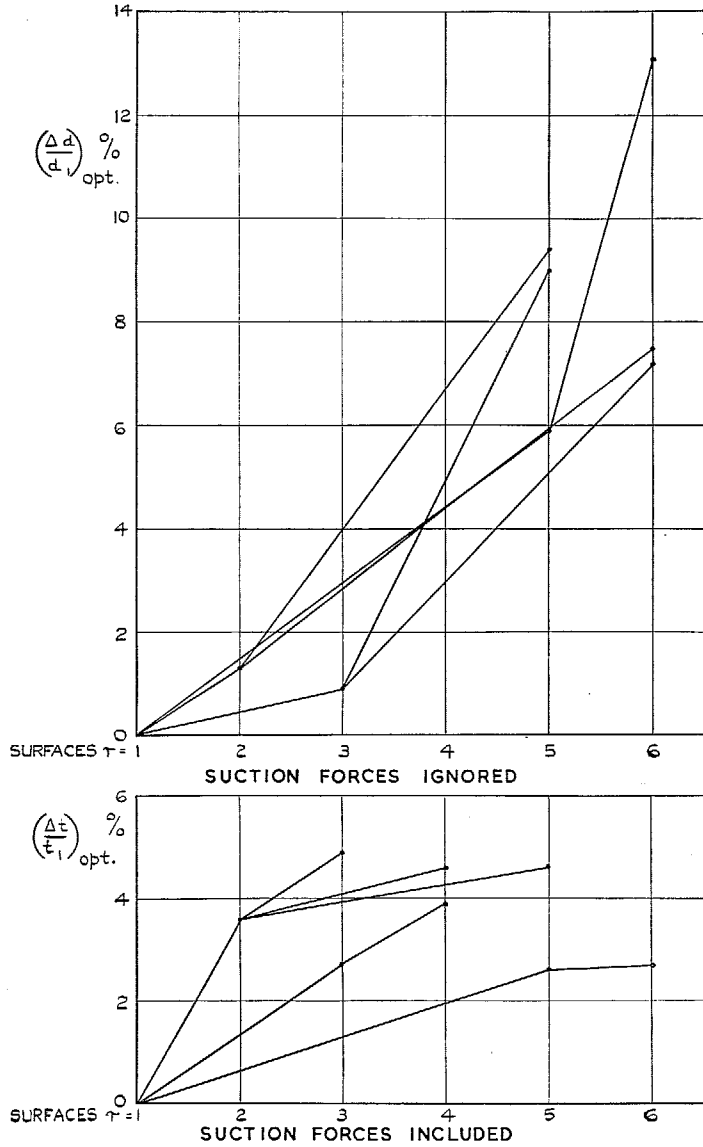
FIG. 2b.   Maximum drag reduction on triangular wings for 'three-surface' combinations, $\tan \gamma/\tan \mu = 0\cdot7338$.
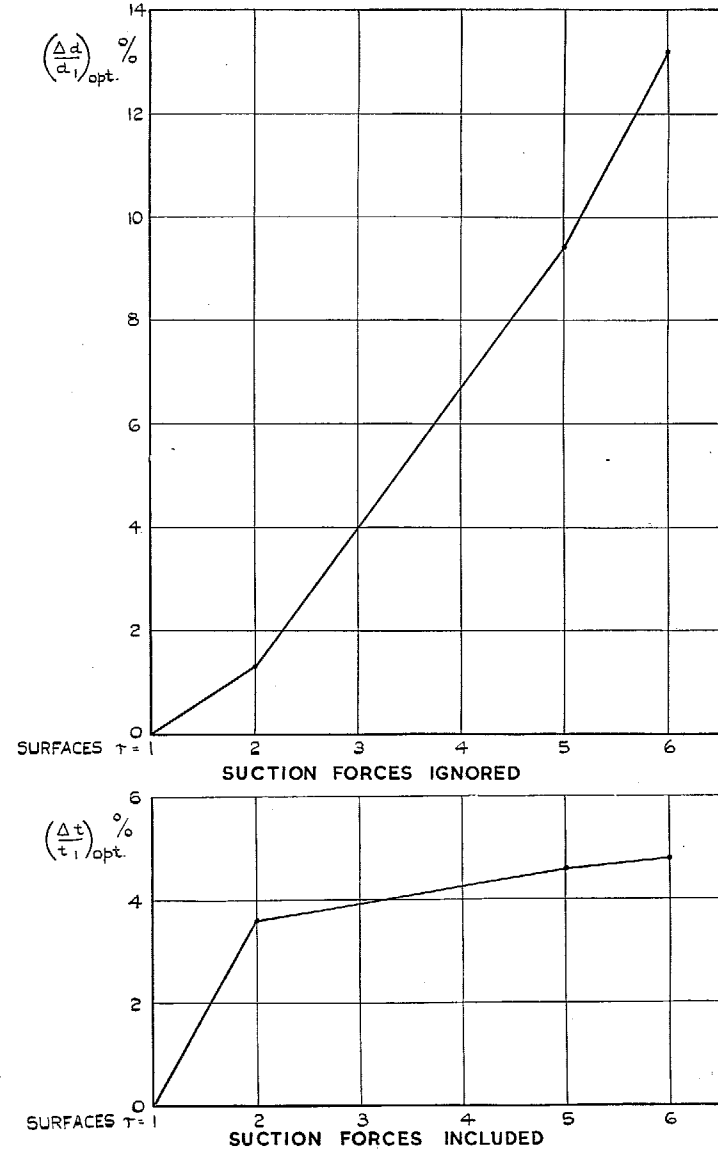
FIG. 2c.   Maximum drag reduction on triangular wings for 'four-surface' combinations, $\tan \gamma/\tan \mu = 0\cdot7338$.
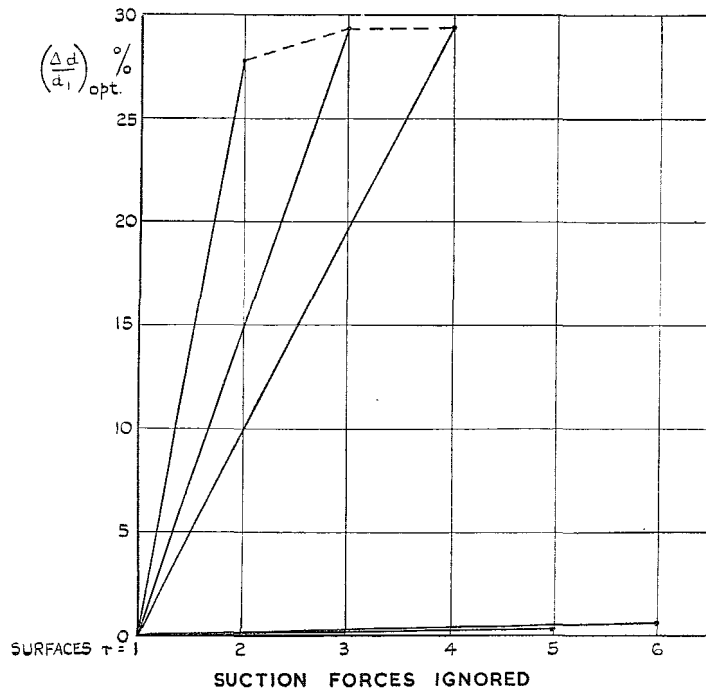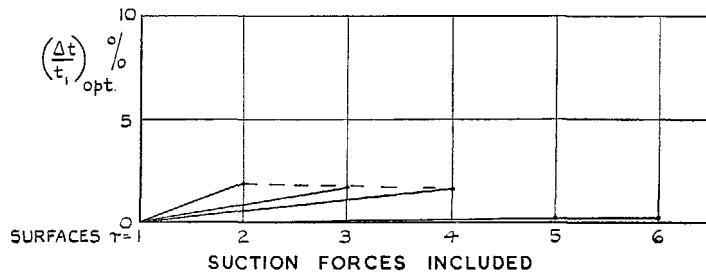
FIG. 3a. Maximum drag reduction on triangular wings for 'two-surface' combinations, tan γ/tan $\mu = 0 \cdot 1184$.
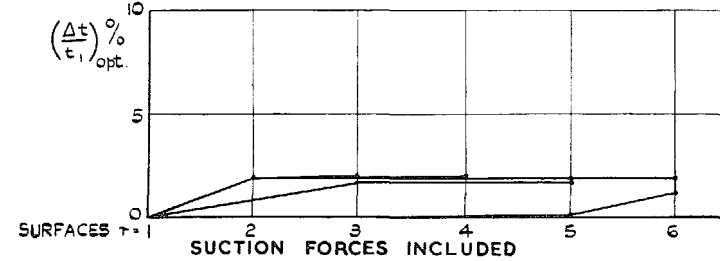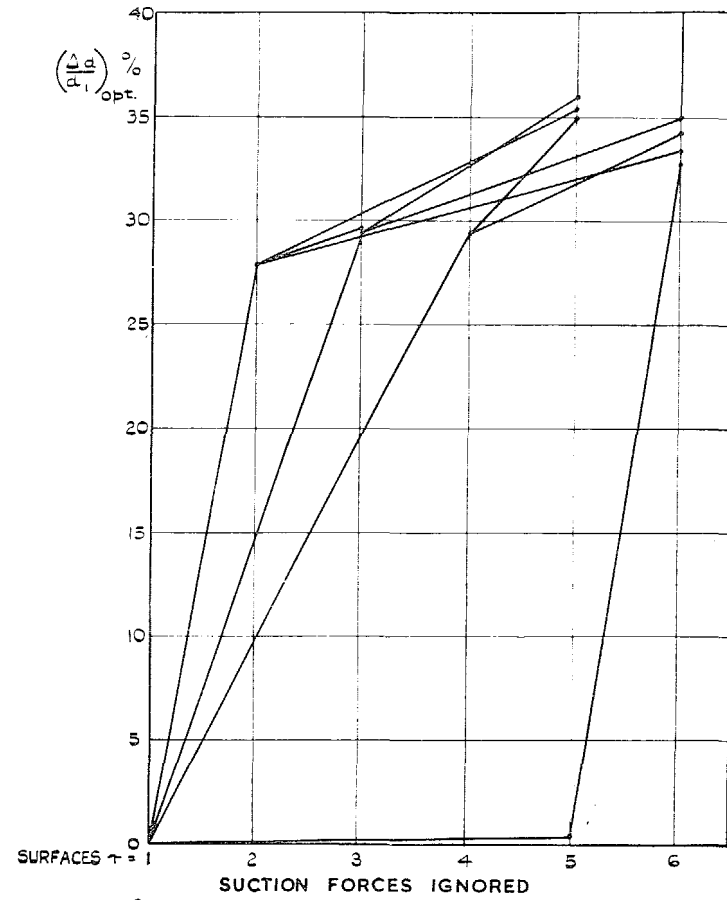
FIG. 3b. Maximum drag reduction on triangular wings for 'three-surface' combinations, tan γ/tan $\mu = 0 \cdot 1184$.
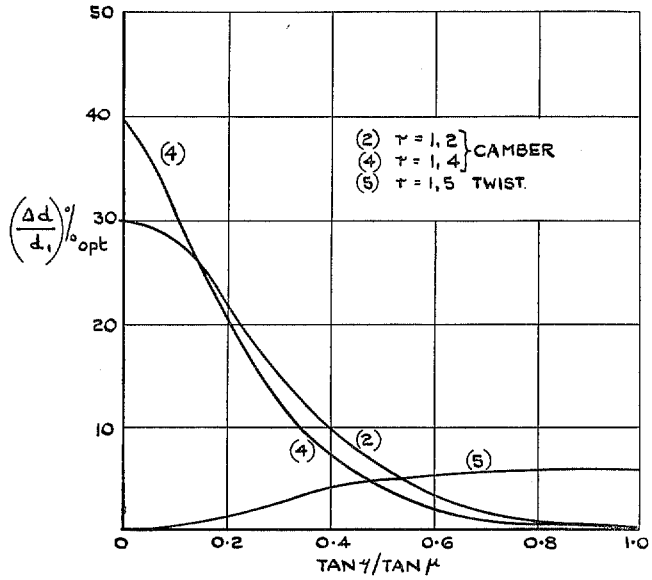
70

ESTIMATED VALUES OF $\left(\Delta d/d_1\right)_{opt}$
(SUCTION IGNORED)

TAN γ / TAN μ

$\left(\dfrac{\Delta d}{d_1}\right)\%_{opt}$

O CALCULATED VALUES.

$\left(\dfrac{\Delta t}{t_1}\right)\%_{opt}$

ESTIMATED VALUES OF $\left(\Delta t/t_1\right)_{opt}$.
(SUCTION INCLUDED)

TAN γ / TAN μ
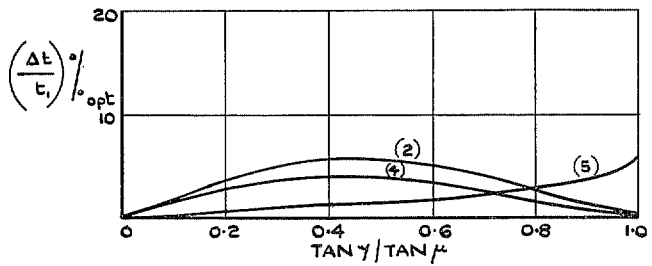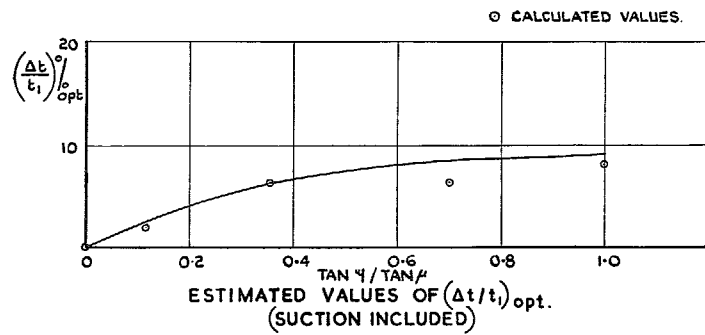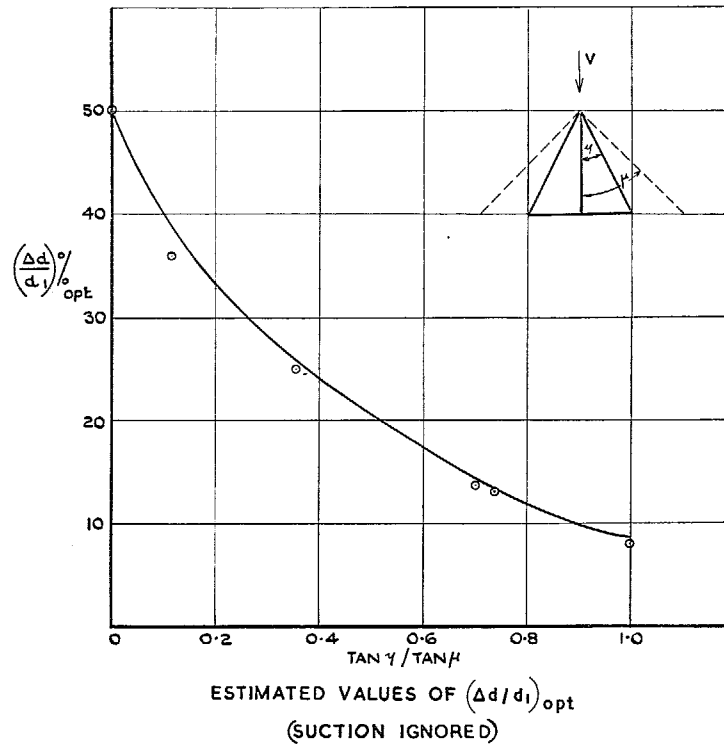
FIG. 5a.　Maximum drag reductions by the use of camber and twist (triangular wings).

$\dfrac{\nabla d}{d_1}$

TAN γ / TAN μ
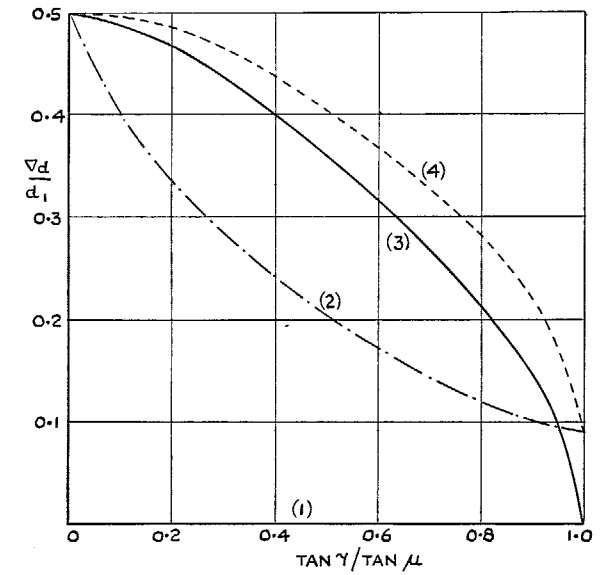
$\dfrac{\nabla d}{d_1} = 0$ ON (1), (FLAT WING WITHOUT SUCTION)

$= \dfrac{d_1 - d_{opt}}{d_1}$ ON (2), (CAMBERED & TWISTED WING, SUCTION IGNORED)

$= \dfrac{d_1 - t_1}{d_1} \equiv \dfrac{S_1}{d_1}$ ON (3), (FLAT WING WITH SUCTION)

$= \dfrac{d_1 - t_{opt}}{d_1}$ ON (4), (CAMBERED & TWISTED WING, SUCTION INCLUDED)

FIG. 5b.　Comparison of drag reductions (on a triangular wing) due to camber and twist, with drag reduction on the flat wing due to suction force.

71
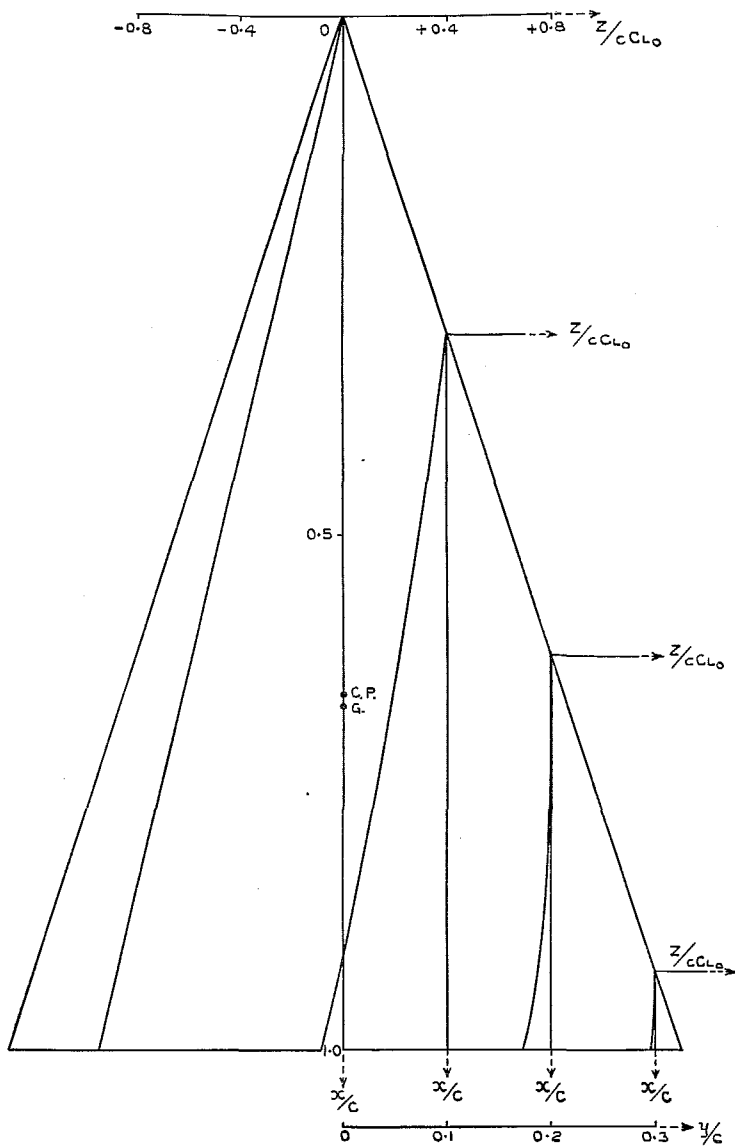
FIG. 6.   Shape of Wing 1a, $\gamma = 18$ deg.—Designed for minimum $C_{Dp}/C_L{}^2$ (suction forces ignored) at $M = 2\cdot47$.
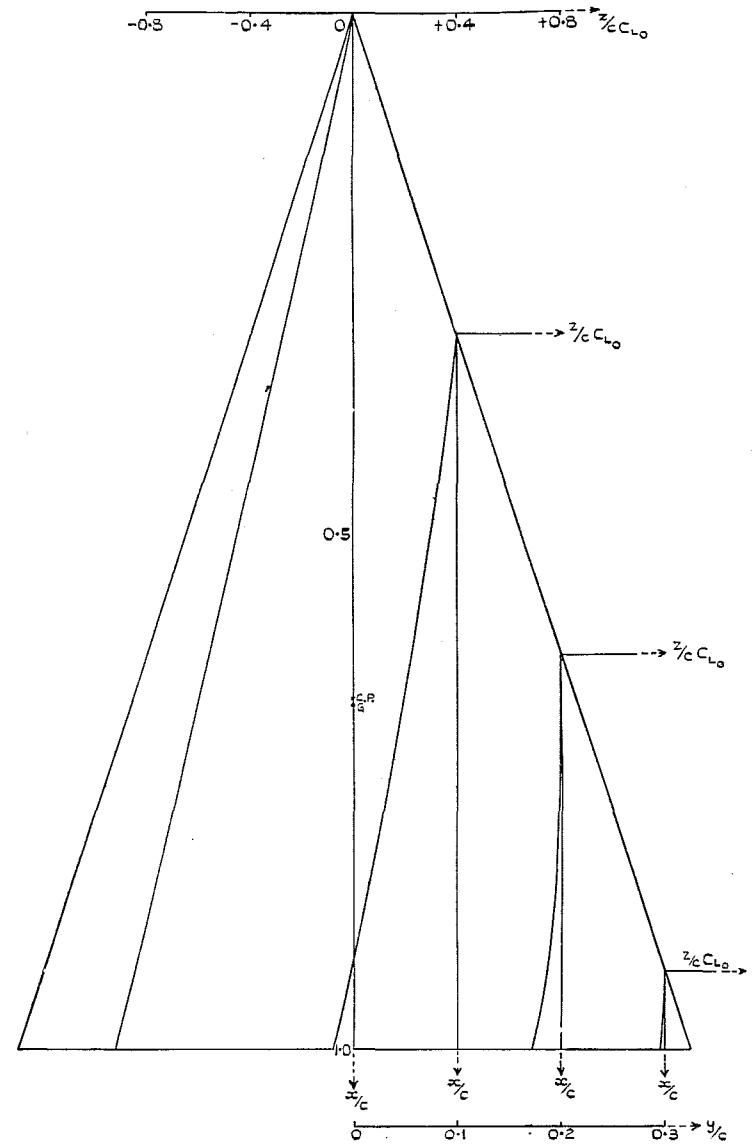
FIG. 7a.   Shape of Wing 1b, $\gamma = 18$ deg.—Designed for minimum $C_{Dp}/C_L{}^2$ (suction forces ignored) at $M = 2\cdot47$.
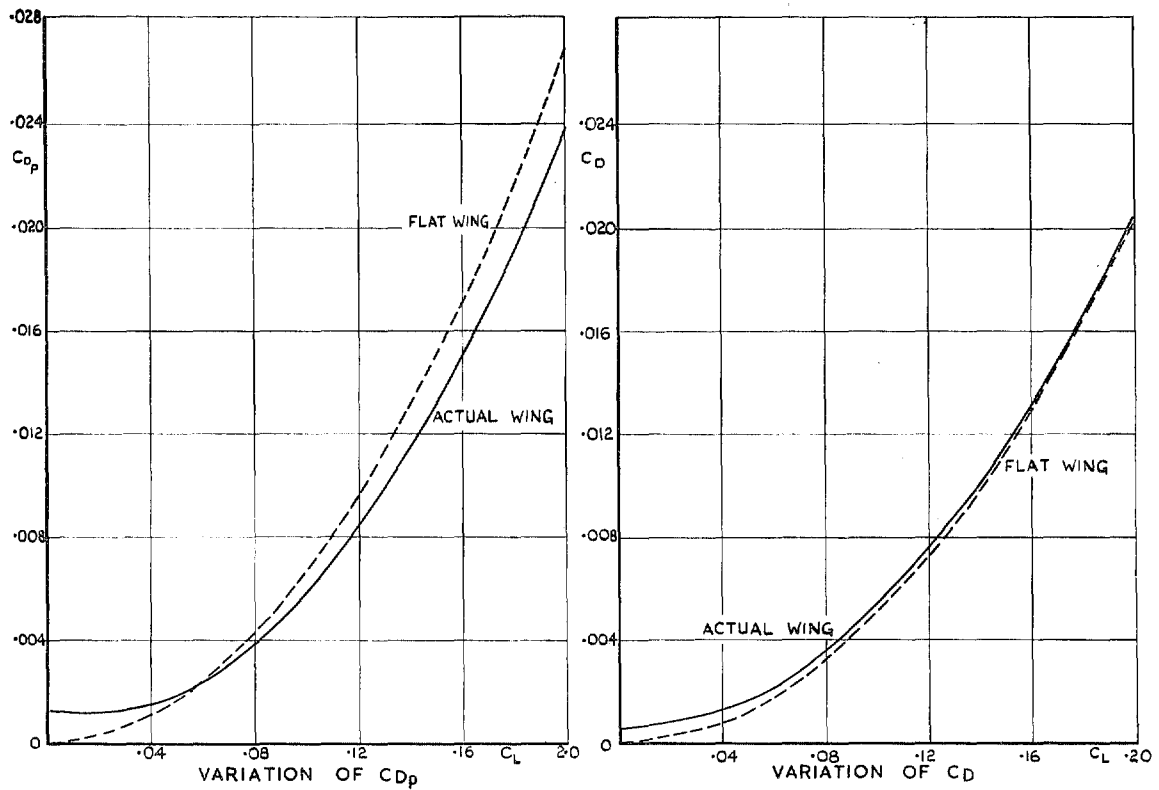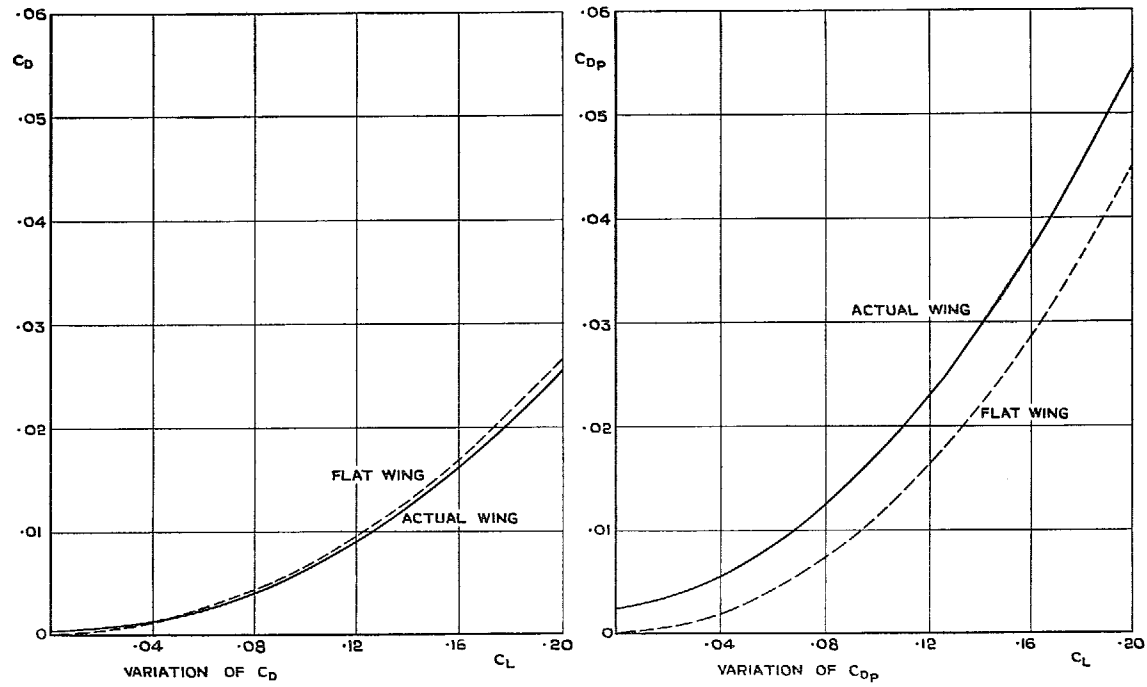
FIG. 7b. Variation of drag with lift for Wing 1b, $\gamma = 18$ deg.—Designed for minimum C_{Dp}/C_L^2 at $M = 2\cdot47$. Design $C_{L0} = 0\cdot12$.
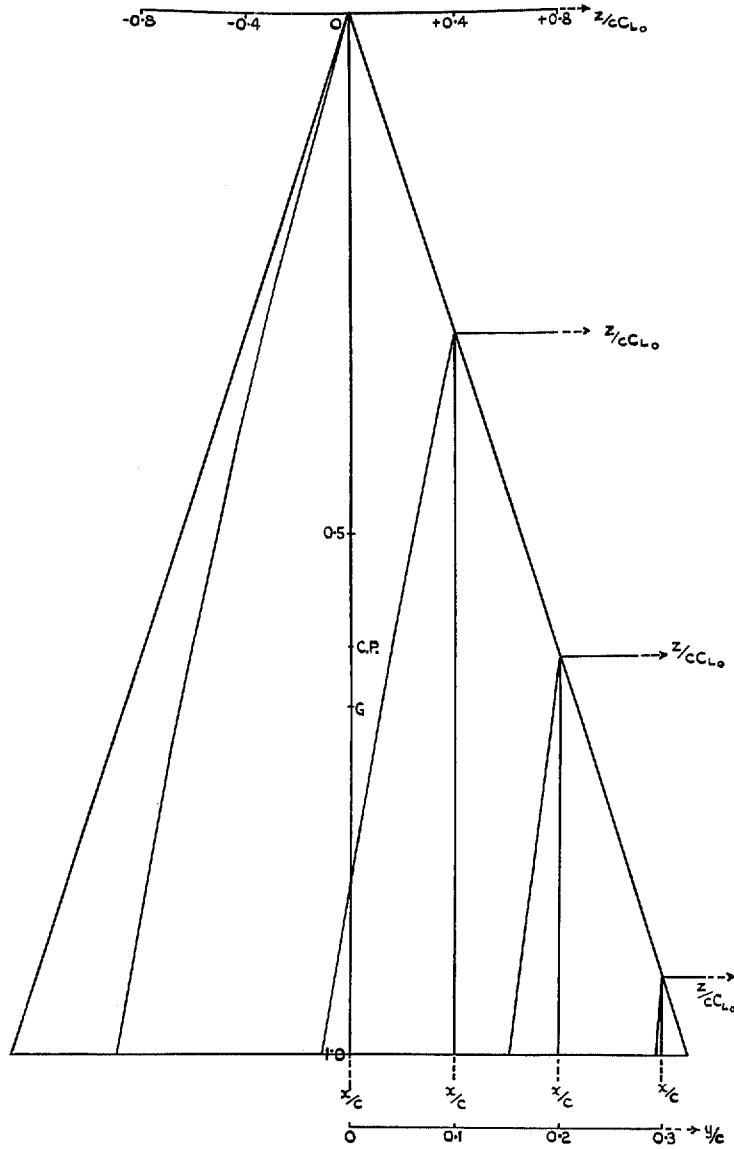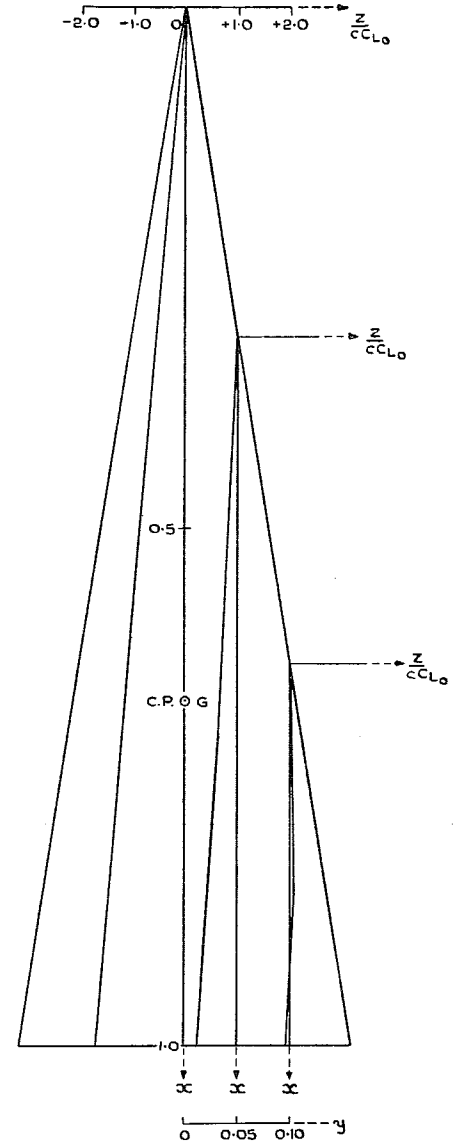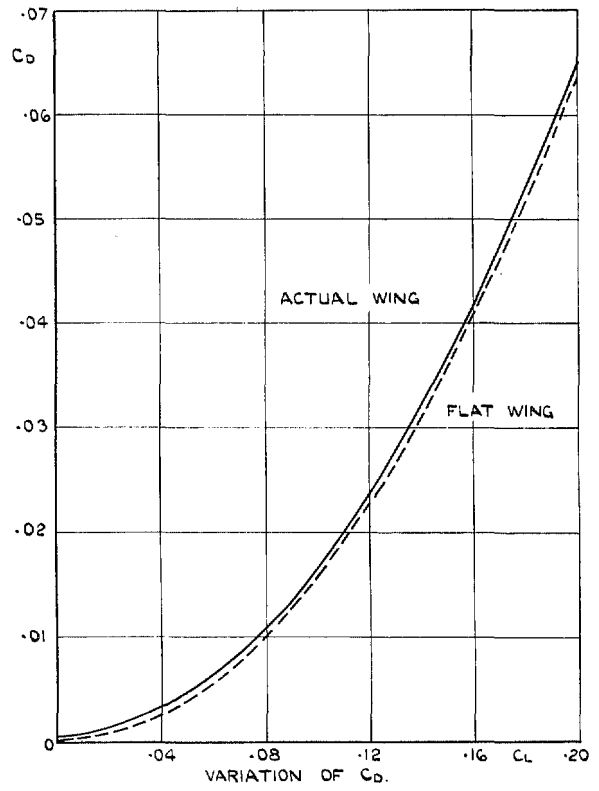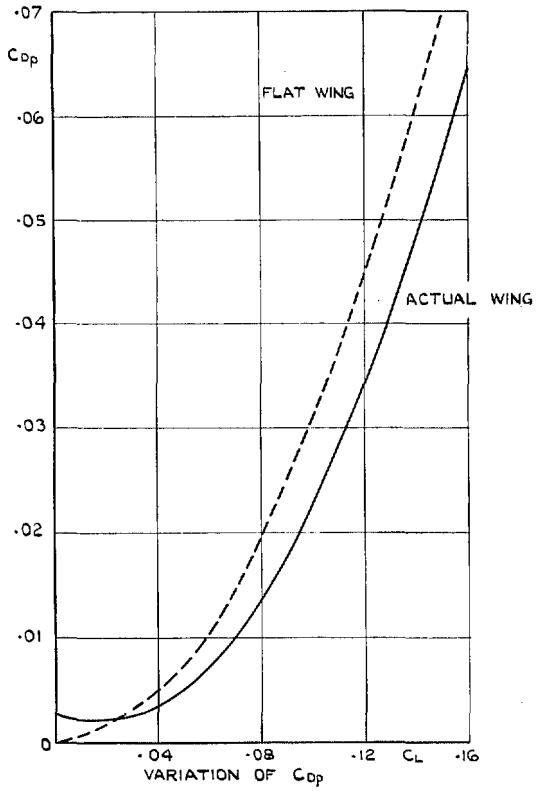
FIG. 8. Shape of Wing 1c, $\gamma = 18$ deg.—Designed for minimum C_D/C_L^2 (suction forces included) at $M = 2\cdot47$.
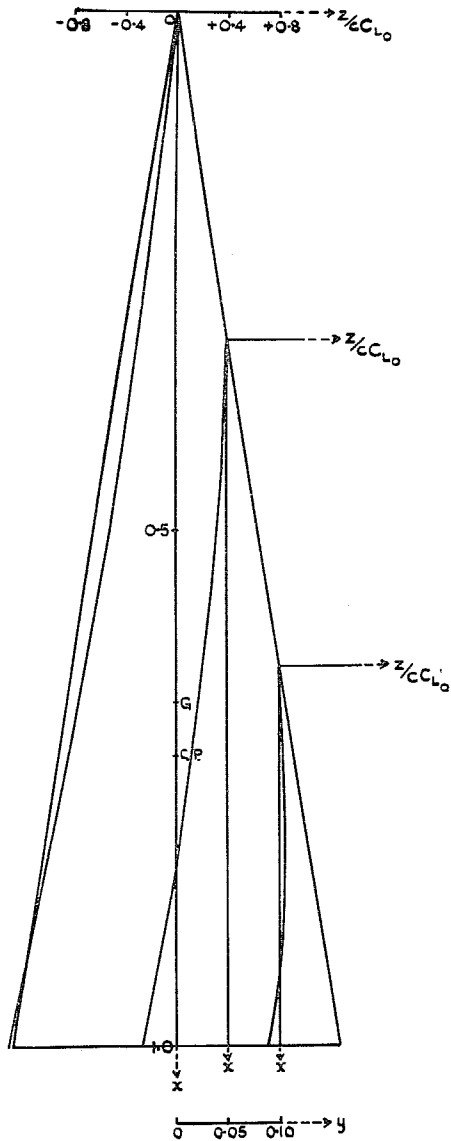
FIG. 9a. Shape of Wing 2a, $\gamma = 9$ deg.
—Designed for minimum C_{Dp}/C_L^2 at
$M = 2\cdot47$.
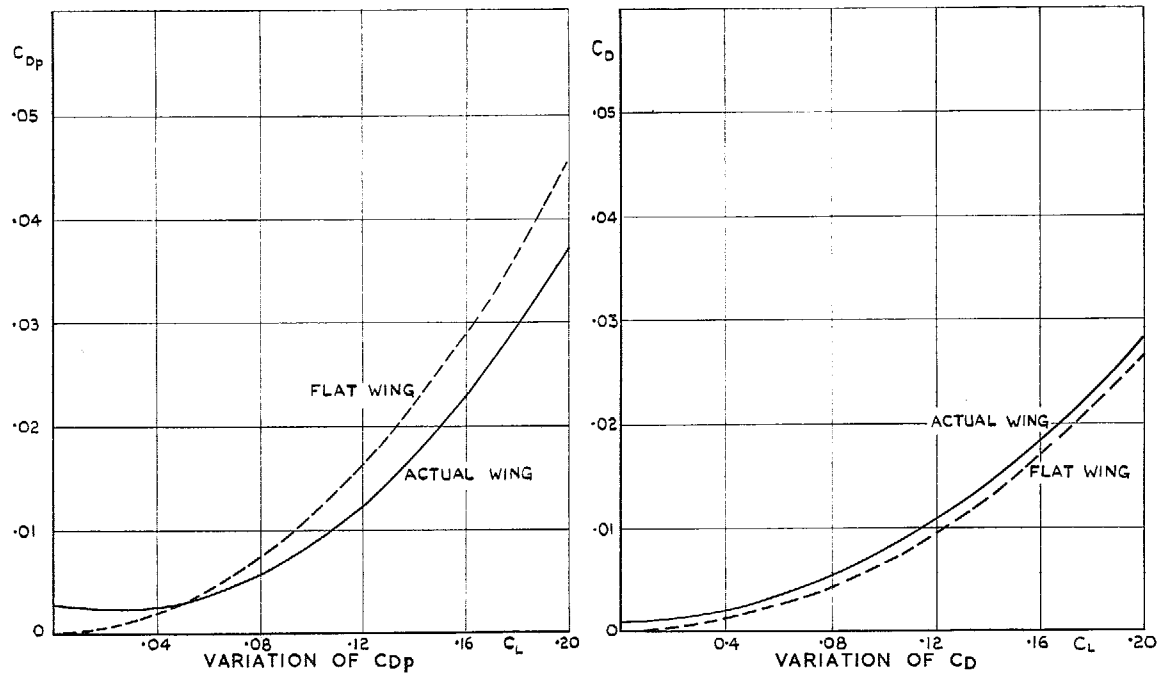
FIG. 9b.   Variation of drag with lift for Wing 2a, $\gamma = 9$ deg.—Designed for minimum C_{Dp}/C_L^2 at $M = 2\cdot47$.   Design $C_{L0} = 0\cdot1$.
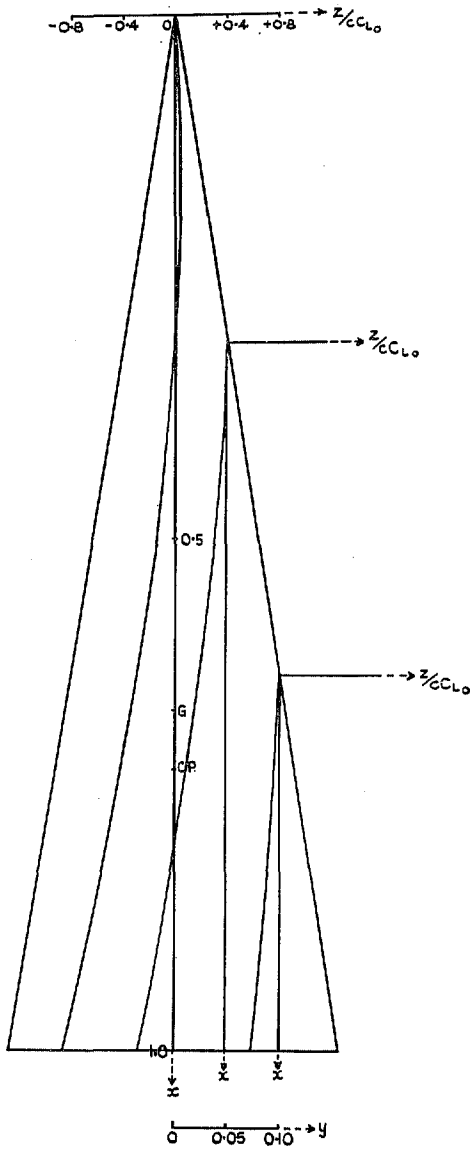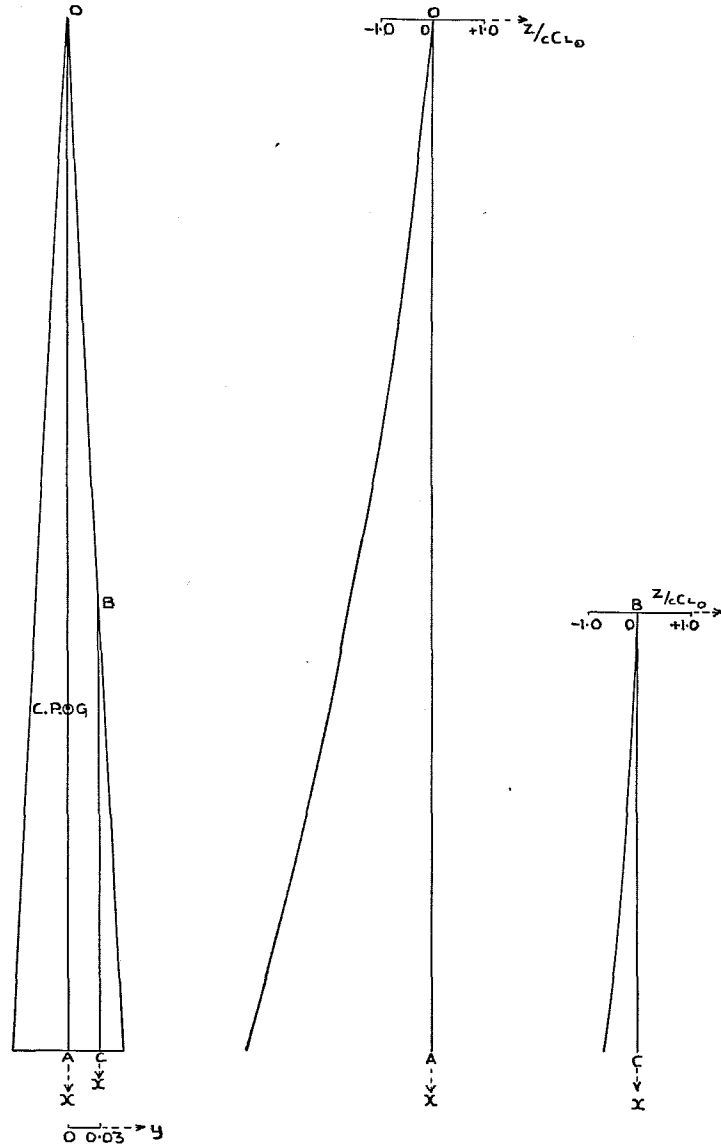
FIG. 10. Shape of Wing 2b, $\gamma = 9$ deg.
—Designed for minimum $C_{Dp}/C_L{}^2$ at
$M = 2 \cdot 47$.
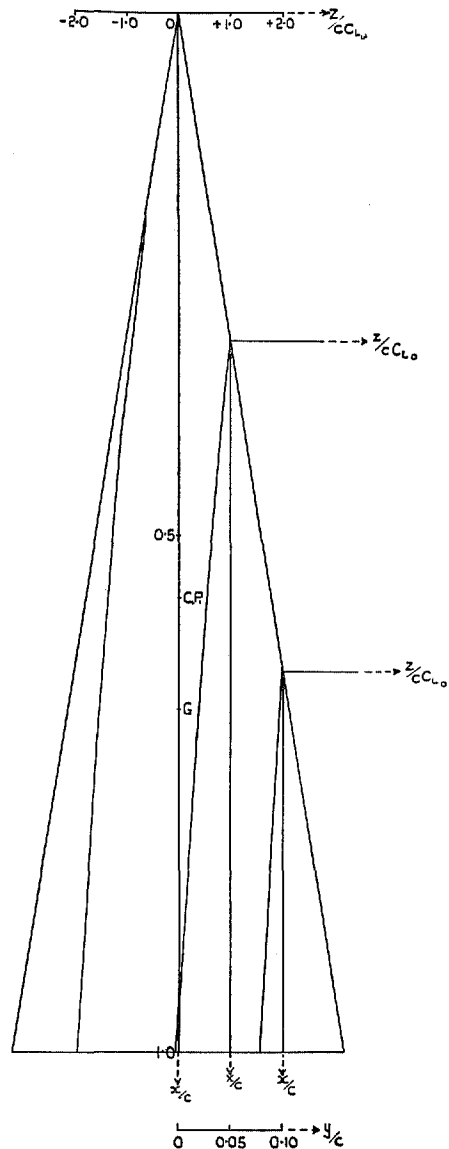
FIG. 11a. Shape of Wing 2c, $\gamma = 9$ deg.
—Designed for minimum $C_D/C_L{}^2$ (suction
forces included), at $M = 2 \cdot 47$.

FIG. 11b. Variation of drag with lift for Wing 2c, $\gamma = 9$ deg.—Designed for minimum $C_D/C_L{}^2$ at $M = 2 \cdot 47$. Design $C_{L\,0} = 0 \cdot 1$.

FIG. 12. Shape of Wing 2d, $\gamma = 9$ deg. —Centre of pressure fixed at G; designed for minimum $C_{D\,v}/C_L{}^2$ at $M = 2 \cdot 47$.
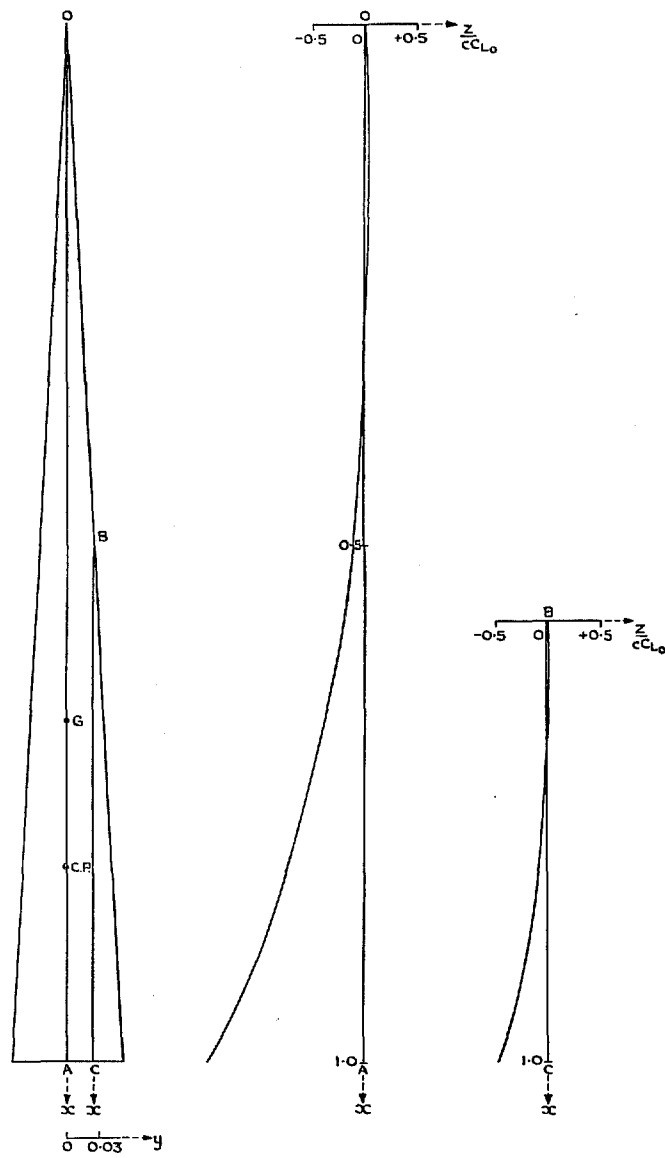
FIG. 13a. Shape of Wing 3a, $\gamma = 3$ deg.—Designed for minimum C_{Dp}/C_L^2 at $M = 2 \cdot 47$.

FIG. 13b. Variation of drag with lift for Wing 3a, $\gamma = 3$ deg.—Designed for minimum $C_{Dv}/C_L{}^2$ at $M = 2 \cdot 47$. Design $C_{L0} = 0 \cdot 05$.

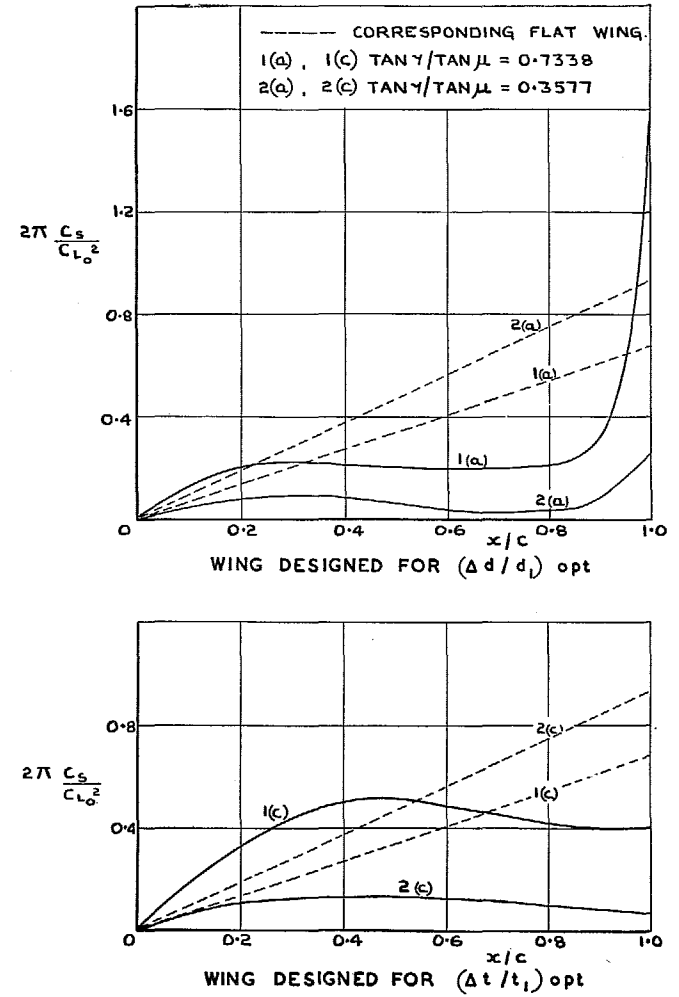FIG. 14. Shape of Wing 3b.—Centre of pressure fixed at G; designed for minimum C_{Dp}/C_L^2 at $M = 2\cdot 47$.

WING DESIGNED FOR $(\Delta d/d_1)$ opt

WING DESIGNED FOR $(\Delta t/t_1)$ opt

FIG. 15. Variation of suction force along the leading edge.

Publications of the
Aeronautical Research Council

ANNUAL TECHNICAL REPORTS OF THE AERONAUTICAL RESEARCH COUNCIL (BOUND VOLUMES)

1939 Vol. I. Aerodynamics General, Performance, Airscrews, Engines. 50s. (52s.).
Vol. II. Stability and Control, Flutter and Vibration, Instruments, Structures, Seaplanes, etc.
63s. (65s.)

1940 Aero and Hydrodynamics, Aerofoils, Airscrews, Engines, Flutter, Icing, Stability and Control, Structures, and a miscellaneous section. 50s. (52s.)

1941 Aero and Hydrodynamics, Aerofoils, Airscrews, Engines, Flutter, Stability and Control, Structures. 63s. (65s.)

1942 Vol. I. Aero and Hydrodynamics, Aerofoils, Airscrews, Engines. 75s. (77s.)
Vol. II. Noise, Parachutes, Stability and Control, Structures, Vibration, Wind Tunnels. 47s. 6d. (49s. 6d.)

1943 Vol. I. Aerodynamics, Aerofoils, Airscrews. 80s. (82s.)
Vol. II. Engines, Flutter, Materials, Parachutes, Performance, Stability and Control, Structures. 90s. (92s. 9d.)

1944 Vol. I. Aero and Hydrodynamics, Aerofoils, Aircraft, Airscrews, Controls. 84s. (86s. 6d.)
Vol. II. Flutter and Vibration, Materials, Miscellaneous, Navigation, Parachutes, Performance, Plates and Panels, Stability, Structures, Test Equipment, Wind Tunnels. 84s. (86s. 6d.)

1945 Vol. I. Aero and Hydrodynamics, Aerofoils. 130s. (132s. 9d.)
Vol. II. Aircraft, Airscrews, Controls. 130s. (132s. 9d.)
Vol. III. Flutter and Vibration, Instruments, Miscellaneous, Parachutes, Plates and Panels, Propulsion. 130s. (132s. 6d.)
Vol. IV. Stability, Structures, Wind Tunnels, Wind Tunnel Technique. 130s. (132s. 6d.)

Annual Reports of the Aeronautical Research Council—

1937   2s. (2s. 2d.)   1938   1s. 6d. (1s. 8d.)   1939-48   3s. (3s. 5d.)

Index to all Reports and Memoranda published in the Annual Technical Reports, and separately—

April, 1950   -   -   -   -   R. & M. 2600   2s. 6d. (2s. 10d.)

Author Index to all Reports and Memoranda of the Aeronautical Research Council—

1909—January, 1954   R. & M. No. 2570   15s. (15s. 8d.)

Indexes to the Technical Reports of the Aeronautical Research Council—

December 1, 1936—June 30, 1939	R. & M. No. 1850	1s. 3d. (1s. 5d.)
July 1, 1939—June 30, 1945	R. & M. No. 1950	1s. (1s. 2d.)
July 1, 1945—June 30, 1946	R. & M. No. 2050	1s. (1s. 2d.)
July 1, 1946—December 31, 1946	R. & M. No. 2150	1s. 3d. (1s. 5d.)
January 1, 1947—June 30, 1947	R. & M. No. 2250	1s. 3d. (1s. 5d.)

Published Reports and Memoranda of the Aeronautical Research Council—

Between Nos. 2251–2349	R. & M. No. 2350	1s. 9d. (1s. 11d.)
Between Nos. 2351–2449	R. & M. No. 2450	2s. (2s. 2d.)
Between Nos. 2451–2549	R. & M. No. 2550	2s. 6d. (2s. 10d.)
Between Nos. 2551–2649	R. & M. No. 2650	2s. 6d. (2s. 10d.)
Between Nos. 2651–2749	R. & M. No. 2750	2s. 6d. (2s. 10d.)

Prices in brackets include postage

HER MAJESTY'S STATIONERY OFFICE